



TOMAS BATA UNIVERSITY IN ZLIN
FACULTY OF TECHNOLOGY
Polymer Centre

Zuzana Kožáková

TAILORING OF MAGNETIC FILLERS FOR POLYMER COMPOSITES AND SUSPENSIONS

Príprava magnetických plnív s vlastnosťami na
mieru pre polymérne kompozity a suspenzie

Doctoral Thesis

Programme:	P 2808 Chemistry and Materials Technology 2808V006
Course:	Technology of Macromolecular Compounds
Supervisor:	doc. Ing. et Ing. Ivo Kuřitka, Ph.D. et Ph.D.
Year:	2014

CONTENT

ACKNOWLEDGEMENT	iii
ABSTRACT	iv
ABSTRAKT	v
LIST OF FIGURES AND TABLES	vi
LIST OF ABBREVIATIONS AND SYMBOLS.....	viii
LIST OF ARTICLES INCLUDED IN THESIS AND AUTHOR'S CONTRIBUTION	ix
INTRODUCTION	10
1. NANOSCOPIC AND MESOSCOPIC MAGNETIC MATERIALS.....	12
1.1 BASIC FEATURES AND PROPERTIES	12
1.2 REDUCTION OF DIMENSIONS AS A SOURCE OF HIGH SURFACE ENERGY ...	13
1.3 IRON OXIDES: STRUCTURE AND MAGNETIC PROPERTIES	13
1.4 SYNTHETIC TECHNIQUES: CONVENTIONAL METHODS AND MICROWAVE-ASSISTED TECHNIQUE	16
1.4.1 CO-PRECIPITATION SYNTHETIC METHOD	17
1.4.2 SOLVOTHERMAL SYNTHESIS.....	18
1.4.3 MICROWAVE-ASSISTED TECHNIQUES	20
1.4.4 TEMPLATE-ASSISTED METHODS	22
2 SMART APPLICATIONS OF MAGNETIC NANO AND SUBMICRO PARTICLES.....	23
2.1 MAGNETIC NANO AND SUBMICRO PARTICLES FOR TARGETING, LABELLING AND SEPARATIONS	23
2.2 MAGNETORHEOLOGICAL FLUIDS IN MEDICINE AND INDUSTRY	24
2.3 SMART MAGNETIC COMPOSITE SYSTEMS.....	26
3 AIMS OF WORK	30
4 METHODOLOGY	31
4.1 MATERIALS.....	31
4.2 SYNTHESIS OF MAGNETIC NANOPARTICLES VIA THE MW-ASSISTED SOLVOTHERMAL TECHNIQUE	31
4.3 SYNTHESIS OF MAGNETIC MICRO-RODS THROUGH THE THERMAL DECOMPOSITION OF PRECURSOR	31
4.3.1 MW-ASSISTED SOLVOTHERMAL SYNTHESIS OF IRON (III) OXALATE PRECURSOR.....	31
4.3.2 THERMAL DECOMPOSITION OF OXALATE PRECURSOR USING MW HEATING	32

4.4	CHARACTERISATION	32
5	SUMMARY OF RESULTS	34
6	CLOSING REMARKS	43
6.1	CONCLUSIONS AND CONTRIBUTION TO SCIENCE AND TECHNOLOGY	43
6.2	FUTURE PROSPECTIVE.....	43
	REFERENCES	44
	CURRICULUM VITAE	52
	LIST OF PAPERS	53
	APPENDIX - PAPERS INCLUDED TO THE THESIS	56

ACKNOWLEDGEMENT

First and foremost, I would like to express my sincere gratitude to my supervisor Assoc. prof. Ing et Ing. Ivo Kuřitka, Ph.D. et Ph.D. for his guidance, mentoring and encouragement throughout doctoral studies.

My thanks belong also to Assoc. prof. Dr. Ing. Vladmír Pavlínek for taking the consultancy of this dissertation, fruitful discussions and cooperation with his research group.

I am deeply grateful to Prof. Ing. Petr Sáha, CSc. for creation of excellent academic and social environment and for giving me the opportunity to participate on the project of Centre of Polymer Systems.

My gratitude goes to all my colleagues from the Polymer Centre, the Centre of Polymer Systems and other departments of the University Institute and Faculty of Technology of the Tomas Bata University in Zlin for their collaboration, help and enthusiasm.

Research work and studies has a social dimension as well. Thanks to my friends, roommates and other colleagues for their nice company.

Thanks to my family for all the support, patience and endless love.

The financial support granted to my research work by the funding providers is partially addressed and acknowledged in the respective places in papers included to this thesis whenever the opportunity to do so was. Here, I would like to thank the Centre of Polymer Systems and Faculty of Technology of the Tomas Bata University in Zlin for the financial assistance during my studies.

ABSTRACT

The presented doctoral thesis is submitted in the form of commented thematically arranged collection of five original scientific articles underpinned by the theoretical background. Synthetic techniques of magnetic particles preparation, their basic features and properties are overviewed with emphasis on the possible application and present trends in many areas are included, too.

At first, original method for the preparation of magnetic nanoparticles based on the iron oxides by the use of microwave-assisted solvothermal techniques is introduced. Mechanisms that take place within this synthesis are also elucidated here. On the basis of discovered mechanisms, we also propose the manner of tailoring of the particles via the precise control of synthesis parameters. Magnetic particles composed of magnetite/maghemite were prepared in 30 minutes while the conventional solvothermal techniques take usually 12-24 hours. Particles size (20-120 nm), shape and organization (single crystal polyhedral particles, polycrystalline spherical assemblies) and presence of crystalline impurities (presence of hematite, goethite and others) were influenced via the selection of the synthetic parameters.

The crystalline composition of these particles was determined by the X-ray diffraction, morphology and particle size distribution were investigated with the help of scanning and transmission electron microscopy. Magnetic properties were measured via the vibrating sample magnetometry and the frequency dependent measurement of complex magnetic permeability. It is well known that for the mesoscopic and nanoscopic materials, contribution of surface and interface atoms to the magnetic anisotropy is great and thus the magnetic behaviour is strongly dependent on the dimension of particles. For this reason, the correlation between the synthesis parameters, structure and morphology of obtained products and the magnetic properties was also discussed.

In order to obtain elongated shape of the magnetic particles that are suitable for the use in magnetorheological suspensions, another method utilizing decomposition of unstable precursor under the elevated temperature was also proposed. It is a two-step process: first step involves solvothermal synthesis of the precursor with the elongated shape, which is, in the second step decomposed into the iron oxide particles that preserve the shape of the precursor. Both steps involve microwaves instead of common heating and thus the process is fast and highly effective.

The performance of prepared nano-particulate systems was demonstrated in magnetorheological experiments as well as by *in vitro* calorimetry for prospective application in hyperthermia.

Keywords: microwave synthesis, iron oxides, nanoparticles, solvothermal synthesis, thermal decomposition, magnetic properties

ABSTRAKT

Prezentovaná dizertačná práca je predložená vo forme komentovaného tematicky aranžovaného súboru piatich pôvodných článkov so sprievodným textom. Metódy syntézy magnetických nanočastíc, ich základné rysy a vlastnosti s dôrazom na potencionálne aplikácie sú zhrnuté do obecného prehľadu, ktorý taktiež zahrňuje súčasné aplikačné trendy v mnohých odvetviach.

Bola vyvinutá originálna metóda na prípravu magnetických častíc oxidov železa pomocou mikrovlnne-asistovanej solvotermálnej techniky. Bol taktiež objasnený mechanizmus vzniku častíc pomocou tejto metódy. Na základe tohto mechanizmu bol navrhnutý spôsob ovplyvňovania vlastností častíc pomocou precízneho riadenia parametrov syntézy. Magnetické častice tvorené magnetitom/maghemitom boli pripravené v priebehu 30 minút, zatiaľ čo konvenčné solvotermálne techniky trvajú 12-24 hodín. Veľkosť častíc (20-120 nm), ich tvar a organizácia (monokryštalické polyhedrálne častice, polykryštalické guľovité zhluky) a prítomnosť kryštalických nečistôt (hematit, goetit a ďalšie) boli riadené nastavením parametrov syntézy. Kryštalická štruktúra častíc bola určená pomocou röntgenovej difrakcie, morfológia a distribúcia veľkosti častíc boli sledované pomocou skenovacej a transmisnej elektrónovej mikroskopie. Magnetické vlastnosti boli študované pomocou vibračnej magnetometrie a frekvenčne závislého meranie komplexnej magnetickej permeability. Je dobre známe, že u materiálov v nano a mezoškále je príspevok povrchových atómov k magnetickej anizotropii značný, a teda magnetické chovanie týchto materiálov je silne závislé na veľkosti častíc. Z tohto dôvodu bola diskutovaná i korelácia medzi parametrami syntézy, štruktúrou a morfológiou častíc a ich magnetickými vlastnosťami.

Za účelom získať magnetické častice podlhovastého tvaru, ktoré sú veľmi vhodné napríklad pre použitie v magnetoreologických suspenziách, bola navrhnutá metóda, ktorá využíva tepelný rozklad málo stabilných prekursorov pri zvýšenej teplote. Jedná sa o proces, ktorý pozostáva z dvoch krokov: prvý krok zahrňuje solvotermálnu syntézu prekursoru podlhovastého tvaru, ktorý je v druhom kroku rozložený na častice oxidov železa, ktoré si ponechávajú tvar prekursoru. Oba kroky zahrňujú mikrovlnný ohrev miesto bežného zahrievania a teda je tento proces rýchly a vysoko efektívny.

Efektivita pripravených nanočasticových systémov bola preukázaná magnetoreologickými experimentmi ako aj *in vitro* kalorimetriou pre perspektívne aplikácie v hypertermii.

Kľúčové slová: mikrovlnná syntéza, oxidy železa, nanočastice, solvotermálna syntéza, termálny rozklad, magnetické vlastnosti

LIST OF FIGURES AND TABLES

- Figure 1.** The percentage of surface atoms changes with the palladium cluster diameter.
p. 12
- Figure 2.** Structural characteristic of magnetite.
p. 14
- Figure 3.** Magnetization curve of ferromagnetic/ ferrimagnetic material.
p. 15
- Figure 4.** The curve of coercivity vs. size of magnetic particles, shown in four regimes: a) superparamagnetic, b) ferromagnetic single domain, c) vortex state, d) multidomain.
p. 16
- Figure 5.** Top-down versus bottom-up techniques.
p. 17
- Figure 6.** Oscillations of polarizable substances under the influence of an alternating electromagnetic field.
p. 21
- Figure 7.** Model of drug delivery system in cross section.
p. 24
- Figure 8.** MR fluid in the absence a) and in the presence b) of an external magnetic field.
p. 25
- Figure 9.** Schema of magnetic fluid hyperthermia process.
p. 26
- Figure 10.** Model cases of the influence of external magnetic field on the elastic modulus of the isotropic and anisotropic elastomers. White arrows show the direction of the force, black arrows demonstrate the direction of magnetic field.
p. 27
- Figure 11.** Mechanism of the controlled release of drug by ferrogel. Symbols MF ON and MF OFF indicate switching of magnetic field.
p. 28

Figure 12. Mechanism of induction activation of shape memory foam with incorporated magnetic particles.

p. 29

Figure 13. TEM images of materials prepared at 220°C for 30 minutes with $(\text{NH}_4)_2\text{CO}_3$ (a), NH_4HCO_3 (b), aq. NH_3 (c) and NH_4Ac (d).

p. 35

Figure 14. TEM image of material prepared with NH_4HCO_3 with the addition of water (left) and magnetization curves of the same material with and without water addition (right).

p. 36

Figure 15. Magnetization curves of materials prepared with NH_4Ac at various temperatures for 30 minutes (left) and at 220°C for 30 minutes with various nucleating agents (right).

p. 37

Figure 16. Magnetic spectra of prepared materials: real part of complex magnetic permeability (a) and imaginary part (b).

p. 38

Figure 17. Temperature increase triggered by Fe_3O_4 nanoparticles suspended in agarose gel measured at 960 kHz and magnetic field amplitude H_{max} 7.5 mT.

p. 39

Figure 18. Flow curves of 15 wt.% suspension of Fe_3O_4 nanoparticles in silicone oil under various magnetic fields strengths; B (mT): squares 0, triangles 82, circles 168 and crosses 253.

p. 40

Figure 19. SEM image of prepared magnetite/maghemite needle-like particles (a) and its magnetic behaviour described by magnetization curve (b).

p. 42

LIST OF ABBREVIATIONS AND SYMBOLS

N	Number of broken bonds pre unit area
γ	Surface energy
u	Energy needed to cut the bonds between neighbouring atoms
γ_0	Contribution of the broken bonds to the surface energy
γ_s	Contribution of the surface stress to the surface energy
ϵ_s	Surface stretching
M	Magnetization
M_s	Saturation magnetization
M_R	Remanent magnetization
T_B	Blocking temperature
H_C	Coercivity
D_{CR}	Critical size parameter of transition to multi-domain state
T_N	Neel temperature
T_M	Morin spin-flip transition
EG	Ethylene glycol
MW	Microwave
ϵ''	Dielectric loss factor
ϵ'	Relative permittivity
$tg \delta$	Loss tangent
MR	Magnetorheological
CT	Computed tomography
SEM	Scanning electron microscopy
TEM	Transmission electron microscopy
XRD	X-ray diffraction
VSM	Vibrating sample magnetometry (or magnetometer)
μ^*	Complex permeability
B	Magnetic flux density
H	Magnetic field inside the material
Oe	Oerstad
emu	Electromagnetic unit
T	Tesla
θ	Diffraction angle
SAR	Specific absorption rate
c_p	specific heat capacity
m_{Fe}	iron content per gram of Fe_3O_4
dT/dt	slope of temperature vs. time dependence

LIST OF ARTICLES INCLUDED IN THESIS AND AUTHOR'S CONTRIBUTION

- I. KOZAKOVA, Z. (50%); BAZANT, P.; MACHOVSKY, M.; BABAYAN, V.; KURITKA, I., Fast Microwave-Assisted Synthesis of Uniform Magnetic Nanoparticles. *Acta Physica Polonica A*, 2010, vol. 118, no. 5, p. 948-949. ISSN 0587-4246.
- II. KOZAKOVA, Z. (50%); KURITKA, I.; KAZANTSEVA, N. E.; BABAYAN, V.; PASTOREK, M.; MACHOVSKY, M. and BAZANT, P., Formation mechanism of iron oxide nanoparticles within the microwave-assisted solvothermal synthesis and its correlation with the structural and magnetic properties. *Manuscript submitted to Materials Research Bulletin*. ISSN 0025-5408.
- III. KOZAKOVA, Z. (50%); KURITKA, I.; BABAYAN, V.; KAZANTSEVA, N.; PASTOREK, M., Magnetic Iron Oxide Nanoparticles for High Frequency Applications. *Ieee Transactions on Magnetics*, 2013, vol. 49, no. 3, p. 995-999. ISSN 0018-9464.
- IV. SEDLACIK, M.; MOUCKA, R.; KOZAKOVA, Z. (30%); KAZANTSEVA, N. E.; PAVLINEK, V.; KURITKA, I.; KAMAN, O.; PEER, P., Correlation of structural and magnetic properties of Fe₃O₄ nanoparticles with their calorimetric and magnetorheological performance. *Journal of Magnetism and Magnetic Materials*, 2013, vol. 326, p. 7-13. ISSN 0304-8853.
- V. KOZAKOVA, Z. (50%); KURITKA, I.; BAZANT, P.; PASTOREK, M. and BABAYAN, V., Synthesis of needle-like iron oxide particles by microwave-assisted thermal decomposition technique. *Manuscript submitted to Materials Letters*. ISSN 0167-577X.

INTRODUCTION

Nowadays, the one of the most growing fields in the materials research is nanotechnology and, as the name suggests, this field deals with the structures having their dimensions in nanoscale. The enormous interest is based on the fact that the present development in many technological areas, especially in electronics, is accompanied with the miniaturization of devices. Miniaturization of electronic components led to the requirement of the decrease of the particles size which compose the building materials.

This work is devoted to the preparation and tailoring of the properties of magnetic nanoparticles and the reason is simple. First of all, their ability to absorb electromagnetic radiation of ultra-high frequencies makes them proper candidates as active component for the polymer matrix microwave absorbers. Combination of small dimensions of particles together with the low weight of polymers is the main advantage of magnetic composites, which can substitute common shielding materials based on metals and thus enable significant decrease of weight of the devices. Moreover, the ability of particles to interact with magnetic field can be used for the numerous technological applications. Besides the industrial applications, small dimensions of particles can be advantageously used also in medicine and pharmacy. Their size is small enough thus they can be incorporated into the organism and flow in the bloodstream. Here they can interact with an external magnetic field and controllably deliver drugs to the affected tissue. Furthermore, magnetic particles can be heated via the alternating magnetic field through the hysteresis losses. This property can be utilized for the magnetic hyperthermia treatment of cancer on the bases of knowledge of the thermal sensibility of tumorous cells. Cancerous cells thus can be selectively destroyed while healthy cells can survive such temperatures and remain unaffected.

The performance of magnetic nanoparticles in all of those applications, of course, depends on the properties of particles; therefore it is necessary to be able to tailor them in desired way. Many synthesis techniques were developed possessing various advantages and also difficulties. We chose solvothermal method since it allows tuning the properties by a simple control of the synthetic parameters, its simplicity and low cost and availability. It is based on the heating of a metallic salt in proper solvent with the addition of other agents, such as nucleating and precipitating. Moreover, we changed the manner of heating from common to microwave what enables reduction of the synthesis time and high efficiency of conversion of raw material into the required product. In addition, the use of pressurized reactor allows the precise control of the synthesis temperature, heating of the reaction mixture above the boiling point of solvent and also indirect control of the pressure via the selection of reactants, filling level of vessels and the temperature.

In recent years, the term magnetorheological suspensions is also pronounced and describes the suspensions of magnetically polarizable particles dispersed in non-magnetic fluid, which are able to change the rheological behaviour dramatically after the application of an external magnetic field via the formation of the chain-like structures. For this purpose, elongated shape of particles seems to be attractive, however, it is usually not reached by the common solvothermal techniques. Therefore we developed microwave-assisted method, which includes the formation of the precursor particles based on iron (III) oxalate via the solvothermal technique and its conversion into the iron oxide particles through the thermal decomposition with the help of microwaves. Iron oxalates tend to grow preferably in one direction at certain conditions and their decomposition products preserve the original shape of the precursor thus the elongated magnetic particles can be obtained. Thanks to microwaves, this method is also very fast and effective and additionally low cost and available chemicals, such as ferrous sulphate and ethylene glycol are used.

To accomplish presented research, its potential usefulness must be shown. Anyway, already formulated intention to apply synthesized particles, requires intensive testing before application. The *in vitro* testing before *in vivo* experiments is a well-established approach in the research pointing towards living systems. Its counterpart in technology oriented to non-living things can be found in so called demonstration experiments which do not usually contribute much to the discovery of the principle. On the other hand, the arrangement of such experiments make the performance of the tested system in certain scale easily visible and the principle of its action understandable in relation to what can be expected as important and useful or dangerous in the real application. In case of magnetic composites and dispersions based on the particles firstly described in this dissertation, it was demonstrated that the materials are able to response to external magnetic fields by intended change of the material's property, such as viscosity or temperature increase through energy dissipation.

1. NANOSCOPIC AND MESOSCOPIC MAGNETIC MATERIALS

1.1 Basic Features and Properties

The field of nanotechnology deals with the nanosized structures called nanostructures. Nanostructures are defined as materials smaller than 100 nm in at least one dimension. Small features permit more functionality in a given space; however, miniaturization of devices is not only their single speciality. Reduced lattice constant, low melting point and high surface energy due to the significant fraction of surface atoms or ions are typical characteristic of nanostructures [1]. The percentage of surface atoms increase with the decrease of particles dimensions is shown in Figure 1. Materials with dimension in the range between quantum and bulk materials are unique by their specific mesoscopic properties. Noticeable increase in the surface to volume ratio leads to the domination of the surface effect, which can contribute to the orientation of spin and thus influence the magnetic properties [2-4].

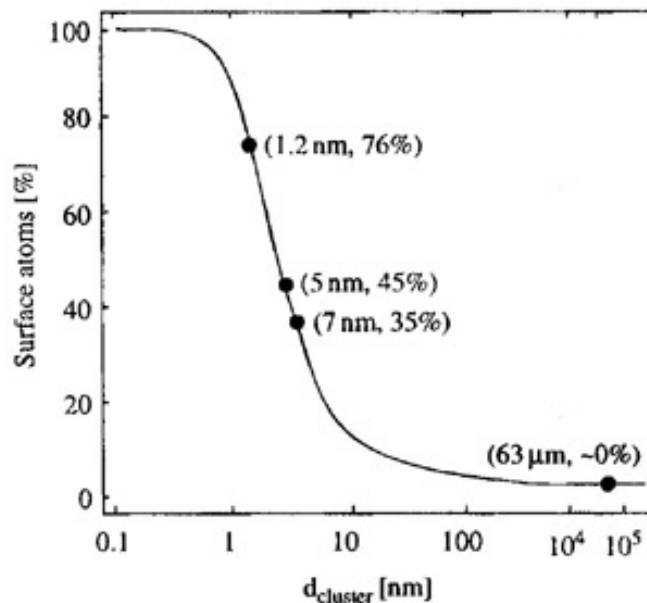


Figure 1. The percentage of surface atoms changes with the palladium cluster diameter [5].

1.2 Reduction of Dimensions as a Source of High Surface Energy

Due to the dramatic reduction of dimensions into the nanoscale, nanostructures possess large fraction of surface atoms per unit volume causing the huge surface energy. The term surface energy can be explained by a model that assumes formation of nanostructures by breaking the large solid pieces into the smaller parts. In order to break the material, energy u is needed to cut the bonds between neighbouring atoms. Then the surface energy is defined as energy required for the creation of a new unit area. The number of broken bonds per unit area N is used to express the contribution of the broken bonds γ_0 to the surface energy [1, 6]:

$$\gamma_0 = Nu/2 \quad (1)$$

Atoms on a solid surface possess reduced number of neighbours thus having the unsatisfied bonds. For that reason, surface atoms are under the force acting perpendicularly to the surface which leads to the stress in the surface plane. Surface stress deforms the surface and causes the surface stretching ϵ_s which also contributes to the surface energy. Surface energy then can be described by the following relation [6]:

$$\gamma = \gamma_0 + \gamma_s(\epsilon_s) \quad (2)$$

where γ_s is the contribution of the surface stress to the surface energy.

Due to high surface energy, nanostructures are thermodynamically unstable or metastable. Therefore, overcoming of the surface energy during the preparation and processing of nanostructures is one of the greatest challenges in the manufacturing of nanoparticles in order to prevent them from the growth in size or aggregation, driven by the reduction of overall surface energy [1].

1.3 Iron Oxides: Structure and Magnetic Properties

Transition metal oxides constitute the class of inorganic solids with very various structures, properties, and phenomena and thus get great attention. From this broad class, iron oxides or ferrites are most interesting due to their magnetic properties; most known representatives are magnetite Fe_3O_4 and maghemite $\gamma\text{-Fe}_2\text{O}_3$. Magnetite has inverse-spinel structure with face-centred cubic unit cell that can be seen in Figure 2. It can be stoichiometric ($\text{Fe}^{\text{II}}/\text{Fe}^{\text{III}} = 0.5$) or non-stoichiometric when a deficiency of trivalent iron exist in sublattice. Similarly, divalent iron can be partly or fully replaced by other divalent ions such as Zn^{II} or Mn^{II} [7].

Maghemite has a structure similar to that of magnetite; however, all or almost all of iron is in the trivalent state and cation vacancies that are confined to tetrahedral sites compensate for the oxidation of Fe^{II} [7].

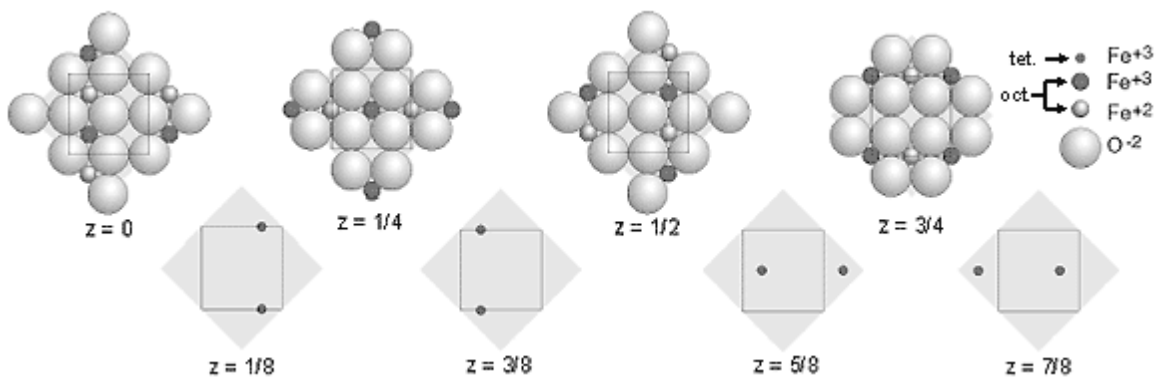


Figure 2. Structural characteristic of magnetite [8].

For the description of magnetic properties, the relationship between the magnetization M (i.e. magnetic polarization) and the magnetic field inside the material H is commonly used and gives the magnetization curve. The typical magnetization curve can be seen in Figure 3. On the basis of behaviour in magnetic field, substances can be classified into two basic groups - materials with weak or strong magnetic behaviour. Weak magnetic behaviour can be divided into the paramagnetic and diamagnetic and features the linear dependence of magnetization on the magnetic field strength. Strong magnetic behaviour embodies ferromagnetic and ferrimagnetic materials and this behaviour is facilitated by the spontaneous ordering of uncompensated magnetic moments of atoms into the magnetic domains. Ordering of magnetic moments is possible under the temperature called Currie temperature while concerning ferromagnetic materials or Neel temperature for ferrimagnets. As a result, magnetization increases with the applied magnetic field until it reaches its saturation M_s which determines maximum field that can be generated by material [9, 10].

Coercivity of material is a further property that can be derived from the magnetization curve and expresses the intensity of the applied magnetic field required to reduce the magnetization of that material to zero after the magnetization of the sample has been driven to saturation. Magnetization of material at zero magnetic field is called remanent magnetization M_R . After the certain time, spins return to their equilibrium with the surroundings. This process is called relaxation and the time of recovery into the equilibrium state is called relaxation time [11]. Small particles do not have permanent magnetic moments in the absence of an external field but can respond to an external magnetic field. These materials are characterized by the blocking temperature T_B at which the thermal energy is comparable to the magnetic anisotropy energy or the energy barrier for spin reorientation. Well above this temperature, the magnetization curve (M-H curve) does not embody any hysteresis. This behaviour is called superparamagnetism [12].

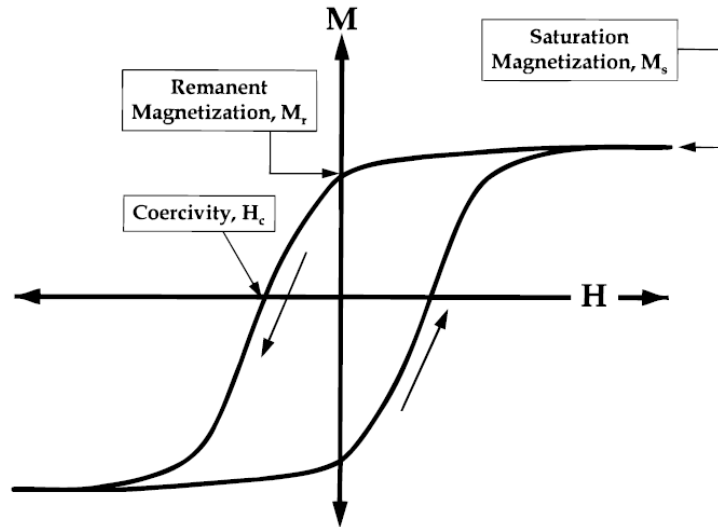


Figure 3. Magnetization curve of ferromagnetic/ ferrimagnetic material [10].

Value of coercivity determines the magnetic hardness of the material: magnetically soft materials have $H_c < 10^3 \text{ A.m}^{-1}$ while magnetically hard materials have the value of coercivity $H_c > 10^3 \text{ A.m}^{-1}$ [11].

Other important characteristic of magnetic materials is magnetic anisotropy that originates from several reasons: crystalline origin, shape of the sample, and stress in the material or atomic segregation. Energy of magnetically ordered sample depends on the relative directions of the magnetization with respect to the structural axes of crystal and it is known as magnetic anisotropy energy [11, 13].

Intrinsic magnetic properties, such as magnetization and anisotropy, are determined on an atomic scale, however, some intrinsic effects are realized on a length scale of several interatomic distances. For the mesoscopic and nanoscopic materials, contribution of surface and interface atoms to the magnetic anisotropy is great and thus the magnetic behaviour is strongly dependent on the dimension of particles [13]. Smaller particles will tend to be in single-domain state while larger ones exhibit multi-domain or vortex configuration if they reach a certain critical parameter D_{cr} . Moreover, other parameters such as Curie temperature and coercivity H_c are also size-dependent [11]. The relation between the coercivity and the particle size as well as their magnetic state can be seen in Figure 4.

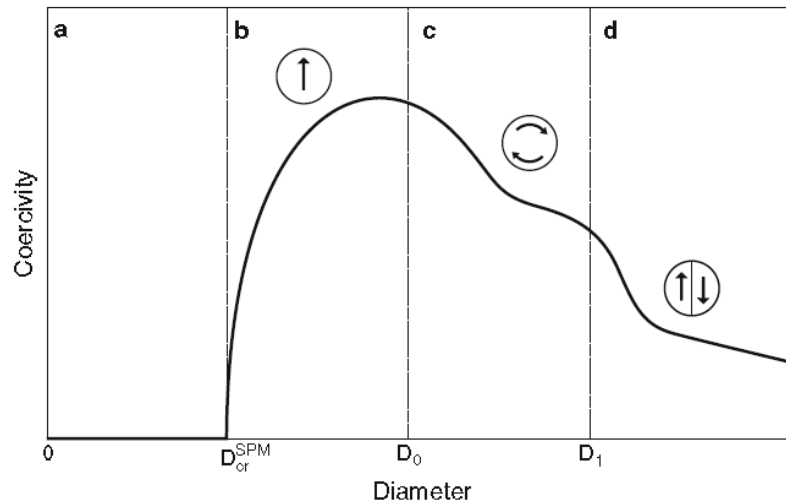


Figure 4. The curve of coercivity vs. size of magnetic particles, shown in four regimes: a) superparamagnetic, b) ferromagnetic single domain, c) vortex state, d) multidomain [11].

On the other hand, paramagnetic, diamagnetic or antiferromagnetic iron oxides, hydroxides or oxide hydroxides can be formed during the preparation of desired magnetic oxides or due to their oxidation by air oxygen such as goethite and hematite. Then the synthesis should be performed in a manner that eliminates the formation of such crystalline impurities [14].

1.4 Synthetic Techniques: Conventional Methods and Microwave-Assisted Technique

Generally, there are two main synthetic approaches for the preparation of magnetic structures: top-down and bottom-up techniques. Top-down methods include physical approaches for the preparation of nanostructures such as milling, attrition, repeated quenching and lithography, however, particles prepared by these methods are often polydispersed, or containing impurities from the preparation procedure. Moreover, the biggest problem with top-down approaches is the imperfection of the surface structure. Bottom-up techniques refer to the atom by atom building of materials on a larger scale. Therefore, these methods promise better chance to obtain nanostructures with fewer defects, impurities and better ordering [1]. Schematic illustration of top-down and bottom-up techniques is given in Figure 5.

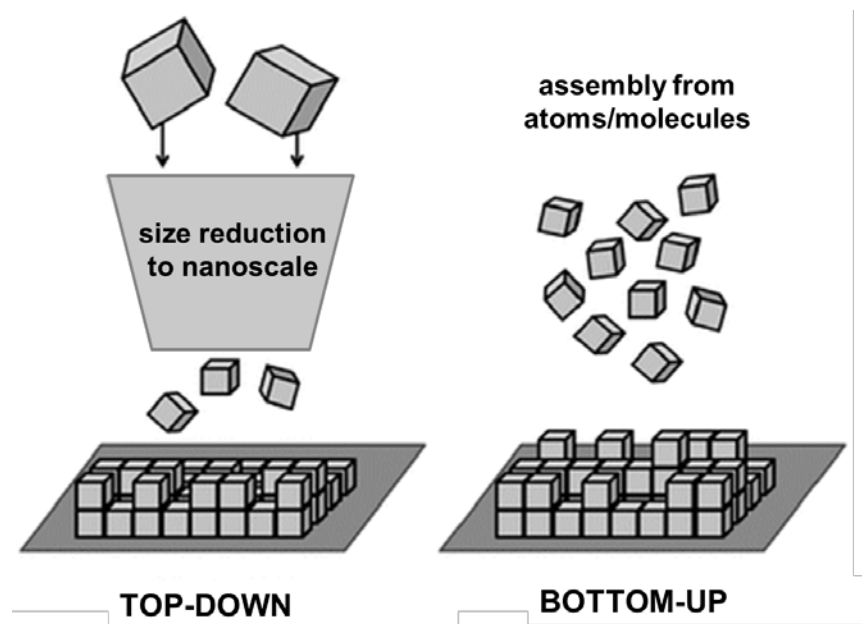


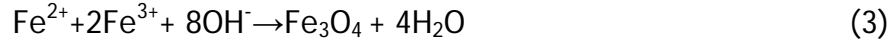
Figure 5. Top-down versus bottom-up techniques [15].

In bottom-up techniques, nanostructures can be formed by a homogenous nucleation from liquids or vapours or by a heterogeneous nucleation on pre-existing surfaces. For the homogenous nucleation of nanoparticles, supersaturation of growth species must be formed firstly. This can be achieved by the temperature decrease or by the conversion of highly soluble chemicals into the less soluble ones by *in situ* chemical reactions. Supersaturation causes that the solution possess high Gibbs free energy and, as a result, this system will tend to reduce the overall surface energy by the segregation of solute from solution [1]. The appearance of the new solid phase is accompanied with the introduction of surface energy into the system until the nuclei are very small and, since they are unstable, they will melt or dissolve. However, if nucleus survives (by a statistical event) and exceeds the critical size, it will tend to grow in order to reduce the overall energy and to form the stable crystal [16].

Due to the rising demand for the magnetic nanostructures of certain properties, numerous methods for their preparation were developed: microemulsions [17], sol-gel syntheses [18], sonochemical reactions [19], hydrothermal and solvothermal reactions [4, 20, 21], flow injection syntheses [22], electrospray syntheses [23] and others.

1.4.1 Co-precipitation Synthetic Method

The most known and used synthetic technique for the preparation of magnetic particles based on magnetite over the years is the classical method of co-precipitation from the stoichiometric mixture of ferrous and ferric salts in aqueous medium by its aging [24] according to the equation:



Magnetite can be formed in a pH range from 8-14 with a stoichiometric ratio of Fe^{3+} to Fe^{2+} 2:1 in a non-oxidizing oxygen environment [24, 25]. In air, magnetite can be oxidized into the hematite $\alpha\text{-Fe}_2\text{O}_3$ which is not desired due to its weak magnetic nature. Hematite is antiferromagnetic below the Morin spin-flip transition ($T_M = 261$ K), paramagnetic above its Neel temperature ($T_N = 955$ K) and exhibits weak ferromagnetic behaviour between the Morin and Neel temperatures [26]. The transformation of magnetite into the hematite in the presence of oxygen runs according to the following equation [24]:



Main advantage of the co-precipitation method is its simplicity and possibility to produce large amounts of materials, however, control of the particle size distribution is limited due to the fact that only kinetic factors control the growth of crystals [24].

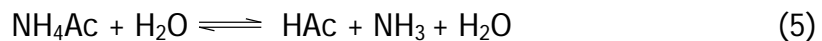
1.4.2 Solvothermal Synthesis

Better control over the size and morphology is enabled within the solvothermal techniques and therefore they were the main object of interest in this dissertation thesis. It is based on the heating of solution of a metallic salt in a suitable solvent in the Teflon-lined stainless autoclave in the presence of other substances, such as nucleating or reducing agents and surfactants [27-29]. In solvothermal synthesis, heating serves for the stimulation of chemical reactions that proceed slowly under the ambient conditions [30], moreover, preparation of nanostructures often requires elevated temperature for the nucleation of nanoparticles [31].

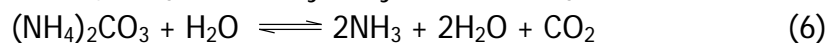
In our experiments, ferric chloride hexahydrate was used as a source of Fe (III) cations, ethylene glycol as a reaction medium and reducing agent and NH_4Ac , $(\text{NH}_4)_2\text{CO}_3$, NH_4HCO_3 and aqueous solution of NH_3 (25 - 27%) as nucleating agents.

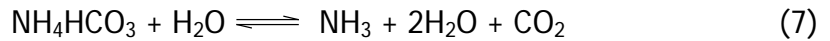
According to the available literature sources [27-29,32,33], a framework of chemical reactions underlying the synthesis can be figured out. The growth of iron oxide particles starts with the nucleation of primary nanocrystals. Nucleation is initiated by the appearance of the first inhomogeneity in the system. In our setup, these inhomogeneity occur due to the generation of colloids, $\text{Fe}(\text{OH})_3$ and $\text{Fe}(\text{OH})_2$, and their formation can be described by the following steps:

Firstly, NH_4Ac , a weak-acid-weak-base salt, can be hydrolyzed in high temperature in the presence of trace amount of water coming from $\text{FeCl}_3 \cdot 6\text{H}_2\text{O}$ as follows [27]:



Similarly, $(\text{NH}_4)_2\text{CO}_3$ and NH_4HCO_3 can be hydrolyzed into NH_3 :

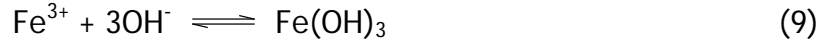




NH_3 , either as the product of hydrolysis reactions or added as aqueous solution yields hydroxide anions:



In our case, Fe (III) salt was used as the precursor. Precipitation of its hydroxide in form of colloidal solution thus proceeds as follows:

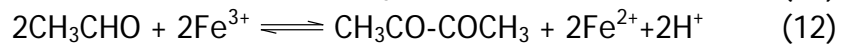


In next, formation of Fe_2O_3 particles may continue according to:

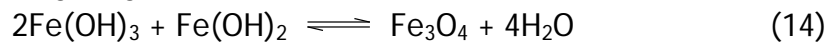


Hence maghemite ($\gamma\text{-Fe}_2\text{O}_3$) and hematite ($\alpha\text{-Fe}_2\text{O}_3$) phases can be formed in this way.

Under the presence of a mild reduction agent (e.g. ethylene glycol), Fe (II) may appear in the system. Ethylene glycol can undergo dehydration and so formed acetaldehyde reduces Fe (III) into Fe (II) and gives ferrous hydroxide in form of a green colloid [32,33]:



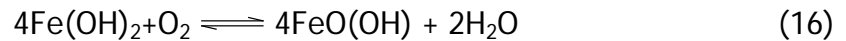
Most likely, both ferric and ferrous oxidation states of iron coexist in the reaction mixture thus enabling magnetite formation:



A minor phase, goethite, was observed and its presence in prepared materials can be explained by partial dehydration:



or by following equation in presence of oxygen:



In the second step, it is generally accepted for conventional solvothermal methods that the fresh formed nanocrystals are unstable due to high surface energy so they tend to aggregate. The driving force for this aggregation is pursuit of reducing the surface energy by both, attachment among the primary nanocrystals and their rotation caused by various interactions including Brownian motion or short-range interactions [34,35].

In contrast to fast nucleation in aqueous solutions, aggregation in ethylene glycol is kinetically slower due to fewer hydroxyl groups on the particle surface and higher viscosity, what allows adequate rotation of nanocrystals to form low-energy configuration of interface and perfect organized assemblies. Subsequently, these aggregates further crystallize and form compact crystals that exhibit features of single-crystal particles [29].

1.4.3 Microwave-Assisted Techniques

Solvothermal methods are relatively simple; however, they take several hours to several days and the yield is often not satisfactory [27-29]. In recent years, the use of microwave energy instead of common heating techniques has emerged due to the possibility to reduce the synthesis duration and thus increase the efficiency of synthesis procedures. In comparison to the conventional techniques, the use of dielectric heating can enhance the reaction rates up to two orders of magnitude and provide higher yields [36]. Microwaves are portion of electromagnetic spectrum with frequencies in a range of 300 MHz to 300 GHz [37]. When the strongly conducting material is irradiated by high-frequency electromagnetic radiation, microwaves are reflected from its surface and thus the material is not effectively heated. However, the movement of electrons on the surface can heat this material through the Ohmic heating mechanism. In the case of insulators, microwaves penetrate through the material without any interaction such as absorption, losses or generation of heat and thus such materials are considered transparent for microwaves [38]. Interaction of materials possessing dipole moment with the electric component of high-frequency electromagnetic field causes the induced polarization of charges within the irradiated material. As a field oscillates, dipoles tend to realign with the alternating electric field and the heat is formed due to the molecular friction and dielectric loss. Radiation of frequency 2.45 GHz used for commercial purposes such as domestic or industrial ovens causes the rotation of polar molecules, but the motion of particles is not sufficient to follow the alternating field precisely. The delay causes the phase difference between the orientation of the field and orientation of dipoles and results in the energy lost from the dipole by molecular friction and collisions, called dielectric loss factor ϵ'' . The ability of substances to convert electromagnetic energy into the heat is determined by the loss tangent $\tan \delta$ that can be expressed by the following equation:

$$\tan \delta = \epsilon'' / \epsilon' \quad (17)$$

where ϵ' is relative permittivity of material which describes the polarizability of molecules in the alternating electric field [30,39]. For this purpose, ethylene glycol (EG) appears to be proper candidate for microwave synthesis due to its high boiling point (197°C) and loss tangent ($\tan \delta = 1.350$) [40]. Figure 6 illustrates the dipole reorientation of polar molecule within the electric component of electromagnetic field as well as the ionic mechanism of electromagnetic field energy absorption.

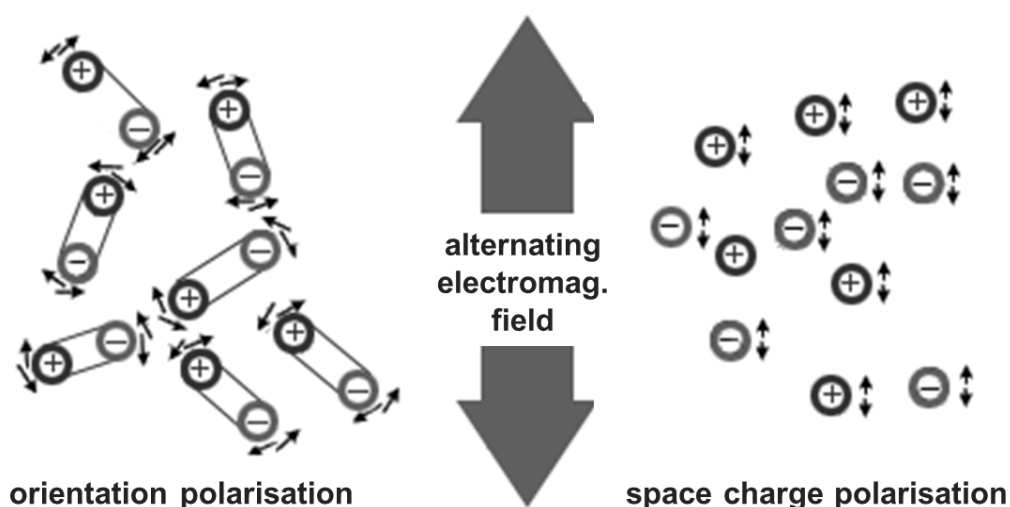


Figure 6. Oscillations of polarizable substances under the influence of an alternating electromagnetic field [41].

Next to the dipolar polarization mechanism, ion conduction mechanism is significantly important. Dissolved charged particles present in the sample oscillate during the ion conduction and collide with neighbour atoms or molecules resulting in the formation of heat. This mechanism is particularly important for the dielectric heating of ionic liquids and it is considered much stronger than the dipolar polarization mechanism [39]. This mechanism can occur also in the case, when described setup of solvothermal synthesis is used. According to our interpretation of available literature sources, we hypothesized that the effect of microwaves during synthesis is as follows. If ethylene glycol is heated to the high temperature (above 200 °C) it becomes less absorbing due to decrease of relative permittivity and loss factor thus the solvent becomes virtually more transparent for microwaves, which means that the ionic mechanism of microwave absorption may be prevailing over dipoles [30]. Once solid particles appear in the solution, another mechanism becomes active due to particles surface polarization that might selectively influence their growth. Moreover, as the heat is generated at the surface of nanoparticles, the local temperature gradient can contribute to the hydroxide-to-oxide transformation described in equations (10) and (14). Besides the dielectric losses, when metal oxides such as ferrites are exposed to high-frequency electromagnetic irradiation, magnetic losses can occur in the microwave region due to the domain wall and electron spin resonance [30]. Moreover, especially in the systems consisted of large amount of ions, superheating of the solvent above its boiling point can occur as a result of dissipation of microwave energy over the whole volume [30, 37]. This sequence of several mechanisms can explain the sudden formation of particles in the reaction mixture as well as very short synthesis time which we observed.

1.4.4 Template-Assisted Methods

Next to the efficiency of the method and formation of nanocrystalline material of high purity, further challenge is the tailoring of the particle morphology. Described hydrothermal and solvothermal methods usually lead to the formation of polyhedral or spherical shapes. However, in recent years, preparation of iron oxide one-dimensional nano- and submicro-structures gets great attention due to their unique properties resulting from the shape anisotropy [42].

Above the common synthetic techniques, template-assisted syntheses offer the possibility to tailor the shape of particles. They include hard templating synthesis that uses hard templates such as silica, which can be, after the synthesis, selectively etched in proper solvent or calcinated at high temperatures, sacrificial templating that utilize templates that are involved in the reaction itself and are consumed during the formation of product or soft templating where soft templates are gaseous or liquid and include emulsion droplets, surfactant micelles or gaseous bubbles [43]. On the other hand, these methods are quite complex and multistep and often bring impurities into the final product [44]. Therefore, methods that utilize organometallic precursors that decompose at relatively low temperature appear to be the most suitable [42]. "Precursor syntheses" are interesting from technological point of view since these methods are simple, cost effective and enable large-scale production [45]. Moreover, combustion procedure is accompanied by generation of gaseous products which suppress the aggregation of forming metal oxide particles thus remaining in nanoscale [46,47]. The tailoring of the morphology can be enabled if the conversion of precursor into the final product runs in such a way that the forming particles preserve the shape given by the precursor. For this purpose, iron oxalates seem to be proper candidates since they grow preferably in a one direction and the shape of the product obtained by their decomposition remains unchanged [42,48-50].

2 SMART APPLICATIONS OF MAGNETIC NANO AND SUBMICRO PARTICLES

2.1 Magnetic Nano and Submicro Particles for Targeting, Labelling and Separations

First of all, magnetic particles in nano and submicro dimensions have the size smaller or comparable to that of cells (10-100 μm), viruses (20-450 nm), proteins (5-50 nm) or genes (2 nm wide and 10-100 nm long) and thus they can 'get close' to a biological entity of interest. Their surface can be modified in order to make them be able to interact with biological molecules and, depending on the surface modification, address them controllably to the desired biological entity [51]. As examples, magnetic particles coated with immuno-specific agents can be bonded to the red blood cells [52], bacteria [53] or urological cancer cells [54], in order to label them or to serve for their separation by an external magnetic field. This could be helpful for the separation of tumorous cells from blood and thus for the early diagnostics of diseases [55]. Other diagnostic methods include magnetic particle imaging, a method emerging as a safe alternative to the computed tomography (CT) angiography. Nowadays, CT-angiography uses iodinated contrast media for the detection of cardiovascular diseases. The use of magnetic particles for the imaging eliminates the risk of contrast-induced nephropathy of patient with renal dysfunction [56]. Magnetic particle imaging is based on a direct measurement of the magnetization of ferromagnetic nanoparticles in order to quantify their local concentration and, in contrast to magnetic resonance imaging (MRI) technique, has the potential to realize high voxel rates, what can serve for the real-time imaging [57].

Next to the magnetic separations, magnetic particles play an irreplaceable role in the drug delivery. Controlled delivery of drug to the desired tissue is enormously important for the drugs with high cytotoxicity and non-specific nature such as chemotherapeutics. Magnetic particulate carriers loaded with the chemotherapeutics are subjected to the organism intravenously or via the arterial injection and guided to the tumour by an external magnetic field. Magnetic particles thus reduce the distribution of the drug within the organism and eliminate the side effects [58]. Model of this drug-delivery system can be seen in Figure 7.

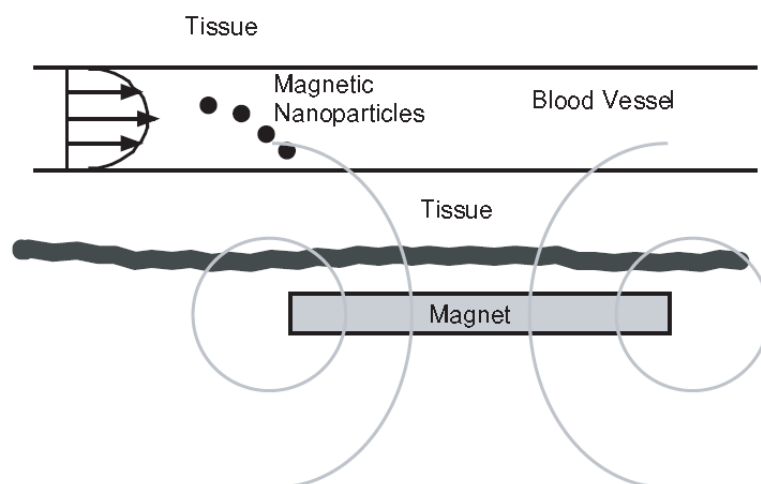


Figure 7. Model of drug delivery system in cross section [51].

Magnetic separation can be useful also for environmental applications. Nowadays, pollution of wastewaters by heavy metals occurs globally and therefore strict regulation on the discharge of heavy metals has been established. For this purpose, magnetic particles have been developed to remove the toxic Hg(II), Pb(II), Cd(II), and Cu(II) from water [59]. In order to prevent them from aggregation in aqueous systems and to alter their sorption ability, their surface is usually treated with an organic coating such as humic acids [58] or dimercaptosuccinic acid [60]. Moreover, magnetic nanoparticles can serve as a magnetic core of core/shell structures intended for the water treatment. The shell can be composed of oxide semiconductor photocatalysts such as titanium or zinc oxides that have been proved to be able to photocatalytically degrade the organic pollutants in waste waters. Magnetic separation provided by the magnetic core solves problem with recovery of the photocatalyst from the treated medium [61].

2.2 Magnetorheological Fluids in Medicine and Industry

Magnetorheological (MR) fluids are materials consisted of magnetically-polarizable particles and non-magnetic medium. In the absence of magnetic field, these fluids exhibit Newtonian-like behaviour; however, after the application of the external magnetic field, magnetic particles dispersed in non-magnetic fluid are polarized and form the chain-like structures due to the interaction of induced dipoles, as can be seen in Figure 8. As a result, MR fluid changes its rheological behaviour what is manifested by the development of a yield stress that monotonically increases with applied field. The field-responsive behaviour of MR fluids is often represented as a Bingham plastic having variable yield stress [62,63].

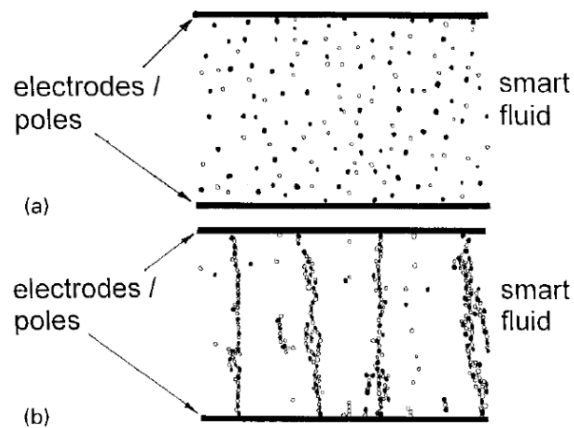


Figure 8. MR fluid in the absence a) and in the presence b) of an external magnetic field [64].

Ability to control the rheological behaviour can be beneficial for numerous practical industrial applications, especially where the control of vibrations or transfer of torque is needed, such as brakes and clutches. Profitable utilization of MR fluids is known in automotive shock absorbers, brakes for physical exercise equipment, actuators, seat dampers and polishing technology [62,64]. For those purposes, MR fluids should consist of soft magnetic materials which are easily magnetized and demagnetized and possess high magnetization saturation value [65].

Controllable rheological behaviour of MR fluids is emerging to be utilized also for medical purposes. After the introduction of MR fluid into the blood vessels that feed the tumour, application of an external magnetic field will cause the change of rheological behaviour of fluid. Formed solid-like structure of MR fluid will cause clogging of vessels and thus also impair the angiogenesis, i.e. formation of new blood vessels feeding the tumour. As a result, supplementation of oxygen and nutrients to the tumour will be prevented resulting in the necrosis of cancerous cells [66,67].

Destruction of the tumorous cells is the main aim also of the method called magnetic fluid hyperthermia. This method arises from the knowledge of the thermal sensitivity of cancerous cells which can be successfully destroyed after the exposition to the elevated temperature (42°C) for 30 minutes [51]. It seems to be simple, however, the challenge is to reach this temperature without the destruction of the surrounding healthy tissue cells. For this purpose, local heating can be reached by the induction heating of the magnetic particles incorporated into the tumorous tissue usually in the form of MR fluid. Magnetic particles are heated when exposed to an alternating magnetic field through the hysteresis losses and relaxation processes, i.e. relaxation of magnetic moments back to their equilibrium orientations (Neel relaxation) and rotational friction between

the particles and the medium (Brownian rotation), while the tissue is inherently nonmagnetic hence it is transparent to magnetic field [67,68-71]. A key parameter characterizing materials used for magnetic hyperthermia is the specific loss power of particles expressed in terms of specific absorption rate (SAR) calculated from the heating rate, specific heat capacity in relation to the amount of iron in the material. The illustration of magnetic fluid hyperthermia process can be seen in Figure 9.

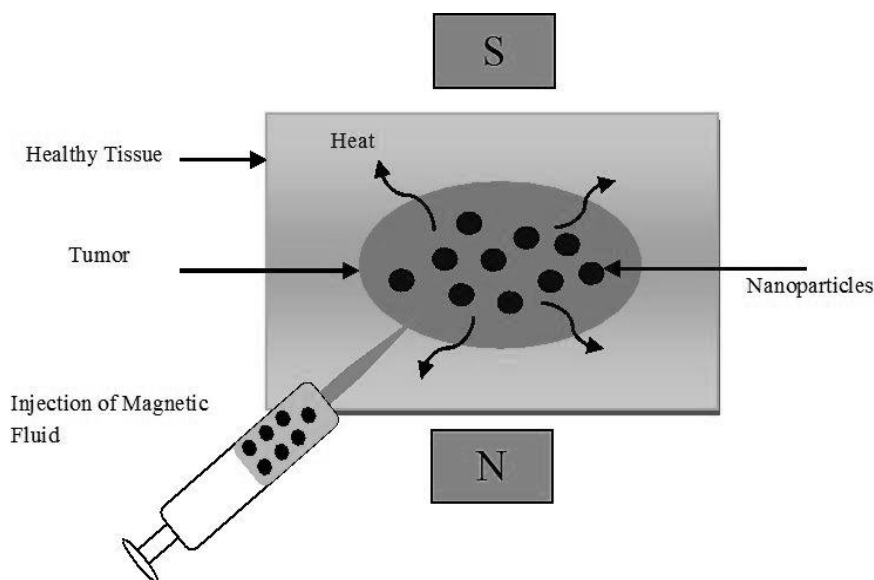


Figure 9. Schematic of magnetic fluid hyperthermia process [72].

2.3 Smart Magnetic Composite Systems

Composite materials are consisted of the two or more different phases. First one is the continuous polymeric matrix and second is the dispersed filler, whether of inorganic or organic nature or the complex core-shell or hybrid system. The aim of the addition of filler into the matrix of desired material is usually the reinforcement or the specific activity of filler such as conductivity, antimicrobial or magnetic properties. In recent years, magnetic nanoparticles are investigated as a promising material for so called smart materials. Smart materials present the group of materials which properties are simply tuneable or have some added value. Magnetic fillers can bring both, make the material to be able to interact with the magnetic field and also, depending on the loading, can reinforce material. Moreover, application of magnetic field during the preparation procedure can ensure desired orientation of filler in the matrix and thus formation of chain-like superstructures through the directed aggregation. As-formed structures, depending on the direction of applied magnetic field, impart the anisotropy to the composite material which is thus manifested also in mechanical properties and is called anisotropic reinforcement [73-76].

Next to the ability to reinforce materials in various manners, magnetic particles are added into the polymeric matrix in order to achieve stimuli-response polymers that possess useful properties such as ability to change swelling behaviour, permeability, and elasticity in a reversible manner [77]. Magnetic field sensitive elastomers are good representative of this group of materials. These materials consist of magnetic particles that are dispersed in highly elastic polymer matrix and couple the shape of elastomer to the external magnetic field. Magnetic particles can be dispersed in the polymer randomly or it is possible to orient them by the magnetic field during the preparation procedure in order to achieve anisotropic magnetic elastomers shown in Figure 10. These materials can serve for many applications due to the tuneable elastic modulus, great deformational effect and quick response to the applied magnetic field [78].

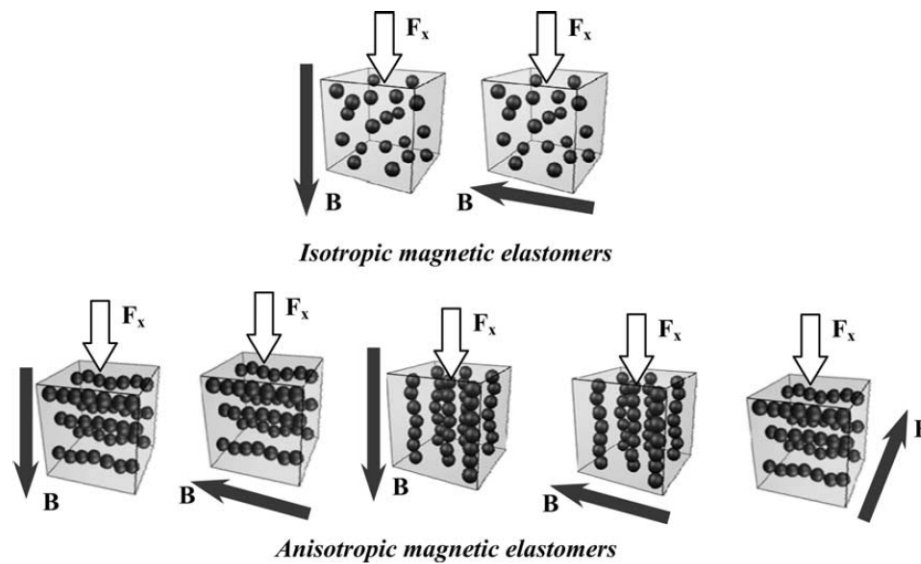


Figure 10. Model cases of the influence of external magnetic field on the elastic modulus of the isotropic and anisotropic elastomers. White arrows show the direction of the force, black arrows demonstrate the direction of magnetic field [78].

Next to the magnetic elastomers, magnetic particles can be incorporated into the matrix of hydrogels. This process can be done by their addition during the gelation or via the diffusion of particles into the previously prepared gel with or without the application of external magnetic field. These magnetic gels, also called ferrogels are smart materials possessing tuneable elastic modulus, deformation and quick response to an external magnetic field [79]. Moreover, they were successfully used for controlling of drugs release by an external magnetic field [77,79-82], as actuators to mimic muscular contraction [83-85] and mechanical actuators [86,87]. Mechanism of controlled release of drug from the ferrogel can be seen in Figure 11.

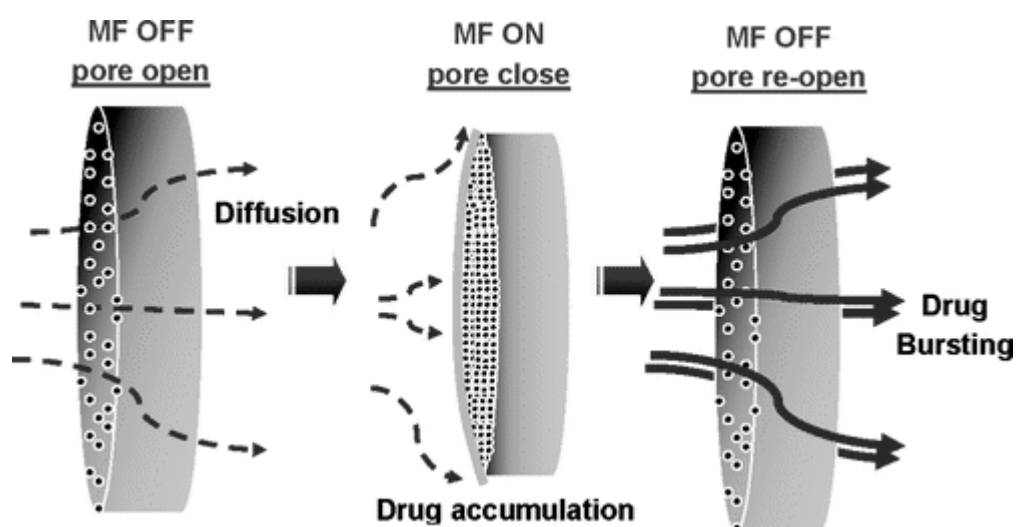


Figure 11. Mechanism of the controlled release of drug by ferrogel. Symbols MF ON and MF OFF indicate switching of magnetic field [77].

Apart from the tuneable mechanical properties, incorporation of magnetic properties into the polymeric matrix brings other benefits, too. Iron oxides and ferrites in nano and submicro dimensions are known to be able to sharply reduce dielectric loss and to absorb microwave energy what makes them attractive candidates for inductive and capacitive materials or microwave absorbers. Polymeric matrix appropriate for this application should be an electrical insulator and should protect electrical components from dust, moisture and short circuiting. For this purpose, epoxy resins seem to be the most profitable materials. At present time there is a huge expansion of microwave electrical devices and telecommunications that produce unwanted electromagnetic signals which can interfere with the electronically controlled devices or can be harmful for the human body [88-90]. For this reason, electromagnetic absorbers present very important group of materials due to ability to eliminate unwanted electromagnetic energy through its redirection. Nanocomposite materials can substitute absorbers based on metallic components and thus reduce the weight of devices what is especially important for the portable communicators etc. [90]. In order to minimize density of absorbers, insulating matrix based on epoxy resins can be replaced with cellular products such as polystyrene foam [91] or polyurethane foam [92]. Incorporation of magnetic particles into the polymeric foam was also found to be interesting for other smart solutions. Vialle et al. [93] proposed material made of shape memory foam where the dispersed particles can serve not only as reinforcement but also for remote activation of shape memory foam. Shape memory foams are smart materials with ability to change the stiffness and recover large strains in response to various stimuli. Incorporation of magnetic particles into the shape memory foam enables its induction activation through

the hysteresis heating of particles instead of the common activation via the conventional heating in the cases when the common thermal activation is complicated due to the temporal limitations of heat transfer from the environment to the sample [93]. This heating mechanism can be seen in Figure 12.

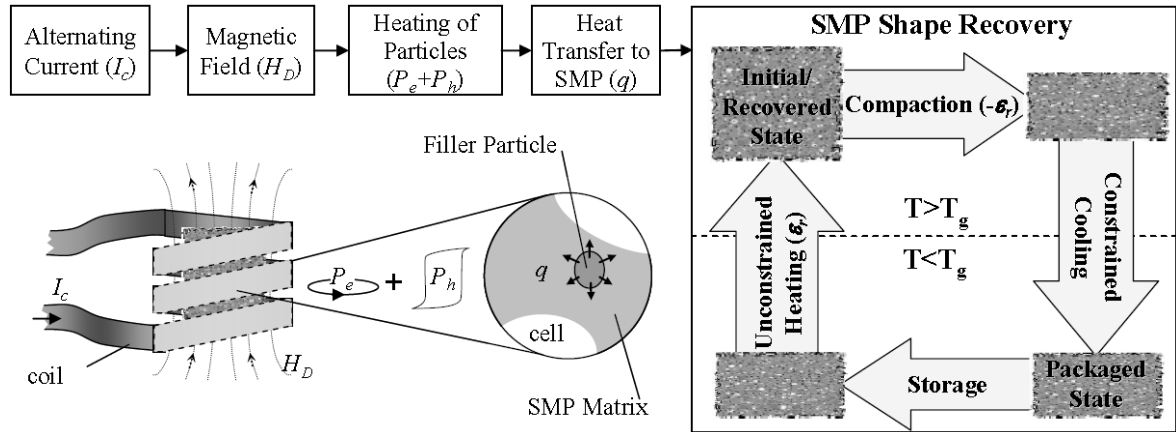


Figure 12. Mechanism of induction activation of shape memory foam with incorporated magnetic particles [93].

3 AIMS OF WORK

The aim of the presented work is to contribute to the field of magnetic nanomaterials, especially in the field of preparation of fillers suitable for composites and magnetorheologic suspensions. For this purpose, four goals were specified according to theoretical and experimental considerations given in the previous chapters:

- preparation of magnetic fillers for magnetorheological suspensions and polymer composites by microwave-assisted techniques,
- elucidation of reaction mechanism that takes place during the solvothermal synthesis of magnetic particles with the help of microwaves,
- tailoring of magnetic properties on the basis of discovered mechanisms,
- demonstration of application potential of prepared fillers in polymer matrix systems and suspensions.

4 METHODOLOGY

4.1 Materials

Ferric chloride hexahydrate $\text{FeCl}_3 \cdot 6\text{H}_2\text{O}$, ferrous sulfate heptahydrate $\text{FeSO}_4 \cdot 7\text{H}_2\text{O}$, ethylene glycol $\text{C}_2\text{H}_6\text{O}_2$, oxalic acid ($\text{H}_2\text{C}_2\text{O}_4$), aqueous ammonia NH_3 (25-27%), ammonium acetate $\text{C}_2\text{H}_3\text{O}_2\text{NH}_4$, ammonium carbonate $(\text{NH}_4)_2\text{CO}_3$ and ammonium bicarbonate $(\text{NH}_4)\text{HCO}_3$ were all supplied by PENTA (Czech Republic) in analytical grade and used without further purification. Distilled and deionized water was used throughout all experiments.

4.2 Synthesis of Magnetic Nanoparticles via the MW-Assisted Solvothermal Technique

Nano- and submicro-sized Fe_3O_4 particles were prepared by a simple solvothermal method in ethylene glycol solution with the help of microwave irradiation. In a standard experiment, 5 mmol of $\text{FeCl}_3 \cdot 6\text{H}_2\text{O}$ (1.352 g) was dissolved in 60 mL of ethylene glycol, followed by the addition of 50 mmol of ammonium acetate - NH_4Ac (3.854 g). This mixture was placed in a 100 mL Teflon reaction vessel (XP-1500 Plus), heated in a pressurized microwave reactor (CEM Mars 5, USA) to the required temperature (200 °C, 210 °C, 220 °C) and maintained at this temperature for 30 minutes. Then, the vessel was cooled to room temperature and black precipitate was collected with the help of permanent magnet. Subsequently, the as-obtained product was washed with distilled water and ethanol for several times and dried naturally on air. Furthermore, in similar experiments, 25 mmol of $(\text{NH}_4)_2\text{CO}_3$ (2.403 g), 50 mmol of NH_4HCO_3 (3.953 g) or 50 mmol of NH_3 in the form of aqueous solution (3.8 mL of 25% water solution) were used as a nucleating agent instead of NH_4Ac . Further experiments involved the addition of 2 to 4 mL of demineralized water to the reaction system while rest of parameters remained unchanged.

4.3 Synthesis of Magnetic Micro-Rods through the Thermal Decomposition of Precursor

4.3.1 MW-Assisted Solvothermal Synthesis of Iron (III) Oxalate Precursor

Organometallic precursor was prepared by a microwave-assisted solvothermal method. Iron (II) sulfate heptahydrate (20 mmol) and oxalic acid dihydrate (20 mmol) were dissolved separately in a mixture of water and ethylene glycol in a ratio of 1:3. Prepared solutions were filtered off and then the solution of oxalic acid was added into the solution of iron (II) sulfate slowly while constantly stirring. As-prepared solution was then transferred into the Teflon liner, sealed and placed into the cavity of a pressurized microwave reactor (CEM Mars 5, USA). The solution was then treated for 30 minutes at 100°C and the obtained yellow precipitate was filtered-off and rinsed with distilled water.

4.3.2 Thermal Decomposition of Oxalate Precursor Using MW Heating

Magnetic needles were prepared by the thermal decomposition of organometallic precursor obtained by the described solvothermal procedure. Small amount (10 mg) of precursor was sealed into the glass tube with the total volume of about 2 mL. Tubes were then placed into the ceramic kiln equipped with the microwave absorbing layer and then kiln was heated in the cavity of common domestic microwave oven (Hyundai, MWM 1417 W) at 750 W for 15 minutes. This setup enables reaching of high temperature in short time and therefore, the decomposition of precursor was complete after 15 minutes. Temperature measured immediately after the decomposition using the contactless pyrometer was found to be of about 450 °C.

4.4 Characterisation

Prepared powder materials were characterized from the point of view of their crystalline structure, particle size, morphology, arrangement into the assemblies, static and dynamic magnetic properties, heating efficiency under the action of an external alternating magnetic field and rheological performance. Methods for the determination of properties of obtained products are listed below:

First of all, macroscopic appearance of prepared powder was observed by naked eye and by digital microscope DVM 2500 (Leica Microsystems, Germany). Scanning electron microscopy was used to investigate the morphology of materials (Vega II/LMU, Tescan, Czech Republic). Due to the small dimensions of product, morphology and particle size were further observed by transmission electron microscopy (JEOL 1200, JEOL). Image analysis was used for estimation of particle size distribution.

X-ray diffraction analysis for the crystalline phase identification of prepared materials was performed on the multi-purpose X-ray diffractometer X'Pert PRO MPD (PANalytical, The Netherlands) with a Cu-K α X-ray source ($\lambda = 1.5418 \text{ \AA}$). Phase composition and size of crystallites were determined according to Rietveld analysis.

Magnetic behaviour of materials under the static and dynamic magnetic field was also studied. The magnetization curves of the samples in the form of powders were measured on a VSM 7407 Vibrating Sample Magnetometer (Lake Shore) at room temperature in air atmosphere. The complex magnetic permeability spectra of materials were studied by the impedance method using an Agilent E4991A Impedance/Material Analyzer in the frequency range from 1 MHz to 3 GHz. The permeability measurements were performed on toroidal samples with an inner diameter of 3.1 mm and an outer diameter of 8 mm. In order to measure the magnetic spectra, magnetic particles were mixed with 10 wt. % of polyvinyl alcohol, dried, and then compressed into toroids at 200 MPa.

The magnetic heating efficiency of prepared materials involved calorimetric determination of specific absorption rate (SAR) was performed with Fe₃O₄ nanoparticles suspended in an aqueous agarose gel (2.5 wt. %). Samples (1.8 mL) in plastic test tubes were placed inside a coil and the temperature vs. time at an exposure to a dynamic magnetic field (field amplitude $H_{\max} = 7.5$ mT and frequency $\nu = 960$ kHz) was recorded. All samples used in the measurement were freshly prepared. The temperature changes were automatically measured by an optical fiber probe (Luxtron STF-2, BFi OPTiLAS SAS, France). Results were corrected for heat losses.

The SAR values for particles dispersed in aqueous suspension can be calculated using following equation [30]:

$$\text{SAR} = \frac{c_p}{m_{\text{Fe}}} \frac{dT}{dt} \quad (18)$$

where c_p is the sample-specific heat capacity under constant pressure ($c_p = 4.18 \text{ Jg}^{-1}\text{K}^{-1}$ for water), m_{Fe} is the iron content per gram of the Fe₃O₄, and dT/dt is the slope of the temperature (from 36 °C to 38 °C) vs. time dependence.

Moreover, magnetic particles in a form of suspension (ferrofluid) were characterized from the point of view of its rheological behaviour with and without the application of an external magnetic field. Steady-shear stress properties under static magnetic field were measured using a rotational rheometer (Physica MCR502, Anton Paar GmbH, Austria) with a Physica MRD 180/1T magnetocell at 37 °C. A parallel-plate measuring system with a diameter of 20 mm and a gap of 0.1 mm was used. True magnetic flux density was measured using a Hall probe and temperature was checked with the help of an inserted thermocouple. Both the Hall probe and the thermocouple were located on the bottom plate. Temperature was set using an Anton Paar circulator Viscotherm VT2 with temperature stability ± 0.02 °C. Maximum magnetic flux density used in all measurements did not exceed 0.3 T to ensure sufficient homogeneity of a magnetic field perpendicular to the shear flow direction. All the steady-shear stress experiments were performed in the shear rate range 0.1-300 s⁻¹.

5 SUMMARY OF RESULTS

On the basis of literature research presented above, there are numerous potential applications of magnetic particles in their separate form, as a magnetic fluid or they can be incorporated into the polymeric matrix. Depending on the expected performance, required properties such as size, purity and magnetic properties can vary with application area.

For this purpose, new microwave-assisted solvothermal synthesis was developed and is described in **Paper I** and **Paper II**. This method combines simplicity and efficiency with possibility to tune the properties of final product through the variation of synthesis parameters. Moreover, mechanisms that take place within the microwave-assisted synthesis were also studied.

Nano- and submicro-sized Fe_3O_4 particles were prepared by a simple solvothermal method in ethylene glycol solution with the help of microwave irradiation. The first step of nucleation starts with the first appearance of heterogeneity in the system. In this case, ammonium nucleating agent is hydrolysed into the ammonia and yields hydroxide anions. Subsequently, precipitation of Fe (III) hydroxide in form of a colloidal solution proceeds and in next step, maghemite can be formed. Similarly, Fe (II) hydroxide can occur in the reaction system due to the presence of mild reductant (in this case ethylene glycol) and enables formation of magnetite. In the second step, freshly formed nanocrystals, which are unstable due to high surface energy, tend to aggregate. The driving force for this aggregation is the pursuit of reducing the surface energy by both an attachment among the primary nanocrystals and their rotation caused by various interactions including Brownian motion or short-range interactions. In case of microwave heating, the solvent at a high temperature (ethylene glycol above 200 °C) becomes less absorbing due to a decrease of the dielectric constant and loss factor; thus, the solvent becomes virtually more transparent for microwaves, which means that the ionic mechanism of the microwave absorption may be prevailing over dipoles. After the solid particles occur in the solution, another mechanism becomes active due to particles' surface polarization that might selectively influence their growth. Moreover, as the heat is generated at the surface of nanoparticles, the local temperature gradient can contribute to the hydroxide-to-oxide transformation. Once the oxide particle reaches the critical size corresponding to the single-domain state, another mechanism of microwaves absorption is assumed to take the main role. Microwave energy is transformed into the heat by magnetic moment rotation and, after some time, in bigger multi-domain particles also by magnetic domain wall motion. This sequence of several mechanisms can explain the sudden formation of particles in the reaction mixture as well as the very short synthesis time.

On the basis of performed experiments, it was found that the composition of reaction mixture, specifically the selection of nucleating agent, plays significant role in the crystalline purity, size and morphology of obtained materials. The influence of various types of nucleation agents added to the reaction mixture is demonstrated in images obtained by Transmission Electron Microscopy (TEM) and can be seen in Figure 13.

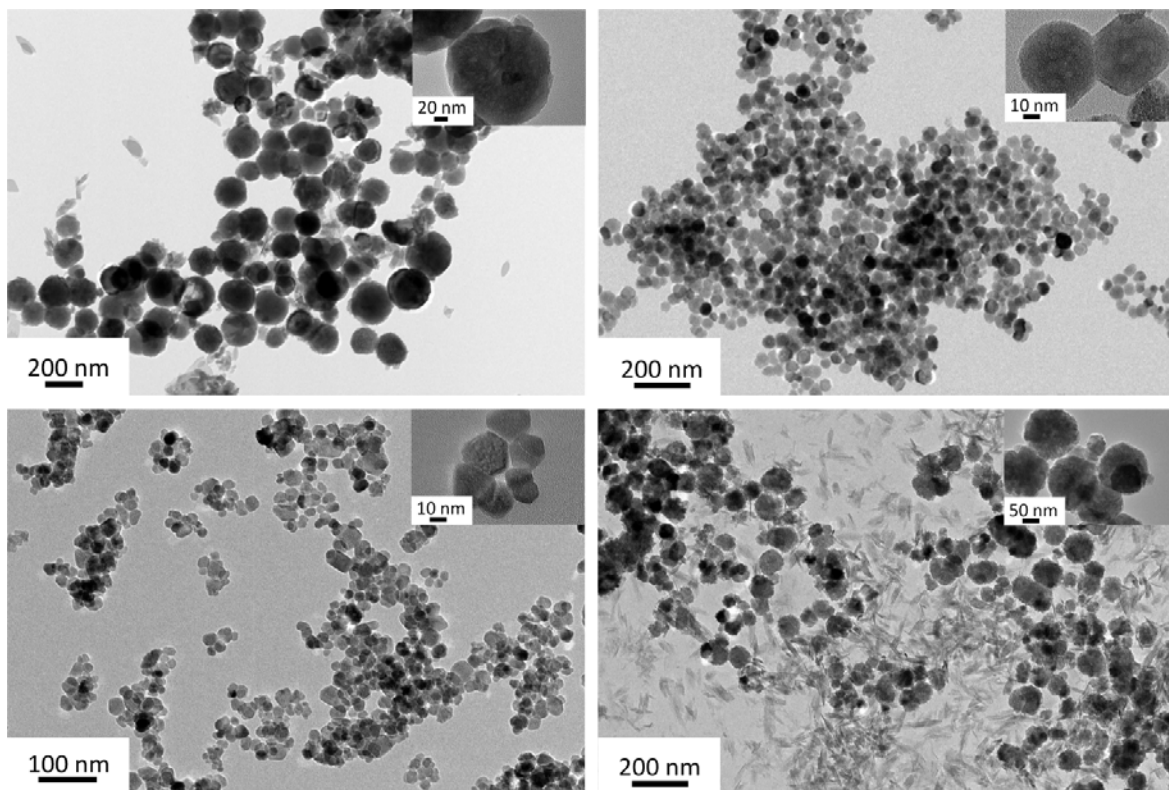


Figure 13. TEM images of materials prepared at 220°C for 30 minutes with $(\text{NH}_4)_2\text{CO}_3$ (a), NH_4HCO_3 (b), aq. NH_3 (c) and NH_4Ac (d).

Due to the possibility to simply vary the properties of prepared materials, their role in the system was studied. On the basis of the reactions that were given in equations (5-7) in this thesis, it is obvious that the selection of the nucleating agent leads to the various amounts of additional water that comes to the reaction system. Cao et al. [35] proposed that if water is present in the reaction system, coordinated ethylene glycol molecules will be substituted by water molecules since the coordination of water molecules with metal ions is stronger than that of ethylene glycol molecules what can significantly affect the morphology of particles. Therefore we performed further experiments which involved the addition of little amount of demineralized water while the rest of parameters remained unchanged. As a consequence, the size of particles is reduced to the one third of the original size what reflects in the significant change of magnetic behaviour and can lead to the formation of single domain magnetic nanoparti-

cles (Figure 14).

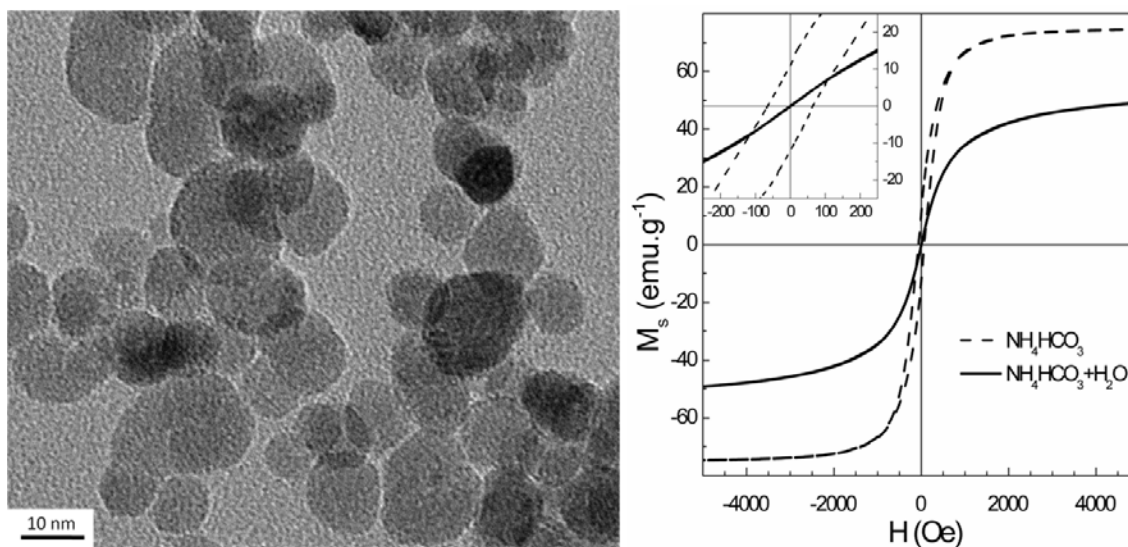


Figure 14. TEM image of material prepared with NH_4HCO_3 with the addition of water (left) and magnetization curves of the same material with and without water addition (right).

Static and dynamic magnetic properties were studied in Paper III. Magneto-static properties of prepared materials were investigated by Vibration Sample Magnetometry (VSM). Differences in the crystalline structure, purity and morphology of studied materials result in different magnetic behaviour of prepared particles. The decrease in the saturation magnetization, especially in the material nucleated by ammonium carbonate, and the atypical shape of the hysteresis loop can be attributed to the defect structure of the particles and the presence of coexisting phases that differ in their magnetic properties. In fact, the XRD analysis revealed, along with the main magnetite phase, the presence of different phases, such as magnetic hematite and nonmagnetic goethite. Figure 15 shows variation of magnetic properties of materials prepared at different temperatures and influence of selected nucleating agents.

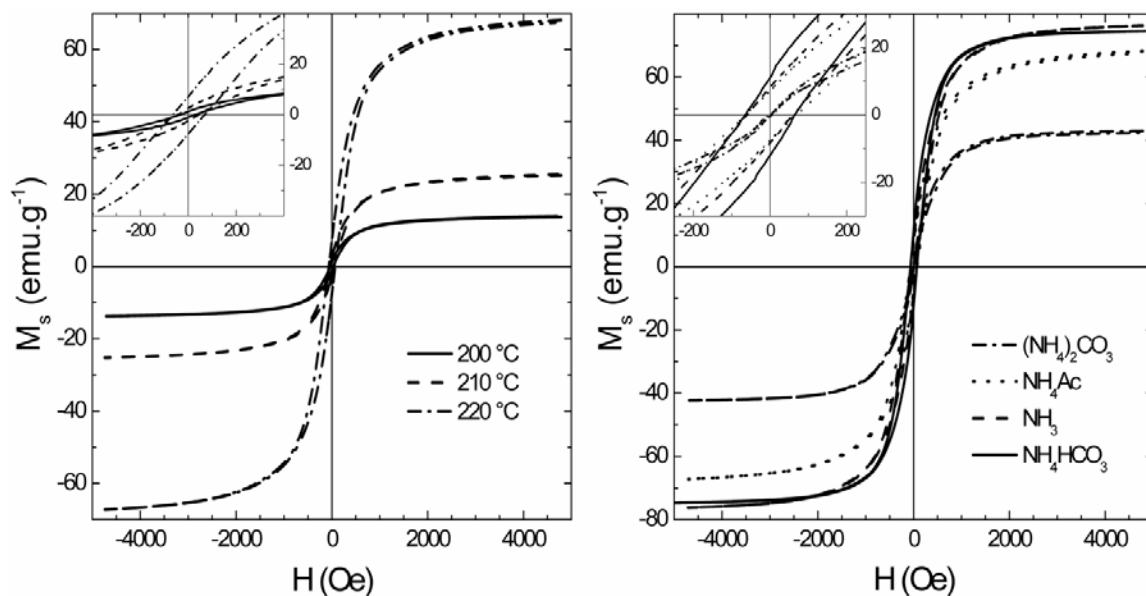


Figure 15. Magnetization curves of materials prepared with NH_4Ac at various temperatures for 30 minutes (left) and at 220°C for 30 minutes with various nucleating agents (right).

Dynamic magnetic properties allow better understanding of the magnetization mechanisms in magnetic nanostructures and are useful as a source of frequency dependent characteristics which are important for potential application in the high frequency range. The complex magnetic permeability spectra of materials were studied by the impedance method using an Agilent E4991A Impedance/Material Analyzer in the frequency range from 1 MHz to 3 GHz. Figure 16 shows the frequency dependence of the complex permeability μ^* (magnetic spectra) for all materials. The complex permeability dispersion of ammonium bicarbonate and ammonium carbonate nucleated samples occupies a frequency interval from 300 MHz to 3 GHz, whereas a sample nucleated by ammonium bicarbonate with additional amount of demineralized water is characterized by a much broader frequency region of dispersion, from 10 MHz to 3 GHz. Moreover, the magnetic spectrum of ammonium carbonate nucleated sample has two regions of complex permeability dispersion with resonance frequencies at 400 MHz and 1.5 GHz. This fact confirms the presence of different coexisting magnetic phases in this sample, which was revealed by XRD measurements.

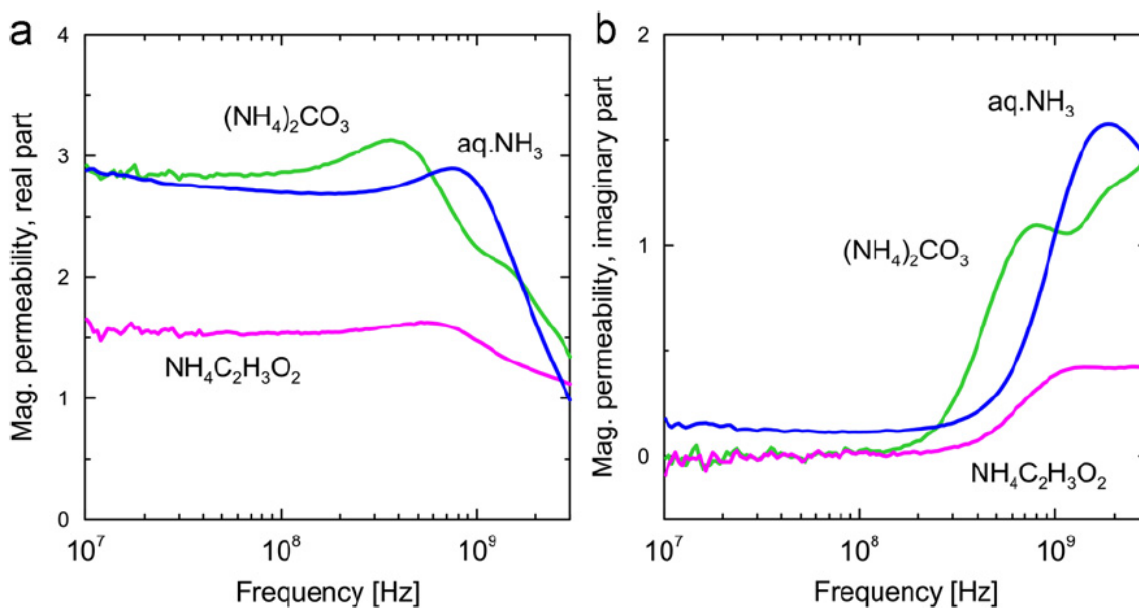


Figure 16. Magnetic spectra of prepared materials: real part of complex magnetic permeability (a) and imaginary part (b).

As it was written in previous chapters, magnetic particles provide possibility to treat the cancer through the destruction of tumorous cells via their incorporation into the affected tissue and their subsequent induction heating (magnetic hyperthermia). The ability to generate heat induced by external alternating magnetic field is dependent on the field amplitude and frequency, concentration of particles and their magnetic properties and was the aim of a study in the **Paper IV**. Main heating mechanisms involve hysteresis losses and relaxation processes, i.e. Neel relaxation and Brownian rotation. Hysteresis losses are determined by magnetic anisotropy. Magnetic anisotropy energy of a nanosized particle is proportional, in first approximation, to the particle volume due to the magnetocrystalline and shape as well as strain induced anisotropy (magnetoelastic anisotropy). The heat generation via the various nucleated Fe_3O_4 particles prepared by the microwave-assisted solvothermal method described above and suspended in agarose gel in terms of the time-dependent temperature curves in the applied AC magnetic field is shown in Figure 17. As can be seen, inductive heating experiments reveal that given magnetic field is able to produce enough energy for temperature increase of the system to 43 °C in time interval 1-10 min for all samples.

The SAR values at 37 °C (the body temperature, which is of primary interest for hyperthermia experiments) for studied systems with variously nucleated Fe_3O_4 nanoparticles are shown in Figure 17 as well. As can be seen, the highest SAR ($\sim 9 \text{ W/g}_{(\text{Fe})}$) was measured for ammonium hydroxide nucleated Fe_3O_4 nano-

particles while for other nucleating agents these values were found to be significantly lower. Based on the structural and magnetic properties, we can assume that the higher value of SAR for aqueous ammonia nucleated Fe_3O_4 nanoparticles is caused by small particle size and narrow particle size distribution. In such a case the prevailing mechanism of heating in AC magnetic field is Neel relaxation. Therefore, the obtained value of SAR can predestine the Fe_3O_4 nanoparticles prepared via the microwave irradiation-assisted solvothermal method to applications such as heating agents in magnetic hyperthermia.

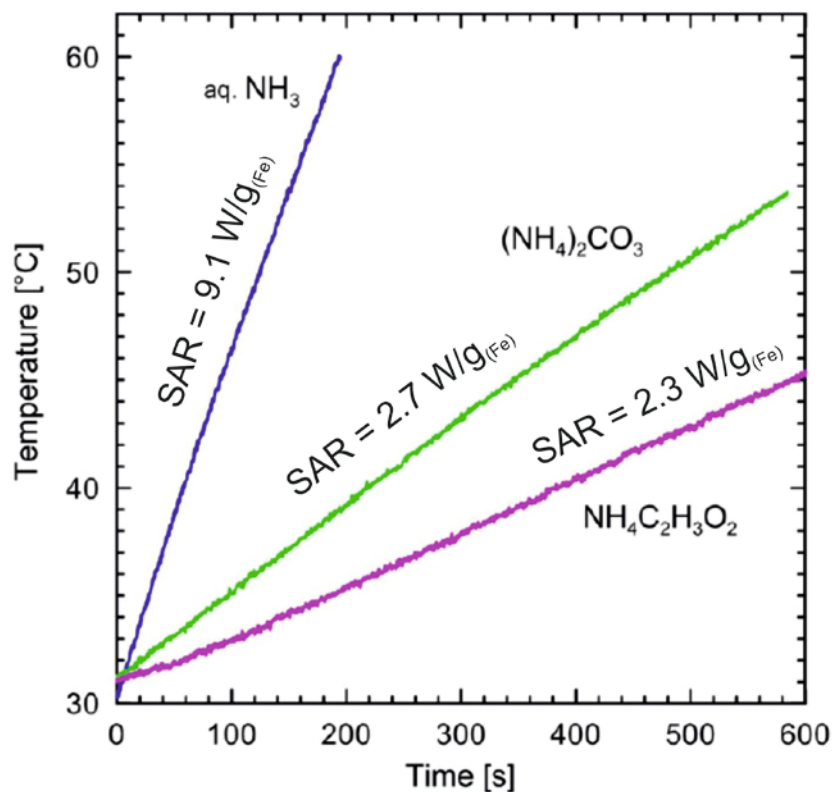


Figure 17. Temperature increase triggered by Fe_3O_4 nanoparticles suspended in agarose gel measured at 960 kHz and magnetic field amplitude H_{max} 7.5 mT.

Other approaches of cancer therapy using magnetic nanoparticles include reducing blood circulation in the tumour area by clogging up blood vessels, which are feeding the tumour, with ferrofluid under an applied magnetic field. The efficiency of this method is based on impairing angiogenesis, i.e., formation of new blood vessels that supply oxygen and nutrients to cancerous tissues. Ferrofluid becomes "solid-like", its viscosity increases by several orders of magnitude when exposed to an external magnetic field, as magnetized particles are aligned into chain-like structures.

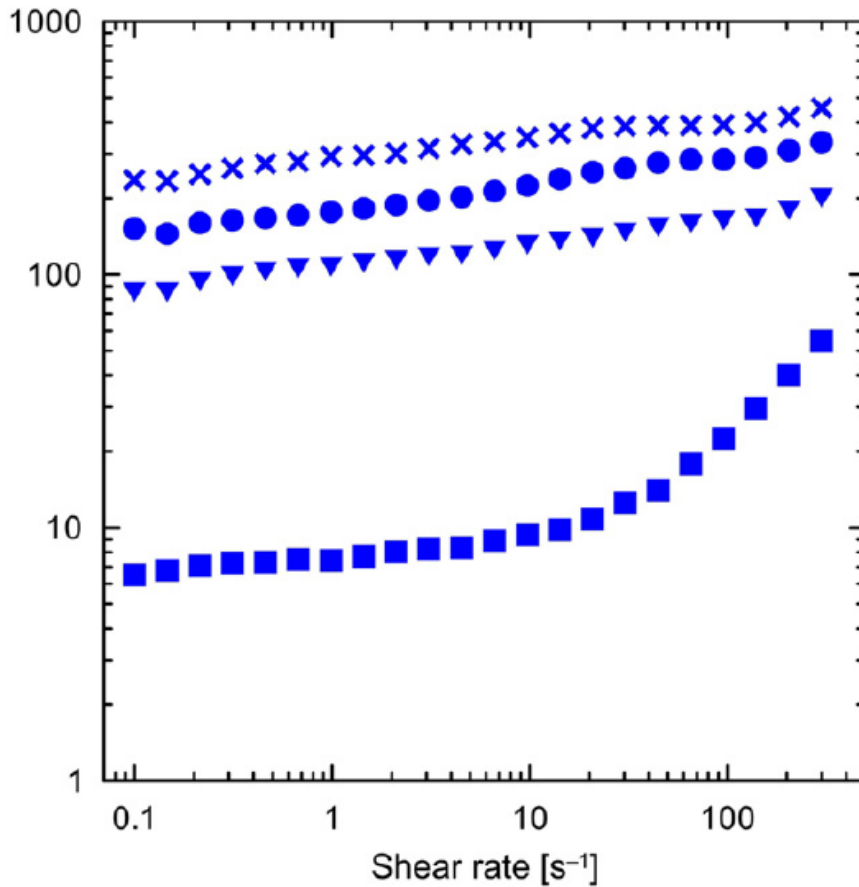


Figure 18. Flow curves of 15 wt% suspension of Fe_3O_4 nanoparticles in silicone oil under various magnetic field strengths; B (mT): squares 0, triangles 82, circles 168 and crosses 253.

On the bases of measurement of magnetic properties via the VSM, ammonia nucleated Fe_3O_4 nanoparticles based ferrofluid was chosen for the evaluation of internal structure formation. Flow curves of shear stress as a function of shear rate for 15 wt. % of ferrofluid based Fe_3O_4 suspension in silicone oil under various magnetic flux densities (B) are shown in Figure 18. The pseudoplastic behaviour in the absence of magnetic field at low shear rates can be attributed to strong interaction between Fe_3O_4 nanoparticles with large specific surface and silicone oil. When a magnetic field is applied to the ferrofluid, the shear stress increases abruptly with magnetic field strength, showing characteristic yield behaviour of a Bingham fluid. This dramatic change in rheological properties (yield stress, representing maximum seal pressure, increases by two orders in magnitude under application of magnetic field) is related to the formation of chain-like structures Fe_3O_4 suspension. In external magnetic field the magnetized Fe_3O_4 nanoparticles attract each other due to magnetic dipole-dipole inter-

actions, forming chains of particles oriented along the field direction. Increase in B induces a higher dipole moment and the particular microstructures become stiffer.

In recent years, preparation of iron oxide one-dimensional nano- and submicro-structures gets great attention due to their unique properties resulting from the shape anisotropy. As it was already shown in previous results, developed microwave-assisted solvothermal syntheses usually led to the particles with polyhedral shape or to the formation of their spherical assemblies. Template assisted synthesis offer the possibility to tailor the shape of particles. For this purpose, methods that utilize organometallic precursor that decompose at relatively low temperature appear to be the most suitable. "Precursor syntheses" are interesting from technological point of view since these methods are simple, low cost, and effective and enable large-scale production. In order to achieve uniform elongated particles with high aspect ratio in short synthesis time we developed microwave-assisted procedure that involves two steps: preparation of precursor and its conversion into the desired product. This procedure is described in **Paper V**. We chose ferric oxalate as a precursor due to its preferred growth in one dimension at proper conditions thus forming rod-like structures. Conversion of precursor into the final product is topotactic reaction thus the forming particles preserve the shape given by the precursor [1]. Ferrous oxalate was prepared from ferrous sulphate heptahydrate in a mixture of water and ethylene glycol via the solvothermal method using the microwave pressurized reactor. The second step involves thermal decomposition of the precursor in common domestic microwave oven using special ceramic kiln accompanied with the internal absorbing layer which is able to be heated in microwaves to the high temperatures in short time and thus allow rapid formation of the required product. Prepared particles are based on magnetite/maghemite, possess needle-like shape and exhibit soft ferromagnetic behaviour. Material prepared by this method can be seen in the SEM image shown in Figure 19 (a) and its magnetic behaviour is demonstrated by the magnetization curve given in Figure 19 (b). Due to the topotactic character of the decomposition process, the shape of the converted product remains preserved. The length of about 20 μm and diameter less than 1 μm gives to the product uniquely high aspect ratio. Obtained magnetization-demagnetization curves show that the prepared iron oxide particles possess ferromagnetic behaviour with the saturation magnetization (M_S) of about 43 emu.g^{-1} and coercivity 124 Oe. XRD-analysis revealed the crystallite size about 40 nm which is in accord with observed magnetic behaviour of the material. The needle-like particles keep the characteristic features of their 40 nm sized nanoparticulate building blocks although we have not TEM images yet.

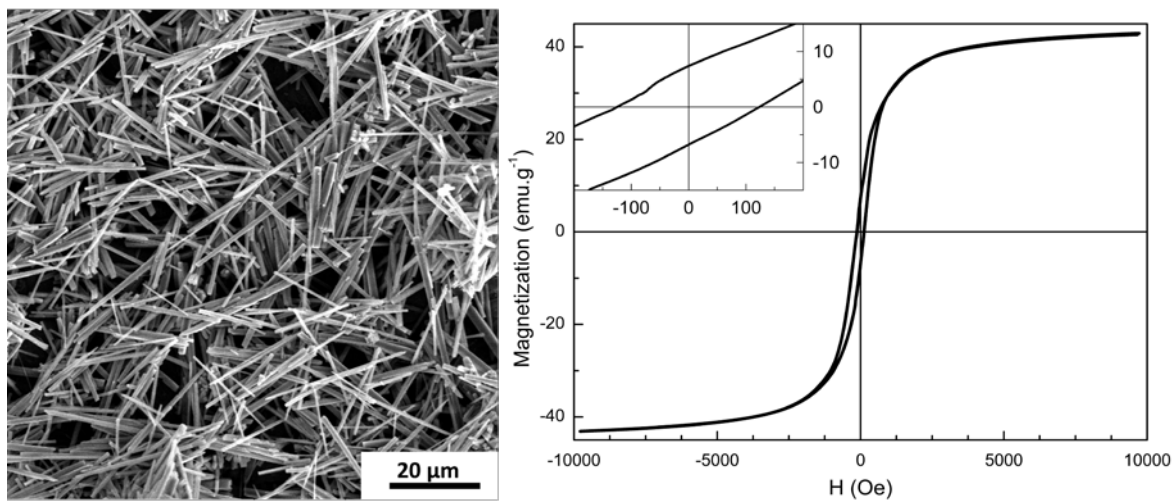


Figure 19. SEM image of prepared magnetite/maghemite needle-like particles (a) and their magnetic behaviour described by magnetization curve (b).

6 CLOSING REMARKS

6.1 Conclusions and Contribution to Science and Technology

The thesis contributes to the general knowledge as well as to technology according to the goals as follows:

- Two novel microwave-assisted techniques were proposed
- Properties of prepared materials were studied from the point of view of their crystalline structure, particle size and morphology and magnetic properties
- Reaction mechanism within the microwave-assisted synthesis was described
- The properties of magnetic particles were tailored according to the discovered mechanism
- Application potential of prepared materials was demonstrated

Imparting the understanding of the reaction and crystal growth mechanisms and further development of the microwave assisted solvothermal methods of magnetic particles synthesis will contribute to the environmental sustainability due to the enormous decrease of the synthesis time, energy and possibly material savings as well as it will conduce to the development of high performance functional materials as demonstrated in enclosed papers.

6.2 Future Prospective

Low-cost and low-toxicity of used chemicals, simplicity, rapidity and efficiency of presented microwave-assisted techniques together with the possibility to influence the properties of magnetic nanoparticles points to the usefulness of this work not only for laboratory use, but also for commercial purposes. Application potential of prepared products is broad, from biomedical uses such as hyperthermia treatment of cancer or controlled delivery of drugs, through the utilization in a form of magnetic fluids for mechanical damping, to the preparation of composite systems for microwave shielding.

REFERENCES

- [1] CAO, G. *Nanostructures & Nanomaterials: Synthesis, Properties & Applications.* London: Imperial College Press, UK, 2004. ISBN 978-981-4322-50-8.
- [2] KOLEV, S.; KOUTZAROVE, T.; YANEV, A. et al. Microwave properties of polymer composites containing combinations of micro- and nano-sized magnetic fillers. *Journal of Nanoscience and Nanotechnology*, 2008, vol. 8, no. 2, p. 650-654. ISSN 1533-4880.
- [3] Y KOSEGLU, Y.; KAVAS, H.; AKTAS, B. Surface effects on magnetic properties of superparamagnetic magnetite nanoparticles. *Physica Status Solidi a-Applications and Materials Science*, 2006, vol. 203, no. 7, p. 1595-1601. ISSN 0031-8965.
- [4] KOZAKOVA, Z.; KURITKA, I.; BABAYAN, V. et al. Magnetic Iron Oxide Nanoparticles for High Frequency Applications. *IEEE Transactions on Magnetics*, 2013, vol. 49, no. 3, p. 995-999. ISSN 0018-9464.
- [5] NUTZENADEL, C.; ZUTTELL, A.; CHARTOUNI, D. et al. Critical size and surface effect of the hydrogen interaction of palladium clusters. *European Physical Journal D*, 2000, vol. 8, no. 2, p. 245-250. ISSN 1434-6060.
- [6] VOLLATH, D. *Nanomaterials : an introduction to synthesis, properties and application.* Weinheim: Wiley-VCH; [Chichester : John Wiley, distributor], 2008. ISBN 9783527315314.
- [7] R. M. CORNELL; R. M., U. SCHVERTMANN, U. *The Iron Oxides: Structure, Properties, Reactions, Occurrences and Uses.* Weinheim: Wiley-VCH; [Chichester: John Wiley, distributor], 2000. ISBN 9783527302741.
- [8] BERGER, P.; ADELMAN, N. B.; BECKMAN, K. J. et al. Preparation and properties of an aqueous ferrofluid. *Journal of Chemical Education*, 1999, vol. 76, no. 7, p. 943-948. ISSN 0021-9584.
- [9] HORAK, D.; BABIC, M.; MACKOVA, H. et al. Preparation and properties of magnetic nano- and micro-sized particles for biological and environmental separations. *Journal of Separation Science*, 2007, vol. 30, no. 11, p. 1751-1772. ISSN 1615-9306.
- [10] LESLIE-PELECKY, D. L.; RIEKE, R. D. Magnetic properties of nanostructured materials. *Chemistry of Materials*, 1996, vol. 8, no. 8, p. 1770-1783. ISSN 0897-4756.
- [11] GUIMARÃES, A. P. *Principles of Nanomagnetism.* Berlin: Springer, 2009. ISBN 978-3-642-01481-9.
- [12] JEONG, U.; TENG, X. W.; WANG, Y. et al. Superparamagnetic colloids: Controlled synthesis and niche applications. *Advanced Materials*, 2007, vol. 19, no. 1, p. 33-60. ISSN 0935-9648.
- [13] SKOMSKI, R. Nanomagnetism. *Journal of Physics-Condensed Matter*,

- 2003, vol. 15, no. 20, p. R841-R896. ISSN 0953-8984. [14] RUSSO, P.; ACIERNO, D.; PALOMBA, M. et al. Ultrafine magnetite nanopowder: Synthesis, characterization, and preliminary use as filler of polymethylmethacrylate nanocomposites. *Journal of Nanotechnology*, 2012. ISSN 1687-9503.
- [15] BIROL, H.; RAMBO, C. R.; GUIOTOKU, M. et al. Preparation of ceramic nanoparticles via cellulose-assisted glycine nitrate process: a review. *Rsc Advances*, 2013, vol. 3, no. 9, p. 2873-2884. ISSN 2046-2069.
- [16] SCHUBERT, U., HÜSING, N. *Synthesis of Inorganic Materials*. Weinheim: Wiley-VCH; [Chichester : John Wiley, distributor], 2000. ISBN 978-3-527-32714-0. .
- [17] CHIN, A. B.; YAACOB, II. Synthesis and characterization of magnetic iron oxide nanoparticles via w/o microemulsion and Massart's procedure. *Journal of Materials Processing Technology*, 2007, vol. 191, no. 1-3, p. 235-237. ISSN 0924-0136.
- [18] ALBORNOZ, C.; JACOBO, S. E. Preparation of a biocompatible magnetic film from an aqueous ferrofluid. *Journal of Magnetism and Magnetic Materials*, 2006, vol. 305, no. 1, p. 12-15. ISSN 0304-8853.
- [19] KIM, E. H.; LEE, H. S.; KWAK, B. K. et al. Synthesis of ferrofluid with magnetic nanoparticles by sonochemical method for MRI contrast agent. *Journal of Magnetism and Magnetic Materials*, 2005, vol. 289, p. 328-330. ISSN 0304-8853.
- [20] WAN, J. X.; CHEN, X. Y.; WANG, Z. H. et al. A soft-template-assisted hydrothermal approach to single-crystal Fe₃O₄ nanorods. *Journal of Crystal Growth*, 2005, vol. 276, no. 3-4, p. 571-576. ISSN 0022-0248.
- [21] KOZAKOVA, Z.; BAZANT, P.; MACHOVSKY, M. et al. Fast Microwave-Assisted Synthesis of Uniform Magnetic Nanoparticles. *Acta Physica Polonica A*, 2010, vol. 118, no. 5, p. 948-949. ISSN 0587-4246
- [22] SALAZAR-ALVAREZ, G.; MUHAMMED, M.; ZAGORODNI, A. A. Novel flow injection synthesis of iron oxide nanoparticles with narrow size distribution. *Chemical Engineering Science*, 2006, vol. 61, no. 14, p. 4625-4633. ISSN 0009-2509.
- [23] BASAK, S.; CHEN, D. R.; BISWAS, P. Electro spray of ionic precursor solutions to synthesize iron oxide nanoparticles: Modified scaling law. *Chemical Engineering Science*, 2007, vol. 62, no. 4, p. 1263-1268. ISSN 0009-2509.
- [24] LAURENT, S.; FORGE, D.; PORT, M. et al. Magnetic iron oxide nanoparticles: Synthesis, stabilization, vectorization, physicochemical characterizations, and biological applications. *Chemical Reviews*, 2008, vol. 108, no. 6, p. 2064-2110. ISSN 0009-2665.

- [25] JOLIVET, J. P.; CHANEAC, C.; TRONC, E. Iron oxide chemistry. From molecular clusters to extended solid networks. *Chemical Communications*, 2004, no. 5, p. 481-487. ISSN 1359-7345.
- [26] BURTON, B.; KIKUCHI, R. THE ANTIFERROMAGNETIC-PARAMAGNETIC TRANSITION IN ALPHA- Fe_2O_3 IN THE SINGLE PRISM APPROXIMATION OF THE CLUSTER VARIATION METHOD. *Physics and Chemistry of Minerals*, 1984, vol. 11, no. 3, p. 125-131. ISSN 0342-1791.
- [27] HU, P.; YU, L. J.; ZUO, A. H. et al. Fabrication of Monodisperse Magnetite Hollow Spheres. *Journal of Physical Chemistry C*, 2009, vol. 113, no. 3, p. 900-906. ISSN 1932-7447.
- [28] CHEN, X. Y.; ZHANG, Z. J.; LI, X. X. et al. Hollow magnetite spheres: Synthesis, characterization, and magnetic properties. *Chemical Physics Letters*, 2006, vol. 422, no. 1-3, p. 294-298. ISSN 0009-2614.
- [29] ZHU, L. P.; XIAO, H. M.; ZHANG, W. D. et al. One-pot template-free synthesis of monodisperse and single-crystal magnetite hollow spheres by a simple solvothermal route. *Crystal Growth & Design*, 2008, vol. 8, no. 3, p. 957-963. ISSN 1528-7483.
- [30] LOUPY, A. *Microwaves in Organic Synthesis*. Weinheim: Wiley-VCH; [Chichester: John Wiley, distributor], 2002. ISBN 3-527-31452-0.
- [31] GERBEC, J. A.; MAGANA, D.; WASHINGTON, A. et al. Microwave-enhanced reaction rates for nanoparticle synthesis. *Journal of the American Chemical Society*, 2005, vol. 127, no. 45, p. 15791-15800. ISSN 0002-7863.
- [32] SKRABALAK, S. E.; WILEY, B. J.; KIM, M. et al. On the polyol synthesis of silver nanostructures: Glycolaldehyde as a reducing agent. *Nano Letters*, 2008, vol. 8, no. 7, p. 2077-2081. ISSN 1530-6984.
- [33] SMITH, W. B. Ethylene glycol to acetaldehyde-dehydration or a concerted mechanism. *Tetrahedron*, 2002, vol. 58, no. 11, p. 2091-2094. ISSN 0040-4020.
- [34] XUAN, S. H.; WANG, Y. X. J.; YU, J. C. et al. Tuning the Grain Size and Particle Size of Superparamagnetic Fe_3O_4 Microparticles. *Chemistry of Materials*, 2009, vol. 21, no. 21, p. 5079-5087. ISSN 0897-4756.
- [35] CAO, S. W.; ZHU, Y. J.; CHANG, J. Fe_3O_4 polyhedral nanoparticles with a high magnetization synthesized in mixed solvent ethylene glycol-water system. *New Journal of Chemistry*, 2008, vol. 32, no. 9, p. 1526-1530. ISSN 1144-0546.
- [36] SHI, S.; HWANG, J. Y. Microwave-assisted wet chemical synthesis: advantages, significance, and steps to industrialization. *Journal of Minerals & Materials Characterization & Engineering*, 2003, vol. 2, p. 101-110. ISSN 2327-4077.

- [37] TSUJI, M.; HASHIMOTO, M.; NISHIZAWA, Y. et al. Microwave-assisted synthesis of metallic nanostructures in solution. *Chemistry-a European Journal*, 2005, vol. 11, no. 2, p. 440-452. ISSN 0947-6539.
- [38] BOGDAL, D.; PROCIAK, A. *Microwave-Enhanced Polymer Chemistry and Technology*. 2008. 1-275 p. Microwave-Enhanced Polymer Chemistry and Technology. ISBN 978-0-8138-2537-3.
- [39] KAPPE, C.O.; DALLINGER, D.; MURPHREE, S. *Practical Microwave Synthesis for Organic Chemists - Strategies, Instruments, and Protocols*. Weinheim: Wiley-VCH; [Chichester: John Wiley, distributor], 2009. ISBN 978-3-527-32097-4.
- [40] LEADBEATER, N. E. *Microwave Heating as a Tool for Sustainable Chemistry*. Boca Raton: CRC Press, 2012. ISBN 9781439812693.
- [41] Available from:
http://www.pueschner.com/basics/phys_basics_en.php
- [42] ZHOU, W. W.; TANG, K. B.; ZENG, S. A. et al. Room temperature synthesis of rod-like FeC₂O₄ center dot 2H₂O and its transition to maghemite, magnetite and hematite nanorods through controlled thermal decomposition. *Nanotechnology*, 2008, vol. 19, no. 6. ISSN 0957-4484.
- [43] CHEN, X. Y.; ZHANG, Z. J.; LI, X. X. et al. Hollow magnetite spheres: Synthesis, characterization, and magnetic properties. *Chemical Physics Letters*, 2006, vol. 422, no. 1-3, p. 294-298. ISSN 0009-2614.
- [44] JIA, Z. G.; REN, D. P.; XU, L. X. et al. Preparation, characterization and photocatalytic activity of porous zinc oxide superstructure. *Materials Science in Semiconductor Processing*, 2012, vol. 15, no. 3, p. 270-276. ISSN 1369-8001.
- [45] HERMANEK, M.; ZBORIL, R. Polymorphous Exhibitions of Iron(III) Oxide during Isothermal Oxidative Decompositions of Iron Salts: A Key Role of the Powder Layer Thickness. *Chemistry of Materials*, 2008, vol. 20, no. 16, p. 5284-5295. ISSN 0897-4756.
- [46] BARINOVA, T. V.; BOROVINSKAYA, I. P.; IGNATE'VA, T.I. et al. Combustion Synthesis of Nanosized Iron Oxides: The Effect of Precursor Composition. *International Journal of Self-Propagating High-Temperature Synthesis*, 2010, vol. 19, no. 4, p. 276-280. ISSN 1061-3862.
- [47] BARINOVA, T. V.; BOROVINSKAYA, I. P. Solution-combustion synthesis of nanosized iron oxide from ferric oxalate. *International Journal of Self-Propagating High-Temperature Synthesis*, 2012, vol. 21, no. 1, p. 1-6. ISSN 1061-3862.
- [48] JIA, Z. G.; REN, D. P.; XU, L. X. Generalized preparation of metal oxalate nano/submicro-rods by facile solvothermal method and their calcined products. *Materials Letters*, 2012, vol. 76, p. 194-197. ISSN 0167-

577X.

[49] GUO, L. M.; ARAFUNE, H.; TERAMAE, N. Synthesis of Mesoporous Metal Oxide by the Thermal Decomposition of Oxalate Precursor. *Langmuir*, 2013, vol. 29, no. 13, p. 4404-4412. ISSN 0743-7463.

[50] HERMANKOVA, P.; HERMANEK, M.; ZBORIL, R. Thermal Decomposition of Ferric Oxalate Tetrahydrate in Oxidative and Inert Atmospheres: The Role of Ferrous Oxalate as an Intermediate. *European Journal of Inorganic Chemistry*, 2010, no. 7, p. 1110-1118. ISSN 1434-1948.

[51] PANKHURST, Q. A.; CONNOLLY, J.; JONES, S. K. et al. Applications of magnetic nanoparticles in biomedicine. *Journal of Physics D-Applied Physics*, 2003, vol. 36, no. 13, p. R167-R181. ISSN 0022-3727.

[52] KULARATNE, B. Y.; LORIGAN, P.; BROWNE, S. et al. Monitoring tumour cells in the peripheral blood of small cell lung cancer patients. *Cytometry*, 2002, vol. 50, no. 3, p. 160-167. ISSN 0196-4763.

[53] MORISADA, S.; MIYATA, N.; IWAHORI, K. Immunomagnetic separation of scum-forming bacteria using polyclonal antibody that recognizes mycolic acids. *Journal of Microbiological Methods*, 2002, vol. 51, no. 2, p. 141-148. ISSN 0167-7012.

[54] ZIGEUNER, R. E.; RIESENBERG, R.; POHLA, H. et al. Isolation of circulating cancer cells from whole blood by immunomagnetic cell enrichment and unenriched immunocytochemistry in vitro. *Journal of Urology*, 2003, vol. 169, no. 2, p. 701-705. ISSN 0022-5347.

[55] LIBERTI, P. A.; RAO, C. G.; TERSTAPPEN, L. Optimization of ferrofluids and protocols for the enrichment of breast tumor cells in blood. *Journal of Magnetism and Magnetic Materials*, 2001, vol. 225, no. 1-2, p. 301-307. ISSN 0304-8853

[56] KHANDHAR, A. P.; FERGUSON, R. M.; ARAMI, H. et al. Monodisperse magnetite nanoparticle tracers for in vivo magnetic particle imaging. *Biomaterials*, 2013, vol. 34, no. 15, p. 3837-3845. ISSN 0142-9612.

[57] BORGERT, J.; SCHMIDT, J. D.; SCHMALE, I. et al. Fundamentals and applications of magnetic particle imaging. *Journal of Cardiovascular Computed Tomography*, 2012, vol. 6, no. 3, p. 149-153. ISSN 1934-5925.

[58] DOBSON, J. Magnetic nanoparticles for drug delivery. *Drug Development Research*, 2006, vol. 67, no. 1, p. 55-60. ISSN 0272-4391.

[59] LIU, J. F.; ZHAO, Z. S.; JIANG, G. B. Coating Fe₃O₄ magnetic nanoparticles with humic acid for high efficient removal of heavy metals in water. *Environmental Science & Technology*, 2008, vol. 42, no. 18, p. 6949-6954. ISSN 0013-936X.

[60] YANTASEE, W.; WARNER, C. L.; SANGVANICH, T. et al. Removal of heavy metals from aqueous systems with thiol functionalized superpara-

- magnetic nanoparticles. *Environmental Science & Technology*, 2007, vol. 41, no. 14, p. 5114-5119. ISSN 0013-936X.
- [61] CUI, B.; PENG, H. X.; XIA, H. Q. et al. Magnetically recoverable core-shell nanocomposites $\gamma\text{-Fe}_2\text{O}_3@\text{SiO}_2@\text{TiO}_2\text{-Ag}$ with enhanced photocatalytic activity and antibacterial activity. *Separation and Purification Technology*, 2013, vol. 103, p. 251-257. ISSN 1383-5866.
- [62] CARLSON, J. D.; JOLLY, M. R. MR fluid, foam and elastomer devices. *Mechatronics*, 2000, vol. 10, no. 4-5, p. 555-569. ISSN 0957-4158.
- [63] JOLLY, M. R.; BENDER, J. W.; CARLSON, J. D. Properties and applications of commercial magnetorheological fluids. *Journal of Intelligent Material Systems and Structures*, 1999, vol. 10, no. 1, p. 5-13. ISSN 1045-389X.
- [64] STANWAY, R. Smart fluids: current and future developments. *Materials Science and Technology*, 2004, vol. 20, no. 8, p. 931-939. ISSN 0267-0836.
- [65] PARK, B. J.; FANG, F. F.; CHOI, H. J. Magnetorheology: materials and application. *Soft Matter*, 2010, vol. 6, no. 21, p. 5246-5253. ISSN 1744-683X.
- [66] CHEN, X. L.; LV, H. Y.; YE, M. et al. Novel superparamagnetic iron oxide nanoparticles for tumor embolization application: Preparation, characterization and double targeting. *International Journal of Pharmaceutics*, 2012, vol. 426, no. 1-2, p. 248-255. ISSN 0378-5173.
- [67] SEDLACIK, M.; MOUCKA, R.; KOZAKOVA, Z. et al. Correlation of structural and magnetic properties of Fe_3O_4 nanoparticles with their calorimetric and magnetorheological performance. *Journal of Magnetism and Magnetic Materials*, 2013, vol. 326, p. 7-13. ISSN 0304-8853.
- [68] BEKOVIC, M.; HAMLER, A. Determination of the Heating Effect of Magnetic Fluid in Alternating Magnetic Field. *Ieee Transactions on Magnetics*, 2010, vol. 46, no. 2, p. 552-555. ISSN 0018-9464.
- [69] KAR, R.; MISRA, A. Increase in temperature of a ferromagnetic substance in rf magnetic field. *Journal of Magnetism and Magnetic Materials*, 2010, vol. 322, no. 6, p. 671-674. ISSN 0304-8853.
- [70] MULLER, S. Magnetic fluid hyperthermia therapy for malignant brain tumors-an ethical discussion. *Nanomedicine-Nanotechnology Biology and Medicine*, 2009, vol. 5, no. 4, p. 387-393. ISSN 1549-9634.
- [71] WANG, X. F.; TANG, J. T.; SHI, L. Q. Induction Heating of Magnetic Fluids for Hyperthermia Treatment. *Ieee Transactions on Magnetics*, 2010, vol. 46, no. 4, p. 1043-1051. ISSN 0018-9464.
- [72] LAHONIAN, M. *Diffusion of Magnetic Nanoparticles within a Biological Tissue during Magnetic Fluid Hyperthermia*. Hyperthermia, 2013. 978-

- 953-51-1129-0. InTech, DOI: 10.5772/52305. Available from: <http://www.intechopen.com/books/hyperthermia/diffusion-of-magnetic-nanoparticles-within-a-biological-tissue-during-magnetic-fluid-hyperthermia>
- [73] HAN, Y.; HONG, W.; FAIDLEY, L. A. E. Field-stiffening effect of magneto-rheological elastomers. *International Journal of Solids and Structures*, 2013, vol. 50, no. 14-15, p. 2281-2288. ISSN 0020-7683.
- [74] HAN, Y.; ZHANG, Z. H.; FAIDLEY, L. E. et al. Microstructure-based modeling of magneto-rheological elastomers. In Goulbourne, N. C. et al. *Behavior and Mechanics of Multifunctional Materials and Composites 2012*. 2012. vol. 8342, p. ISBN 0277-786X 978-0-8194-8999-9.
- [75] JESTIN, J.; COUSIN, F.; DUBOIS, I. et al. Anisotropic reinforcement of nanocomposites tuned by magnetic orientation of the filler network. *Advanced Materials*, 2008, vol. 20, no. 13, p. 2533-+. ISSN 0935-9648.
- [76] TJONG, S. C. Structural and mechanical properties of polymer nanocomposites. *Materials Science & Engineering R-Reports*, 2006, vol. 53, no. 3-4, p. 73-197. ISSN 0927-796X.
- [77] LIU, T. Y.; HU, S. H.; LIU, D. M. et al. Magnetic-sensitive behavior of intelligent ferrogels for controlled release of drug. *Langmuir*, 2006, vol. 22, no. 14, p. 5974-5978. ISSN 0743-7463.
- [78] VARGA, Z.; FILIPCSEI, G.; ZRINYI, M. Magnetic field sensitive functional elastomers with tuneable elastic modulus. *Polymer*, 2006, vol. 47, no. 1, p. 227-233. ISSN 0032-3861.
- [79] GELIR, A.; ALVEROGLU, E.; TULUN, M. et al. Controlling the Size and the Stability of Magnetic Clusters Formed in Polyacrylamide Hydrogels via Cobalt-Anionic Fluoroprobe Interactions. *Polymer Engineering and Science*, 2010, vol. 50, no. 4, p. 843-850. ISSN 0032-3888.
- [80] LIU, T. Y.; HU, S. H.; LIU, K. H. et al. Study on controlled drug permeation of magnetic-sensitive ferrogels: Effect of Fe₃O₄ and PVA. *Journal of Controlled Release*, 2008, vol. 126, no. 3, p. 228-236. ISSN 0168-3659.
- [81] SATARKAR, N. S.; HILT, J. Z. Magnetic hydrogel nanocomposites for remote controlled pulsatile drug release. *Journal of Controlled Release*, 2008, vol. 130, no. 3, p. 246-251. ISSN 0168-3659.
- [82] GUPTA, R.; BAJPAI, A. K. Magnetically Guided Release of Ciprofloxacin from Superparamagnetic Polymer Nanocomposites. *Journal of Biomaterials Science-Polymer Edition*, 2011, vol. 22, no. 7, p. 893-918. ISSN 0920-5063.
- [83] MITSUMATA, T.; IKEDA, K.; GONG, J. P. et al. Magnetism and compressive modulus of magnetic fluid containing gels. *Journal of Applied*

Physics, 1999, vol. 85, no. 12, p. 8451-8455. ISSN 0021-8979.

[84] ZRINYI, M. Intelligent polymer gels controlled by magnetic fields. *Colloid and Polymer Science*, 2000, vol. 278, no. 2, p. 98-103. ISSN 0303-402X.

[85] ZRINYI, M.; SZABO, D.; KILIAN, H. G. Kinetics of the shape change of magnetic field sensitive polymer gels. *Polymer Gels and Networks*, 1998, vol. 6, no. 6, p. 441-454. ISSN 0966-7822.

[86] HERNANDEZ, R.; SARAFIAN, A.; LOPEZ, D. et al. Viscoelastic properties of poly(vinyl alcohol) hydrogels and ferrogels obtained through freezing-thawing cycles. *Polymer*, 2004, vol. 45, no. 16, p. 5543-5549. ISSN 0032-3861.

[87] CHATTERJEE, J.; HAIK, Y.; CHEN, C. J. Biodegradable magnetic gel: synthesis and characterization. *Colloid and Polymer Science*, 2003, vol. 281, no. 9, p. 892-896. ISSN 0303-402X.

[88] LI, X. C.; GONG, R. Z.; FENG, Z. K. et al. Effect of particle size and concentration on microwave-absorbing properties of $Cu_xCo_{2-x}Y$ ($x=0, 1$) hexaferrite composites. *Journal of the American Ceramic Society*, 2006, vol. 89, no. 4, p. 1450-1452. ISSN 0002-7820.

[89] YU, M. X.; LI, X. C.; GONG, R. Z. et al. Magnetic properties of carbonyl iron fibers and their microwave absorbing characterization as the filler in polymer foams. *Journal of Alloys and Compounds*, 2008, vol. 456, no. 1-2, p. 452-455. ISSN 0925-8388.

[90] RAMAJO, L. A.; CRISTOBAL, A. A.; BOTTA, P. M. et al. Dielectric and magnetic response of Fe_3O_4 /epoxy composites. *Composites Part a-Applied Science and Manufacturing*, 2009, vol. 40, no. 4, p. 388-393. ISSN 1359-835X.

[91] YANG, Y. L.; GUPTA, M. C. Novel carbon nanotube-polystyrene foam composites for electromagnetic interference shielding. *Nano Letters*, 2005, vol. 5, no. 11, p. 2131-2134. ISSN 1530-6984.

[92] DAVINO, D.; MEI, P.; SORRENTINO, L. et al. Polymeric Composite Foams With Properties Controlled by the Magnetic Field. *Ieee Transactions on Magnetics*, 2012, vol. 48, no. 11, p. 3043-3046. ISSN 0018-9464.

[93] VIALLE, G.; DI PRIMA, M.; HOCKING, E. et al. Remote activation of nanomagnetite reinforced shape memory polymer foam. *Smart Materials & Structures*, 2009, vol. 18, no. 11. ISSN 0964-1726.

CURRICULUM VITAE

Name: Zuzana Kožáková

Date of birth: 1985, April 04

Place of birth: Bratislava, Slovak Republic

Permanent address: SNP 387/17, Nové Mesto n. V., 915 01, Slovak Republic

Nationality: Slovak

Affiliation: Polymer Centre, Faculty of Technology, Tomas Bata University in Zlín, Nám. T.G. Masaryka 275, Zlín 762 72, Czech Republic

Centre of Polymer Systems, University Institute, Tomas Bata University in Zlín, Nad Ovčírnou 3685, 760 01 Zlín, Czech Republic

Phone: (+420)-57-603-8049

E-mail: zkozakova@ft.utb.cz

Education:

2004 - 2007 Faculty of Technology, Tomas Bata University in Zlín
Bc. (BSC.) degree in study programme Chemistry and Food Technology
Bachelor thesis: Stanovenie riboflavínu v kvasniciach metódou HPLC

2007 - 2009 Faculty of Technology, Tomas Bata University in Zlín
Ing. (MSc.) degree in study programme Technology, Hygiene and Economics of Food Production
Master thesis: Chromatografické stanovenie B-komplexu

2009 - Polymer Centre, Faculty of Technology, Tomas Bata University in Zlín
PhD student in the doctoral programme Technology of Macromolecular Substances

LIST OF PAPERS

Journal articles:

1. Z. Kozakova, P. Bazant, M. Machovsky, V. Babayan, and I. Kuritka, "Fast Microwave-Assisted Synthesis of Uniform Magnetic Nanoparticles," *Acta Physica Polonica A*, vol. 118, pp. 948-949, 2010.
2. M. Machovsky, I. Kuritka, and Z. Kozakova, "Microwave assisted synthesis of nanostructured Fe₃O₄/ZnO microparticles," *Materials Letters*, vol. 86, pp. 136-138, 2012.
3. M. Sedlacik, R. Moucka, Z. Kozakova, N. E. Kazantseva, V. Pavlinek, I. Kuritka, *et al.*, "Correlation of structural and magnetic properties of Fe₃O₄ nanoparticles with their calorimetric and magnetorheological performance," *Journal of Magnetism and Magnetic Materials*, vol. 326, pp. 7-13, 2013.
4. Z. Kozakova, I. Kuritka, V. Babayan, N. Kazantseva, and M. Pastorek, "Magnetic Iron Oxide Nanoparticles for High Frequency Applications," *IEEE Transactions on Magnetics*, vol. 49, pp. 995-999, 2013.
5. M. Sedlacik, M. Mrlik, Z. Kozakova, V. Pavlinek, and I. Kuritka, "Synthesis and electrorheology of rod-like titanium oxide particles prepared via microwave-assisted molten-salt method," *Colloid and Polymer Science*, vol. 291, pp. 1105-1111, 2013.
6. M. Sedlacik, S. Almajdalawi, M. Mrlik, V. Pavlinek, Z. Kozakova, I. Kuritka, "Electrorheological properties of suspensions of rod-like titanium oxide/polypyrrole particles," *Plasty a kaučuk*, vol. 49, pp. 33-35, 2012

Conference proceedings:

1. Z. Kozakova, P. Bazant, M. Machovsky, V. Babayan, and I. Kuritka, "Fast Microwave-Assisted Synthesis of Uniform Magnetic Nanoparticles," in *14th Czech and Slovak Conference on Magnetism CMAG '10*, Košice, 2010, ISBN 978-80-7097-804-7.
2. B. Altangerel, Z. Kozakova, D. Kramářová, O. Rop, I. Hoza, "The Determination of water soluble vitamins in multivitamin pharmaceuticals", in *Bezpečnost' a kontrola potravin*, Nitra, 2010, ISBN 978-80-552-0350-8.
3. R. Moucka, M. Sedlacik, Z. Kozakova, N. Kazantseva, O. Kaman, "Magnetite nanoparticles for magnetic mediated hyperthermia," in *20th International Conference on Soft Magnetic Materials*, Kos, Greece, 2011, ISBN

978-960-9534-14-7.

4. Z. Kozakova, I. Kuritka, M. Machovsky, P. Bazant, M. Pastorek, "Application of microwave pressurized reactor in synthesis of magnetic particles," in *Plastko*, Zlín, 2010, ISBN 978-80-7318-909-9.
5. P. Bažant, M. Machovský, Z. Kožáková, I. Kuřitka, P. Žlebek, M. Pastorek, "Open vessel microwave synthesis of hybrid fillers for medical plastics," in *Plastko*, Zlín, 2010, ISBN 978-80-7318-909-9.
6. Z. Kozakova, V. Babayan, M. Sedlacik, I. Kuritka, V. Pavlinek, "Rapid microwave-assisted method for preparation of magnetic nanoparticles for hyperthermia treatment," in *Third International NanoBio Conference 2010*, Zurich, 2010, published in *European Cells and Materials* Vol. 20. Suppl. 3, 2010, ISSN 1473-2262.
7. Z. Kozakova, M. Machovsky, V. Babayan, M. Pastorek, I. Kuritka, „Influence of synthesis parameters on the growth process of magnetic nanoparticles synthesized by microwave-assisted solvothermal method," in *Nanocon*, Brno, 2011, ISBN 978-80-87294-27-7.
8. Z. Kozakova, M. Mrlik, M. Sedlacik, V. Pavlinek, I. Kuritka, „Preparation of TiO₂ powder by microwave-assisted molten-salt synthesis," in *Nanocon*, Brno, 2011, ISBN 978-80-87294-27-7.
9. M. Machovsky, P. Bazant, Z. Kozakova, M. Pastorek, P. Zlebek, I. Kuritka, *et al.*, „Open vessel microwave-assisted synthesis of Ag/ZnO hybrid fillers with antibacterial activity," in *Nanocon*, Brno, 2011, ISBN 978-80-87294-27-7.
10. J. Sedlak, P. Bazant, Z. Kozakova, M. Machovsky, M. Pastorek, I. Kuritka, *et al.*, „Nanostructured zinc oxide microparticles with various morphologies," in *Nanocon*, Brno, 2011, ISBN 978-80-87294-27-7.
11. Z. Kozakova, I. Kuritka, V. Babayan, N. Kazantseva, M. Pastorek, „Synthesis and properties of magnetic nanoparticles for polymer composite systems," in *BYPOS 2012*, Liptovský Ján, 2012, ISBN 978-80-970923-2-0.
12. Z. Kozakova, I. Kuritka, V. Babayan, N. Kazantseva, and M. Pastorek, "Magnetic Iron Oxide Nanoparticles for High Frequency Applications," in *ICMM 2012*, Kaiserslautern, 2012, ISBN 978-1-4673-5625-1.
13. Z. Kozakova, I. Kuritka, P. Bazant, M. Machovsky, P. Pastorek, V. Babayan, „Simple and effective preparation of cobalt ferrite nanoparticles by

microwave-assisted solvothermal method," in *Nanocon*, Brno, 2012, ISBN 978-80-87294-32-1.

14. P. Bazant, Z. Kozakova, I. Kuritka, M. Machovsky, „Microwave assisted hydrothermal synthesis of Ag-ZnO nano-micro structures: comparison of closed and open vessel reactor influence on nitrate solution preparation route," in *Nanocon*, Brno, 2012, ISBN 978-80-87294-32-1.

15. M. Sedlacik, M. Mrlik, V. Pavlinek, Z. Kozakova, and P. Saha, „Electrorheological behaviour under oscillatory shear of TiO₂ rod-like particles prepared via microwave-assisted molten-salt synthesis," in *13th International Conference on Electrorheological Fluids and Magnetorheological Suspensions*. vol. 412, H. I. Unal, Ed., 2013.

APPENDIX - PAPERS INCLUDED TO THE THESIS

Paper I.

Kozakova, Z.; Bazant, P.; Machovsky, M.; Babayan, V.; Kuritka, I., Fast Microwave-Assisted Synthesis of Uniform Magnetic Nanoparticles. *Acta Physica Polonica A* 2010, 118, (5), 948-949. (50%)

Fast Microwave-Assisted Synthesis of Uniform Magnetic Nanoparticles

Z. KOZAKOVA, P. BAZANT, M. MACHOVSKY, V. BABAYAN AND I. KURITKA*

Polymer Centre, Faculty of Technology, Tomas Bata University in Zlin
Nam. T.G. Masaryka 275, 762 72 Zlin, Czech Republic

In recent time, magnetic nanoparticles have become widely used for preparation of advanced magnetic materials and also for biomedical applications. Requirement for preparation of particles of suitable shape and size has appeared, hence, various methods have been developed. Here we present rapid and energy saving one-pot solvothermal synthesis using microwave pressurized system. This method allows tuning the size of the particles as well as their magnetic properties. Spherical Fe_3O_4 nanoparticles are obtained in 30 min; they are uniform with average dimensions of 200 nm and exhibit ferromagnetic behavior dependent on synthesis temperature.

PACS numbers: 75.50.Tt, 75.60.Ej, 75.75.Cd

1. Introduction

In the past decades, the interest in synthesis of uniform magnetic particles in micro- or nanodimensions expanded due to their potential application in many fields. They can be applied in medicine for controlled drug delivery, hyperthermia or medical diagnostic for magnetic resonance imaging. These particles are also used as fillers in magnetic composites or in electromagnetic shielding materials. They are investigated as a key component of magnetorheological fluids, too. Moreover, external magnetic field can be used for preparation of oriented anisotropic structures from this particular system thus achieving novel properties [1–6]. Lots of methods have been introduced for preparation of magnetic particles, employing both dry and wet chemistry. The most popular among them have become simple one-pot solvothermal methods [7–10].

2. Experimental

In a standard experiment, 5 mmol of $\text{FeCl}_3 \cdot 6\text{H}_2\text{O}$ was dissolved in 60 mL of ethylene glycol, followed by the addition of nucleating agent (50 mmol of NH_4Ac , 25 mmol of $(\text{NH}_4)_2\text{CO}_3$ or 200 mmol of aqueous NH_3). This mixture was placed in a teflon reaction vessel (XP-1500 Plus), heated in pressurized CEM Mars 5 microwave system (CEM Corporation) to a required temperature (200, 210 or 220 °C) and maintained at this temperature for 30 min. After the reaction, the vessel was cooled to a room temperature and the as-obtained product was filtered off, washed with water and ethanol for

several times and dried naturally on air. The structure of the final product was characterized by X-ray diffraction method (XRD; PANalytical X'Pert PRO). The particle size and shape was visualized by scanning electron microscopy (SEM; VEGA\LMU, Tescan) and magnetic properties were identified by a vibrating sample magnetometer (VSM; VSM 7400, Lake Shore).

3. Results and discussion

Magnetic particles were obtained by a simple microwave-assisted solvothermal method in 30 min in nearly 100%. As can be seen from XRD pattern in Fig. 1, all the diffraction peaks are attributed to cubic Fe_3O_4 , although we cannot distinguish whether it is magnetite or maghemite. Key factor for obtaining well crystallized structures are synthesis time and temperature. The required product can be obtained if the time of synthesis is about 30 min. Experiments with different synthesis temperatures showed that the crystallic structure of particles improves with the temperature increment. The typical SEM image of the product prepared with NH_4Ac at 220 °C in Fig. 2 shows that the prepared particles are spherical, uniform and their dimension are about 200 nm. Figure 3 gives magnetization curves of particles prepared with NH_4Ac at different temperatures and that these particles exhibit ferromagnetic behavior. A strong effect of the synthesis temperature is manifested: with increase of the temperature used for preparation of particles, saturation magnetization and coercivity of prepared material are significantly higher.

4. Conclusion

To conclude, in this work there is presented an efficient, rapid and facile one-pot solvothermal microwave-assisted

* corresponding author; e-mail: ivo@kuritka.net

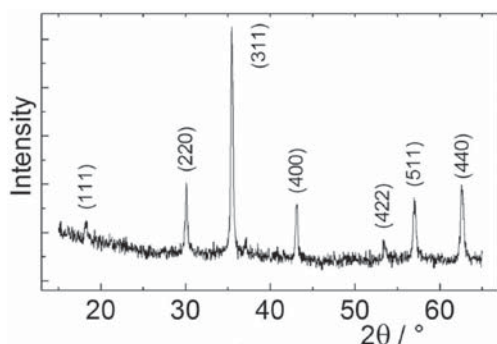


Fig. 1. XRD pattern of Fe_3O_4 particles prepared with NH_4Ac at 220°C for 30 min.

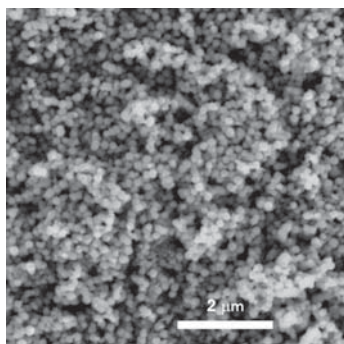


Fig. 2. SEM image of Fe_3O_4 particles prepared with NH_4Ac at 220°C for 30 min.

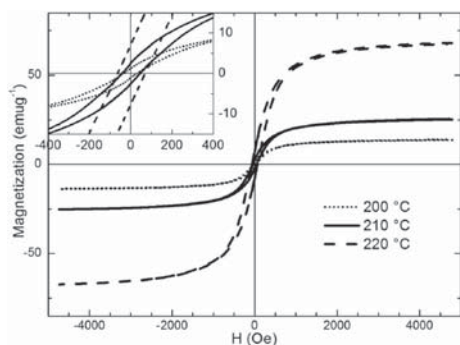


Fig. 3. Room temperature magnetization curves of Fe_3O_4 particles prepared with NH_4Ac at 200, 210 and 220°C for 30 min. In the inset is given a detailed view of magnetization curves is given, showing variation of coercivity while different temperatures are used within the synthesis.

synthesis of magnetic Fe_3O_4 nanoparticles by which they can be obtained in 30 min without requirement of further treatment such as calcination, which can cause disruption of particles. The as-obtained spherical particles are uniform with an average dimension of 200 nm and exhibit ferromagnetic behavior. The method allows particle size tuning and refinement of magnetic properties by simple changing the synthesis parameters, i.e. temperature or nucleating agent, which can be profitable in future medical application as well as in formation of advanced magnetic materials.

Acknowledgments

This work was supported by the internal grant of TBU in Zlín No. IGA/25/FT/10/D funded from the resource of specific university research.

References

- [1] A.K. Gupta, M. Gupta, *Biomaterials* **26**, 3995 (2005).
- [2] D.K. Kim, Y. Zhang, J. Kehr, T. Kalson, B. Bjelke, M. Muhammed, *J. Magn. Magn. Mater.* **225**, 256 (2001).
- [3] A.S. Lübke, Ch. Alexiou, Ch. Bergemann, *J. Surg. Res.* **95**, 200 (2001).
- [4] C. Schao-Wen, Z. Ying-Jie, M. Ming-Yan, L. Liang, Z. Ling, *J. Phys. Chem. C* **112**, 1851 (2008).
- [5] J. Jestin, F. Cousin, I. Dubois, C. Ménager, R. Schveins, J. Oberdisse, F. Bouté, *Adv. Mater.* **20**, 2533 (2008).
- [6] C. Scherer, A.M. Figueiredo, Neto, *Braz. J. Phys.* **35**, 718 (2005).
- [7] H. Peng, Y. Lingjie, Z. Ahui, G. Chenyi, Y. Fangli, *J. Phys. Chem. C* **113**, 900 (2009).
- [8] Ch. Xiangying, Z. Zhongjie, L. Xiaoxuan, S. Chengwu, *Chem. Phys. Lett.* **422**, 294 (2006).
- [9] Z. Lu-Ping, X. Hong-Mei, Z. Wei-Dong, Y. Guo, F. Shao-Yun, *Cryst. Growth Design* **8**, 957 (2008).
- [10] D. Hong, L. Xiaolin, P. Qing, W. Xun, Ch. Jinping, L. Yadong, *Angew. Chem. Int. Ed.* **44**, 2782 (2005).

Paper II.

Kozakova, Z.; Kuritka, I.; Kazantseva, N. E.; Babayan, V.; Pastorek, M.; Machovsky, M. and Bazant, P., Formation mechanism of iron oxide nanoparticles within the microwave-assisted solvothermal synthesis and its correlation with the structural and magnetic properties. *Manuscript submitted to Material Research Bulletin.* (50%)

Elsevier Editorial System(tm) for Materials Research Bulletin
Manuscript Draft

Manuscript Number:

Title: Formation mechanism of iron oxide nanoparticles within the microwave-assisted solvothermal synthesis and its correlation with the structural and magnetic properties

Article Type: Research Article

Section/Category: Nanomaterials

Keywords: inorganic compounds; magnetic materials; nanostructures; oxides; chemical synthesis; magnetic structure

Corresponding Author: Ms. Zuzana Kozakova,

Corresponding Author's Institution: Tomas Bata University in Zlin

First Author: Zuzana Kozakova

Order of Authors: Zuzana Kozakova; Ivo Kuritka; Natalia Kazantseva; Vladimir Babayan; Miroslav Pastorek; Michal Machovsky; Pavel Bazant; Petr Saha

Abstract: Magnetic nanoparticles on the base of Fe₃O₄ were prepared by a facile and rapid one-pot solvothermal synthesis using FeCl₃·6H₂O as a source of iron ions, ethylene glycol as a solvent and NH₄Ac, (NH₄)₂CO₃, NH₄HCO₃ or aqueous NH₃ as precipitating and nucleating agents. In contrast to previous reports we reduce the synthesis time to 30 minutes using pressurized microwave reactor without requirement of further post-treatment such as calcination, which can cause defects of particles. The as-obtained particles have dimension in range of 20 to 130 nm, uniform shape and exhibit magnetic properties with saturation magnetization ranging from 8 to 76 emu·g⁻¹. Suggested method allows simple particle size and crystallinity tuning resulting in improved magnetic properties by changing the synthesis parameters, i.e. temperature and nucleating agent. Moreover, efficiency of conversion of raw material into the product is almost 100 %. Description of the grow process under the solvothermal conditions is a crucial tool for tailoring the properties of magnetic nanoparticles.

Suggested Reviewers: Thierry Caillot

Institut de Recherches sur la Catalyse et l'Environnement de Lyon, Université Lyon 1, France
thierry.caillot@univ-lyon1.fr

Jeffrey A. Gerbec

Mitsubishi Chemical Center for Advanced Materials, University of California, Santa Barbara
jgerbec@mrl.ucsb.edu

Alejandro G. Roca

Department of Physics, University of York
agr506@york.ac.uk

New Manuscript Checklist

[Click here to view linked References](#)

Materials Research Bulletin (MRB) New Manuscript Checklist

All new manuscripts should have the following:

- Text no smaller than 12 point type, double-spacing of all text pages including the references.
- Page numbers on each page.
- High quality figures, i.e. no photocopies of photographic plates, laser prints are acceptable.
- Large symbols used in figures, good enough for reproduction.
- Tables and figures at the end of the manuscript (no embedded tables/figures in text).
- Correct order:
 - Abstract
 - Introduction
 - Experimental
 - Results
 - Discussion
 - Conclusions
 - References
 - Tables (one table per 8½ X 11 page)
 - Figure captions page
 - Figures, with figure number, no caption (one figure per 8½ X 11 page)

***Manuscript**

[Click here to view linked References](#)

Formation mechanism of iron oxide nanoparticles within the microwave-assisted solvothermal synthesis and its correlation with the structural and magnetic properties

Zuzana Kozakova*, Ivo Kuritka, Natalia Kazantseva, Vladimir Babayan, Miroslav Pastorek, Michal Machovsky, Pavel Bazant and Petr Saha

Centre of Polymer Systems, University Institute, Tomas Bata University in Zlin, Nad Ovcirnou 3685, 760 01 Zlin, Czech Republic

zkozakova@ft.utb.cz *corresponding author

ivo@kuritka.net

nekazan@yahoo.com

babayan@ft.utb.cz

pastorek@ft.utb.cz

machovsky@ft.utb.cz

bazantik@centrum.cz

saha@utb.cz

Abstract

Magnetic nanoparticles on the base of Fe_3O_4 were prepared by a facile and rapid one-pot solvothermal synthesis using $\text{FeCl}_3 \cdot 6\text{H}_2\text{O}$ as a source of iron ions, ethylene glycol as a solvent

and NH_4Ac , $(\text{NH}_4)_2\text{CO}_3$, NH_4HCO_3 or aqueous NH_3 as precipitating and nucleating agents. In contrast to previous reports we reduce the synthesis time to 30 minutes using pressurized microwave reactor without requirement of further post-treatment such as calcination, which can cause defects of particles. The as-obtained particles have dimension in range of 20 to 130 nm, uniform shape and exhibit magnetic properties with saturation magnetization ranging from 8 to 76 $\text{emu}\cdot\text{g}^{-1}$. Suggested method allows simple particle size and crystallinity tuning resulting in improved magnetic properties by changing the synthesis parameters, i.e. temperature and nucleating agent. Moreover, efficiency of conversion of raw material into the product is almost 100 %. Description of the grow process under the solvothermal conditions is a crucial tool for tailoring the properties of magnetic nanoparticles.

Keywords: inorganic compounds; magnetic materials; nanostructures; oxides; chemical synthesis; magnetic structure

1. Introduction

Recently, the interest in preparation of nano-sized magnetic particles has risen due to their potential utilization in many areas of use. The most ambitious applications are in medicine and pharmacy for magnetic resonance imaging, biomaterials diagnostics, and drug delivery and in cancer treatment: magnetically mediated hyperthermia. Furthermore, they are used for preparation of functional magnetic materials, high recording media, colored pigments and ferrofluids [1-6]. All of these applications require defined nanoparticles features together with high magnetization. Therefore, the development of synthetic method enabling the preparation of tailor-made product with truly wide range of requesting properties gets great attention. Lots of methods have been introduced for preparation of magnetite nanoparticles, by using both dry and wet chemistry. Thanks to the simplicity of solvothermal method it became one of the

most popular among them. It is based on the principle of heating of solution of a metallic salt in a suitable solvent in the Teflon-lined stainless autoclave in the presence of other substances, such as nucleating or reducing agents and surfactants. Recently, several teams have described relatively simple preparation of well-crystallized magnetic nanoparticles where ferric chloride is the source of iron cations and ethylene glycol serves both as a solvent and reducing agent. Moreover, other substances used in synthesis were ethylenediamine serving as both, coordinating agent and quasi-surfactant, urea or different ammonium salts used as nucleating agents, sodium acetate or other chemicals [7-10]. However, tardiness of all of these methods (synthesis time at least 12 hours) is their main disadvantage which should be solved in order to improve efficiency and applicability of solvothermal syntheses. Microwave heating, using the transformation of electromagnetic energy to heat, seems to be the proper alternative to conventional heating leading to acceleration of synthetic procedure. Common microwave reactors use radiation of frequency 2.45 GHz and the wavelength 12.2 cm. Microwave synthesis is used in both organic and inorganic chemistry as a rapid method durable usually several minutes and therefore it is also energy saving. Moreover, it is possible to operate with a reflux system at atmospheric pressure that provide preparation of particles of various sizes and shapes, such as spheres, sheets, rods, tubes and others as it was demonstrated in recently [11-13].

Several microwave-assisted methods using the reflux system have been used for synthesis of magnetic particles. However, these methods are relatively tedious and time-consuming as it turned out. As an example, two hours are required for preparation of Fe_3O_4 nanoparticles by MW heating of product obtained by mixing solutions of FeCl_3 and FeSO_4 under argon protection with the addition of aqueous NH_3 [14]. In another case, magnetite and maghemite nanoparticles were synthesized by the fast and simple method based on MW heating of precursor obtained from the mixture of FeCl_3 and polyethylene glycol ($M_w = 20000$) in

distilled water with the addition of hydrazine hydrate; however, the as-obtained particles have relatively wide size distribution and irregular shapes [15]. According to our experience, heating limited by boiling temperature, intense mass flows accompanying the evaporation and subsequent condensation of the solvent in external coolers and foaming of the reaction mixture are strong limitations for these systems. Although a pressurized system for solvothermal synthesis offers relatively simple control over the morphology and particle size, examples of microwave pressurized reactors are reported very rarely in this field. Caillot et al used microwave applicator connected with an autoclave (RAMO system, Reacteur Autoclave Micro Onde) for the synthesis of magnetic nanoparticles using $\text{FeCl}_2 \cdot 4\text{H}_2\text{O}$ and sodium ethoxide as starting material [16]. The resulting products were Fe_2O_3 , Fe_3O_4 or their mixture in the dependence on the concentration of sodium ethoxide.

Microwave-assisted synthesis using pressurized system are based on exposure of reaction mixtures to MW radiation in sealed vessels made from PTFE (Teflon) or even glass in microwave ovens. Products of such synthesis are influenced by the initial setting of synthetic parameters, namely concentration of metallic salts and type of solvent. On the other hand, a programmable MW system with precise control of temperature and pressure may offer full control over the synthesis conditions [17].

In many cases, temperature increase is needed for initiation of nucleation in nanoparticles synthesis. If using the conventional heating, reaction mixture is heated through the wall of reaction vessel via conduction and convection of heat, and thus created temperature gradient causes non-uniform nucleation and growth conditions. Microwave heating can solve this problem, since the energy is directly transferred to the microwave absorbing materials and the total volume of reactant is therefore uniformly heated [18].

There are two MW heating effects that determine the quality of final substance: thermal and non-thermal effects. The thermal effect is considered as a fast and effective heating of reaction

mixture providing uniform nucleation and growth conditions thus leads to preparation of uniform nanoparticles with small sizes and high crystallinity. Non thermal effects include the creation of hot spots and hot surfaces within the heating of solid materials on the liquid-solid surfaces which support the reduction of metal precursors, nucleation and formation of metal clusters [11]. These effects are still a matter of intensive discussion and controversies in synthetic chemistry. Moreover, the mechanisms of microwave effects playing the role in solvothermal synthesis of magnetic nanoparticles remain uncovered in recent literature.

The goal of this work is threefold. First is to establish simple, fast and highly efficient method of magnetic nanoparticles synthesis with a view to the scientific and commercial uses.

Towards this purpose we decided to combine the simplicity of solvothermal methods and efficiency of microwave heating into novel, environmental friendly method providing the product of fine quality in high yields. In next, this work contributes to the elucidation of effects of microwave heating on the processes and reactions that occur during the synthesis. Understanding the correlation among the reaction mechanism, conditions and properties of resulting particles enables to fulfill the third goal – development of a simple method with possibility to tailor the properties of product.

2. Materials and methods

2.1 Solvothermal synthesis of magnetic nanoparticles

Nano- and submicro-sized Fe_3O_4 particles were prepared by a simple solvothermal method in ethylene glycol solution with the help of microwave irradiation. All reagents used within the synthesis were purchased from Penta Ltd. (Czech Republic) in analytical grade and used without further purification. In a standard experiment, 5 mmol of $\text{FeCl}_3 \cdot 6\text{H}_2\text{O}$ (1.352 g) was dissolved in 60 mL of ethylene glycol, followed by the addition of 50 mmol of ammonium

acetate - NH_4Ac (3.854 g). This mixture was placed in a 100 mL Teflon reaction vessel (XP-1500 Plus), heated in a CEM Mars 5 microwave oven to the required temperature (200 °C, 210 °C, 220 °C) and maintained at this temperature for 30 minutes. After the reaction, the vessel was cooled to a room temperature and black precipitate was collected with the help of permanent magnet. Subsequently, the as-obtained product was washed with distilled water and ethanol for several times and dried naturally on air. Furthermore, in similar experiments, 25 mmol of $(\text{NH}_4)_2\text{CO}_3$ (2.403 g), 50 mmol of NH_4HCO_3 (3.953 g) or 50 mmol of NH_3 in the form of aqueous solution (3.8 mL of 25% water solution) were used as a nucleating agent instead of NH_4Ac . Further experiments involved the addition of 2 to 4 mL of demineralized water to the reaction system while rest of parameters remained unchanged.

2.2 Characterization of as-prepared magnetic nanoparticles

First of all, macroscopic appearance of prepared powder was observed by naked eye and by digital microscope DVM 2500 (Leica Microsystems, Germany). The structure of the final product was characterized by the X-ray Diffraction (PANalytical X'Pert PRO) with $\text{Cu K}\alpha 1$ radiation ($\lambda = 1.540598 \text{ \AA}$). Phase composition and crystallites sizes were determined according to Rietveld analysis. Particle size and morphology were preliminary investigated with the help of Scanning Electron Microscopy (VEGA\LMU, Tescan). Particles shape, organization and proportions were further specified by Transmission Electron Microscopy (JEOL 1200, JEOL). Image analysis was used for estimation of particle size distribution. Magnetic properties were measured by a vibrating sample magnetometer (VSM 7400, Lake Shore).

3. Results and discussion

3.1 Correlation of particle properties with reaction conditions

X-ray diffraction (XRD) patterns of samples exemplified on materials prepared with NH_4Ac at 200, 210 and 220 °C for 30 minutes can be seen in figure 1. Diffraction pattern of material prepared at 220°C is clearly attributed to the cubic crystal structure of Fe_3O_4 , however, presence of peaks that do not belong to the magnetite are observed in patterns of materials prepared at 200 and 210° C, indicating creation of other crystalline phases at lower synthesis temperatures. In addition, although the diffraction pattern of product of synthesis proceeding at 200°C includes broaden regions mostly seen between 30 and 40° 2θ that indicate presence of amorphous portion and broad peaks characteristic for very small particles, these features gradually disappear while the synthesis temperature increases, and at 220 °C are even absent. Therefore we can consider this system very sensitive within the range of a few tens of degrees centigrade and exploit elevated temperature to accelerate the nucleation and growth of the nanoparticles of required crystalline phase. Demonstrated development of sample crystallinity with the temperature increment is also followed by the set of the samples nucleated by other ammonium salts used in our experiments, not shown here for the sake of brevity. Calculation according to the Rietveld analysis showed that the crystallites size of magnetite phase depends on the used nucleating agent and varies from 20 to 80 nm. Phase composition also differs with the manner of nucleation. While the product prepared with aqueous ammonia is composed of pure Fe_3O_4 without other crystalline impurities, the presence of minor ferric compounds such as $\text{FeO}(\text{OH})$ and $\alpha\text{-Fe}_2\text{O}_3$ is evident in samples nucleated by ammonium carbonate and ammonium bicarbonate and utilization of ammonium acetate leads to the formation of product with $\text{FeO}(\text{OH})$ in bigger portions.

FIGURE 1. HERE

It is well known that maghemite always accompanies magnetite in all materials due to the slow oxidation of magnetite into the maghemite by air oxygen and results in the formation of

the maghemite layer on the surface. In nanoscaled materials, this effect becomes considerable due to the large surface area and can be observed even in single crystals [19-21]. Moreover, reactants and mechanism (will be discussed later) of presented synthesis allows formation of maghemite and magnetite. Usually, maghemite phase can be determined by Mössbauer spectrometry [22,23]. However, the differentiation between non-stoichiometric magnetite and magnetite–maghemite mixture is considerably challenging and was even claimed to be almost impossible [24,25]. The same spinel structure and almost identical lattice parameters makes identification of magnetite ($\text{Fe(II)Fe(III)}_2\text{O}_4$) and maghemite ($\gamma\text{-Fe(III)}_2\text{O}_3$) by XRD technique complicated. However, a deep detailed analysis of (511) Bragg peak at 2θ range $56.5\text{-}57.5^\circ$ and (440) peak at $62\text{-}63.5$ 2θ provide insight in this issue [26]. Pure magnetite has the central position of the diffraction peak at 57.0 while maghemite has this peak slightly shifted to higher values, i.e. 57.3 . Under the certain conditions, observed peaks can be analyzed by deconvolution with the use of proper magnetite and maghemite standards. A detailed analysis of XRD patterns obtained for our samples are shown in figure 2. It is evident that all peaks are composed from more than one Gaussian contribution which can be attributed to the presence of both magnetite and maghemite phases in all samples. On the other hand, the peak positions at X-axes can be slightly shifted because the used diffractometer is not equipped with the Göbel mirror. Without the use of high resolution XRD and pure magnetite and maghemite nanoparticulate standards, the deconvolution cannot be successfully performed and the ratio between the phases cannot be exactly estimated.

FIGURE 2. HERE

Scanning electron microscopy image (SEM) of particles prepared with ammonium acetate is shown in figure 3. The particles have quasi spherical shape and occur in a form of clusters. Similarly, SEM study of all types of prepared products provides analogical results, which can be influenced by the resolution of the used method.

FIGURE 3. HERE

Images of better resolution were obtained by transmission electron microscopy (TEM) (Figure 4). Analyses of the TEM images shown the importance of nucleation agent on the particle size, shape and organization is evident. The use of aqueous NH_3 as well as NH_4HCO_3 provides single-crystalline material composed of uniform-shaped polyhedral nanoparticles with narrow size distribution and dimension below 30 nm. However, the use of $(\text{NH}_4)_2\text{CO}_3$ and NH_4Ac for nucleation lead to the creation of clusters consisted of nano-sized grains and ranging to several hundred nanometers. The hierarchical structure of clusters affects the magnetic properties of materials obtained and therefore we further studied the reason for their formation within the microwave-assisted solvothermal process.

FIGURE 4. HERE

The size of clusters obtained with the use of ammonium acetate on the base of TEM analysis is 60 nm. Since the size of grains of the magnetite phase calculated by Rietveld analysis is about 40 nm, these clusters seems to be formed by the binding of the small crystallites of the goethite phase together with the magnetite crystals, as can be seen in the TEM image at high magnification (figure 3d). While the ammonium carbonate is used, particles with diameter about 120 nm are formed due to the twinning of crystallites of magnetite with the diameter of 80 nm induced by the incorporation of crystalline impurities (such as $\text{FeO}(\text{OH})$ and $\alpha\text{-Fe}_2\text{O}_3$) produced during the synthesis. Nanoparticles sizes are confirmed by calculations on the base of Rietveld analysis as described above. Information on particle sizes obtained by TEM image analyses were further used for creation of histograms which give us conception of particle size distribution in prepared materials (figure 5).

FIGURE 5. HERE

Magnetostatic properties of samples were investigated by using of vibrating sample magnetometer (VSM) at the room temperature. Figure 6 (left) demonstrates magnetization

curves of material prepared with ammonium acetate synthesized at 200, 210 and 220° C. Saturation magnetization (M_s) of nanoparticles obtained with NH_4Ac varies from 13.8 to 67.7 emu.g^{-1} with regard to the increase of temperature. The increase of M_s can be explained on the one hand to the crystallinity improvement seen in Figure 1, and on the other hand probably due to the phase transition at higher temperature which led to formation of material with major magnetite (maghemite) fraction. Similar results were obtained for the samples nucleated by $(\text{NH}_4)_2\text{CO}_3$ with saturation magnetization ranging from 8.4 to 46.2 emu.g^{-1} , as well as for NH_4HCO_3 with M_s in a range of 33.2 to 75.2 emu.g^{-1} and, also for aqueous NH_3 with the highest saturation magnetization among the forenamed materials that reaches 44.5 to 76.3 emu.g^{-1} . Lower values of M_s of prepared materials than that of the bulk magnetite (92–100 emu.g^{-1}) [27] are common for nanoparticulate systems and can be attributed to the canted spins on the surfaces [28]. On the other hand, maghemite phase present on the surface of nanoparticles could also lead to the decrease of M_s . For better understanding of effects influencing the magnetic properties of prepared materials the magnetization curves obtained with the use of different nucleating agents were plotted together in figure 6 (right). Obviously, particles prepared with aqueous ammonia and ammonium bicarbonate have the highest saturation magnetization; particles prepared with ammonium carbonate have the lowest one. It is well known that coercivity is determined by effective magnetic anisotropy and thus depends on the material composition as well as the grain size and shape. Figure 6 shows the rise of the coercivity depending on the synthesis temperature. It can be attributed to the already mentioned presence of the magnetite phase in the sample at the expense of other less magnetic phases such as hematite or non-magnetic goethite and the growth of the particles to the larger dimensions. However, despite of variations of particle size with the use of different nucleating agents, the coercivity of the materials prepared by different way of nucleation is very similar and reaches about 60 Oe. Nevertheless, material prepared with the use of ammonium

carbonate is the only exception with nearly zero value of coercivity. The squeezed shape of hysteresis loop (see the inset graph in Figure 6) indicates pronounced influence of the clusters formation on the hysteresis and confirms presence of two magnetic phases that differs in magnetic properties [29].

FIGURE 6. HERE

3.2 The mechanism of nanoparticle formation by MW-assisted synthesis

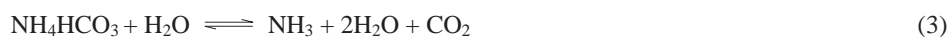
As the starting point for the description of the growth of Fe₃O₄ nanoparticles can be adopted the two-stage growth model of nanoparticles in supersaturated solutions [30]. In the first stage, nucleation of primary nanocrystals occurs what is followed by their aggregation into the secondary nanoparticles and, especially, this second step has to be reconsidered for specific microwave conditions.

We used NH₄Ac, (NH₄)₂CO₃, NH₄HCO₃ and aqueous NH₃ as nucleating agents. NH₄Ac is weak-acid-weak-base salt that can be hydrolyzed in high temperature in the presence of trace amount of water coming from FeCl₃.6H₂O as follows [7]:



Although NH₃.H₂O is used in reference [7], we do not expect the formation of solid ammonium hydrates in the system and we consider this formula to be an expression of presence of ammonia and water (NH₃ + H₂O) as it was most likely author's original intention.

Similarly, (NH₄)₂CO₃ and NH₄HCO₃ can be hydrolyzed into NH₃:



NH₃, either as the product of above reactions or added as aqueous solution yields hydroxide anions.



In our case, Fe (III) salt was used as the precursor. Precipitation of its hydroxide in form of colloidal solution proceeds as follows:

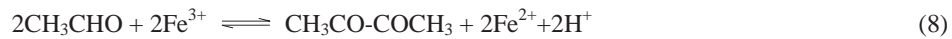


In next, formation of Fe₂O₃ particles may continue according to:



Hence maghemite phase can be formed in this way.

Under the presence of a mild reduction agent (e.g. ethylene glycol), Fe (II) may appear in the system. Ethylene glycol can undergoes dehydration and so-formed acetaldehyde [31,32] reduces Fe (III) into Fe (II) and gives ferrous hydroxide in form of a green colloid:



Most likely, both ferric and ferrous oxidation states of iron coexist in the reaction mixture thus enabling magnetite formation:



A minor phase, goethite, was observed and its presence in prepared materials can be explained by partial dehydration:



or by following equation in presence of oxygen:



The first step of nucleation starts with the first appearance of heterogeneity in the system similarly, as in common solvothermal methods. Hu et al. [7] proposed the mechanism with the key role of NH₃.H₂O. Aqueous ammonia evaporates and forms gaseous bubbles that provide

heterogeneous nucleation centers for new-formed nanoparticles, which can then aggregate around the gas–liquid interface. In our case, we used various precipitation agents and all of them lead to nanocrystalline products in the same reaction time; however, we did not obtain any evidence of hollow structures. Moreover, other authors used ammonia-less techniques with sodium acetate and obtained similar results, albeit this was achieved without MW assistance [30,33]. Lou et al. in their review [34] consider gas templating mechanism that uses soluble gases especially that originated from decomposition of organic molecules such as urea, as highly speculative. Therefore we propose that the reaction starts with formation of colloid according to the equations (5) and (9) rather than with formation of nanobubbles. In the second step, it is generally accepted for conventional solvothermal methods that the fresh formed nanocrystals are unstable due to high surface energy so they tend to aggregate. The driving force for this aggregation is pursuit of reducing the surface energy by both, attachment among the primary nanocrystals and their rotation caused by various interactions including Brownian motion or short–range interactions [30,35]. In our case of MW heating, the solvent at a high temperature (above 200 °C) becomes less absorbing due to decrease of dielectric constant and loss factor thus the solvent becomes virtually more transparent for microwaves, which means that the ionic mechanism of microwave absorption may be prevailing over dipoles [12]. After the solid particles occur in the solution, another mechanism becomes active due to particles surface polarization that might selectively influence their growth. Moreover, as the heat is generated at the surface of nanoparticles, the local temperature gradient can contribute to the hydroxide-to-oxide transformation described in equations (6) and (10). Once the oxide particle reaches the critical size corresponding to single-domain state, another mechanism of MW absorption is assumed to take the main role. Microwave energy is transformed into the heat by magnetic moment rotation and after some time in bigger multi-domain particles also by magnetic domain wall motion. This sequence of

several mechanisms can explain the sudden formation of particles in the reaction mixture as well as the very short synthesis time. Time required for the formation of nanoparticles with magnetic properties exceeds 12 hours for common solvothermal synthesis. Assuming simply just the fast heating of reaction mixture and no non-thermal effects supporting the transformation of raw material into the product we reduced synthesis time firstly to 20 minutes. However, the time of microwave treatment was not sufficient for the precipitate formation and only opaque yellow colloid was obtained with no magnetically separable fraction. Prolongation of the exposure to microwaves to 30 minutes provides formation of black precipitate and, moreover, the conversion of starting material into the product runs with almost 100% efficiency. This fact refers to the sudden formation of final product, the relatively narrow particle size distribution and support the concept of sequential action of MW absorption mechanisms as a non-thermal effect.

The role of solvent has to be reconsidered in comparison to conventional processes as well. Ethylene glycol is an exceptionally good microwave absorbing solvent at 2.45 GHz ($\tan \delta = 1.350$) [36] which assures very fast increase of temperature at the beginning of the synthesis together with fast achievement of quasi-stable reaction condition in the pressurized reaction vessel. On the other hand, it is not directly involved in chemistry of ferric hydroxide or oxide formation. EG can disproportionate according to equation (7) but the equilibrium must be shifted to the left side of the reaction, however the acetaldehyde enters the redox reaction (8) and yields Fe^{2+} cations. Liberation of one H_2O molecule per each Fe^{2+} cation occurs according to equations (7) and (8). Stoichiometric amount of water is delivered to the reaction system with $\text{FeCl}_3 \cdot 6\text{H}_2\text{O}$. The water plays crucial role in cation solvation, nucleation agent hydrolysis, see equations (1-4), and in formation of ferric and ferrous hydroxides, equations (5) and (9). Hence, the water is not present in excess but in stoichiometric amount as one of the reactants. Moreover, it has the highest dielectric constant

among common solvents although its loss factor ($\tan \delta = 0.123$) [36] is approximately eleven times lower than that of EG.

In contrast to fast nucleation in aqueous solutions, aggregation in ethylene glycol is kinetically slower due to fewer hydroxyl groups on the particle surface and higher viscosity, what allows adequate rotation of nanocrystals to form low-energy configuration of interface and perfect organized assemblies. Subsequently, these aggregates further crystallize and form compact crystals that exhibit features of single-crystal particles [9]. As it was possible to see in figure 3, particles obtained with the use of aqueous NH_3 are single crystals with polyhedral shape, the second most perfectly developed crystallites were observed for NH_4HCO_3 then followed by less developed spherical multi-grains obtained by the use of $(\text{NH}_4)_2\text{CO}_3$, whereas nucleation by NH_4Ac led to the biggest and polycrystalline particles with spherical shape. The same trend was observed for phase composition of prepared materials. As can be seen in table 1, the use of aqueous ammonia yielded single phase material while NH_4Ac gave the highest fraction of goethite in product. The other nucleation agents NH_4HCO_3 and $(\text{NH}_4)_2\text{CO}_3$ gave moderate results. Observed trend of perfection of crystalline structure development correlates well with the virtually hidden presence of water in nucleating agents. Hydrolysis of NH_4Ac does not provide any extra water molecule per each NH_3 in equation (1). Hydrolysis of $(\text{NH}_4)_2\text{CO}_3$ yields one extra H_2O molecule per two NH_3 and hydrolysis of NH_4HCO_3 yields two extra water molecules per each NH_3 , see equations (2, 3). About 2,5 mL of water gets to the reaction system with addition of aqueous ammonia (25 % water solution), which means approximately 3 molecules of H_2O per each NH_3 . Since the synthesis conditions such as temperature and duration are the same in all four cases, the influence of composition of reaction mixture on particle shape and organization was further investigated.

TABLE 1. HERE

Similar system was described by Cao et al. [35] and denominated as (EG)-H₂O system. By the addition of different amounts of water (1-3 mL) into the reaction system, Fe₃O₄ polyhedral particles with different size are formed whereas samples prepared without water addition led to the formation of product consisted of spherical particles assembled by smaller particles. If water is added to reaction system, coordinated EG molecules will be substituted by water molecules since the coordination of water molecules to metal ions is stronger than that of EG molecules. Selecting the amount of added water, particle size can be influenced in agreement with Cao et al. we considered the role of addition of deionized water as one of the most important factors in the control of particle size and size distribution, too. For this purpose we also performed experiments with the addition of water into the reaction mixture. According to the TEM figures showed above, sample nucleated by NH₄HCO₃ was chosen due to the narrow size distribution and shape uniformity of particles. Apparently from TEM image seen in figure 7, addition of small amount of demineralized water causes reduction of particles from 30 to 10 nm, even if the design of the as-prepared particles remains unchanged and they also possess single-crystalline character with polyhedral shape. This reduction of size significantly reflects in the magnetic properties of final product: figure 7 (right) clearly demonstrates transition from ferromagnetic to the superparamagnetic state.

FIGURE 7. HERE

Next to the synthetic conditions that can be directly controlled such as the synthetic temperature and composition of reaction mixture, pressure in reaction vessels can be influenced only indirectly, through the setting the level of the vessel filling, type of solvent and temperature (reaction temperature below or above the boiling point of solvent) and also by the type of used reactants. Since the used solvent and the level of vessel filling was almost the same in our experiments, the pressure in reaction vessels during the synthesis depended on the used nucleation agent and varied from 900 to 3800 kPa. When aqueous ammonia and

ammonium acetate were used within the synthesis, the lowest pressure (800-1000 kPa) was obtained. On the other hand, the decomposition of ammonium carbonate was accompanied with the increasing the pressure up to 3800 kPa due to the significant change of mole ratio of reaction (see equation (2)). The use of ammonium bicarbonate leads to medium value of pressure about 2000 kPa, since smaller change of mole ratio of reaction accompanying the decomposition reaction.

The importance of the use of pressurized reactor lies in the possibility to superheat the solvent what means that the synthesis can be performed above the boiling point. Moreover, above the boiling point, ethylene glycol becomes virtually transparent for microwaves thus the reaction mixture behaves similarly as ionic liquids that are consisted entirely of ions and ionic effect becomes prevailing reaction mechanism. The ionic effect is considered to be much stronger than the dipolar rotation mechanism and therefore the conversion of raw material into the solid product in the reaction system can be significantly enhanced. Moreover, the use of pressurized microwave reactors with sealed vessels ensure limited amount of oxygen from the ambient to be involved in the reaction system thus preventing the complete oxidation of Fe (II) into the Fe (III) cations that lead to the formation of undesired byproducts such as α - Fe_2O_3 .

4. Conclusions

Simple and effective method for preparation of magnetic material based on Fe_3O_4 in nano- and submicro-dimension has been proposed. Efficiency of this method is to provide the transformation of common solvothermal method using conventional heating into the microwave-assisted method. The change of heating manner causes considerable acceleration of the reaction due to the direct heating of absorbing material and non-thermal effects supporting the transformation of raw material into the final product. Thanks to the use of

pressurized system enabling the control of the synthesis temperature and time as well as indirectly total pressure in the reaction vessel, materials with various properties that reflect the requirements of the specific applications were prepared. Particles ranging from 20 to more than 100 nm based on single-crystals or crystalline assemblies were prepared selecting the type of nucleating agent. It is established that appropriate composition of the starting reaction mixture leads to the formation of the pure one-phase or multiphase materials. Magnetic properties of materials obtained by proposed microwave-assisted method can be tailored as a consequence of the changes in the phase composition, crystalline structure, particles size, shape and their self-organization into clusters. Beside the change of reaction mixture by the variation of nucleating agents, reaction medium represented by ethylene glycol can be modified by the addition of demineralized water. Small portion of demineralized water in the reaction medium results in the reduction of nanoparticles sizes to the one third of original size that significantly reflects in the magnetic properties and can lead to the formation of single domain nanoparticles in superparamagnetic and ferromagnetic states. Even the addition of minor amount of demineralized water to the reaction system can serve as the tool for tailoring the magnetic properties of the final product and makes this microwave-assisted solvothermal method more flexible to the current requirements. Consequently, simplicity, low cost and variability and reproducibility of this method makes it proper candidate for the routine preparation of ferromagnetic and superparamagnetic material in nano-dimensions.

Acknowledgements

This work was supported by the internal grant of TBU in Zlín No.IGA/FT/2013/014 funded from the resource of specific university research.

This article was written with support of Operational Program Education for Competitiveness co-funded by the European Social Fund (ESF) and national budget of Czech Republic, within

the framework of project Advanced Theoretical and Experimental Studies of Polymer Systems (reg. number: CZ.1.07/2.3.00/20.0104).

This article was written with support of Operational Program Research and Development for Innovations co-funded by the European Regional Development Fund (ERDF) and national budget of Czech Republic, within the framework of project Centre of Polymer Systems (reg. number: CZ.1.05/2.1.00/03.0111).

References

- [1] Gupta A K and Gupta M 2005 Synthesis and surface engineering of iron oxide nanoparticles for biomedical applications *Biomaterials* **26** 3995-4021
- [2] Kim D K, Zhang Y, Kehr J, Klason T, Bjelke B and Muhammed M 2001 Characterization and MRI study of surfactant-coated superparamagnetic nanoparticles administered into the rat brain *Journal of Magnetism and Magnetic Materials* **225** 256-61
- [3] Lubbe A S, Alexiou C and Bergemann C 2001 Clinical applications of magnetic drug targeting *Journal of Surgical Research* **95** 200-6
- [4] Cao S W, Zhu Y J, Ma M Y, Li L and Zhang L 2008 Hierarchically nanostructured magnetic hollow spheres of Fe₃O₄ and gamma-Fe₂O₃: Preparation and potential application in drug delivery *Journal of Physical Chemistry C* **112** 1851-6
- [5] Jestin J, Cousin F, Dubois I, Menager C, Schweins R, Oberdisse J and Boue F 2008 Anisotropic reinforcement of nanocomposites tuned by magnetic orientation of the filler network *Advanced Materials* **20** 2533-+
- [6] Scherer C and Neto A M F 2005 Ferrofluids: Properties and applications *Brazilian Journal of Physics* **35** 718-27
- [7] Hu P, Yu L J, Zuo A H, Guo C Y and Yuan F L 2009 Fabrication of Monodisperse Magnetite Hollow Spheres *Journal of Physical Chemistry C* **113** 900-6

- [8] Chen X Y, Zhang Z J, Li X X and Shi C W 2006 Hollow magnetite spheres: Synthesis, characterization, and magnetic properties *Chemical Physics Letters* **422** 294-8
- [9] Zhu L P, Xiao H M, Zhang W D, Yang G and Fu S Y 2008 One-pot template-free synthesis of monodisperse and single-crystal magnetite hollow spheres by a simple solvothermal route *Crystal Growth & Design* **8** 957-63
- [10] Deng H, Li X L, Peng Q, Wang X, Chen J P and Li Y D 2005 Monodisperse magnetic single-crystal ferrite microspheres *Angewandte Chemie-International Edition* **44** 2782-5
- [11] Tsuji M, Hashimoto M, Nishizawa Y, Kubokawa M and Tsuji T 2005 Microwave-assisted synthesis of metallic nanostructures in solution *Chemistry-a European Journal* **11** 440-52
- [12] Loupy A 2002 *Microwaves in organic synthesis – a review* Wiley VHC: Weinheim
- [13] Lidstrom P, Tierney J, Wathey B and Westman J 2001 Microwave assisted organic synthesis - a review (vol 57, pg 9225, 2001) *Tetrahedron* **57** 10229-
- [14] Hong R Y, Pan T T and Li H Z 2006 Microwave synthesis of magnetic Fe₃O₄ nanoparticles used as a precursor of nanocomposites and ferrofluids *Journal of Magnetism and Magnetic Materials* **303** 60-8
- [15] Wang W W, Zhu Y J and Ruan M L 2007 Microwave-assisted synthesis and magnetic property of magnetite and hematite nanoparticles *Journal of Nanoparticle Research* **9** 419-26
- [16] Caillot T, Aymes D, Stuerge D, Viart N and Pourroy G 2002 Microwave flash synthesis of iron and magnetite particles by disproportionation of ferrous alcoholic solutions *Journal of Materials Science* **37** 5153-8
- [17] [2] Kozakova Z, Bazant P, Machovsky M, Babayan V and Kuritka I 2010 Fast Microwave-Assisted Synthesis of Uniform Magnetic Nanoparticles *Acta Physica Polonica A* **118** 948-9

- [18] Gerbec J A, Magana D, Washington A and Strouse G F 2005 Microwave-enhanced reaction rates for nanoparticle synthesis *Journal of the American Chemical Society* **127** 15791-800
- [19] Grosvenor A P, Kobe B A and McIntyre N S 2004 Examination of the oxidation of iron by oxygen using X-ray photoelectron spectroscopy and QUASES (TM) *Surface Science* **565** 151-62
- [20] Guardia P, Labarta A and Batlle X 2011 Tuning the Size, the Shape, and the Magnetic Properties of Iron Oxide Nanoparticles *Journal of Physical Chemistry C* **115** 390-6
- [21] Tang J, Myers M, Bosnick K A and Brus L E 2003 Magnetite Fe₃O₄ nanocrystals: Spectroscopic observation of aqueous oxidation kinetics *Journal of Physical Chemistry B* **107** 7501-6
- [22] Roca A G, Marco J F, Morales M D and Serna C J 2007 Effect of nature and particle size on properties of uniform magnetite and maghemite nanoparticles *Journal of Physical Chemistry C* **111** 18577-84
- [23] Doriguetto A C, Fernandes N G, Persiano A I C, Nunes E, Greneche J M and Fabris J D 2003 Characterization of a natural magnetite *Physics and Chemistry of Minerals* **30** 249-55
- [24] Vandenberghe R E, Barrero C A, da Costa G M, Van San E and De Grave E 2000 Mossbauer characterization of iron oxides and (oxy)hydroxides: the present state of the art *Hyperfine Interactions* **126** 247-59
- [25] Gorski C A and Scherer M M 2009 Influence of Magnetite Stoichiometry on Fe-II Uptake and Nitrobenzene Reduction *Environmental Science & Technology* **43** 3675-80
- [26] Kim W, Suh C Y, Cho S W, Roh K M, Kwon H, Song K and Shon I J 2012 A new method for the identification and quantification of magnetite-maghemite mixture using conventional X-ray diffraction technique *Talanta* **94** 348-52

- [27] Cornell R M, Schwertmann U *The iron oxides: structure, properties, reactions occurrences, and uses* 2003 Wiley-VCH, Weinheim
- [28] Morales M P, Veintemillas-Verdaguer S, Montero M I, Serna C J, Roig A, Casas L, Martinez B and Sandiumenge F 1999 Surface and internal spin canting in gamma-Fe₂O₃ nanoparticles *Chemistry of Materials* **11** 3058-64
- [29] Skomski R 2003 Nanomagnetism *Journal of Physics-Condensed Matter* **15** R841-R96
- [30] Xuan S H, Wang Y X J, Yu J C and Leung K C F 2009 Tuning the Grain Size and Particle Size of Superparamagnetic Fe₃O₄ Microparticles *Chemistry of Materials* **21** 5079-87
- [31] Skrabalak S E, Wiley B J, Kim M, Formo E V and Xia Y N 2008 On the polyol synthesis of silver nanostructures: Glycolaldehyde as a reducing agent *Nano Letters* **8** 2077-81
- [32] Smith W B 2002 Ethylene glycol to acetaldehyde-dehydration or a concerted mechanism *Tetrahedron* **58** 2091-4
- [33] Yan A, Liu X H, Qiu G, Zhang N, Shi R R, Yi R, Tang M and Che R C 2007 A simple solvothermal synthesis and characterization of round-biscuit-like Fe₃O₄ nanoparticles with adjustable sizes *Solid State Communications* **144** 315-8
- [34] Lou X W, Archer L A and Yang Z C 2008 Hollow Micro-/Nanostructures: Synthesis and Applications *Advanced Materials* **20** 3987-4019
- [35] Cao S W, Zhu Y J and Chang J 2008 Fe₃O₄ polyhedral nanoparticles with a high magnetization synthesized in mixed solvent ethylene glycol-water system *New Journal of Chemistry* **32** 1526-30
- [36] Leadbeater N E 2012 *Microwave heating as a tool for sustainable chemistry* CRC Press: Boca Raton

Table 1. Variations of properties of materials prepared with different nucleating agents.

Type of nucleating agent	NH ₃ to H ₂ O molecules ratio	Crystalline impurities	Fe ₃ O ₄ crystallites size by XRD (nm)	Particle Size by TEM (nm)	M _s (emu.g ⁻¹)	H _c (Oe)
		minor				
(NH ₄) ₂ CO ₃	1:0,5	Fe ₂ O ₃ .H ₂ O, Fe ₂ O ₃	84	130	46	2
		minor				
NH ₄ HCO ₃	1:1	Fe ₂ O ₃ .H ₂ O	32	40	75	65
NH ₃ aq.	1:3	-	17	20	76	61
		minor				
NH ₄ Ac	1:0	α-FeO(OH)	42	60	68	67

Figure captions

Figure 1. XRD patterns of magnetic particles prepared with NH_4Ac at various temperatures for 30 minutes.

Figure 2. Distinguishing between the magnetite and maghemite by the detailed analysis of the diffraction peaks localized in angle range $56.5\text{-}57.5^\circ 2\theta$.

Figure 3. SEM figure of material prepared with NH_4Ac for 30 minutes.

Figure 4. TEM images of materials prepared at 220°C for 30 minutes with $(\text{NH}_4)_2\text{CO}_3$ (a), NH_4HCO_3 (b), aq. NH_3 (c) and NH_4Ac (d).

Figure 5. Size distribution histograms of materials prepared at 220°C for 30 minutes with various nucleating agents.

Figure 6. Magnetization curves of materials prepared with NH_4Ac at various temperatures for 30 minutes (left) and at 220°C for 30 minutes with various nucleating agents (right).

Figure 7. TEM image of material prepared with NH_4HCO_3 with the addition of water (left) and magnetization curves of the same material with and without the water addition (right).

Figure 1.

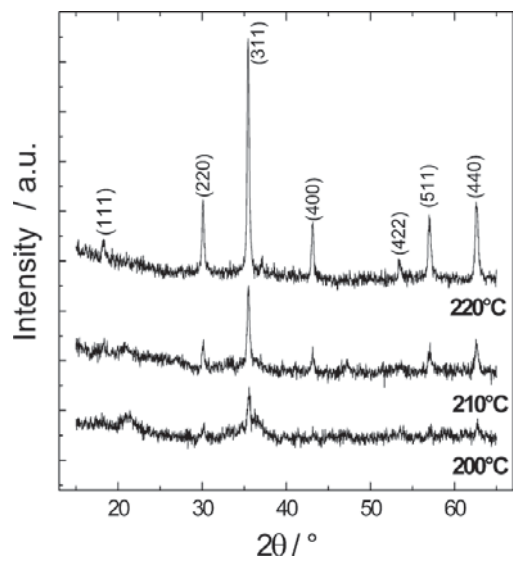


Figure 2.

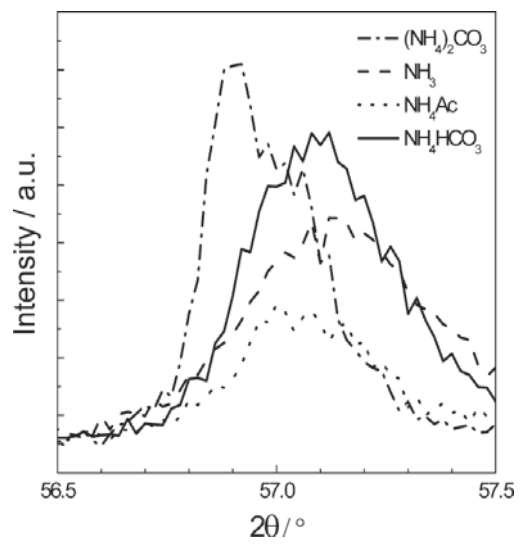


Figure 3.

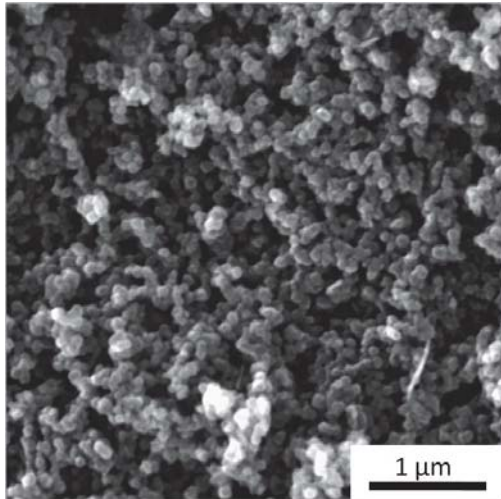


Figure 4.

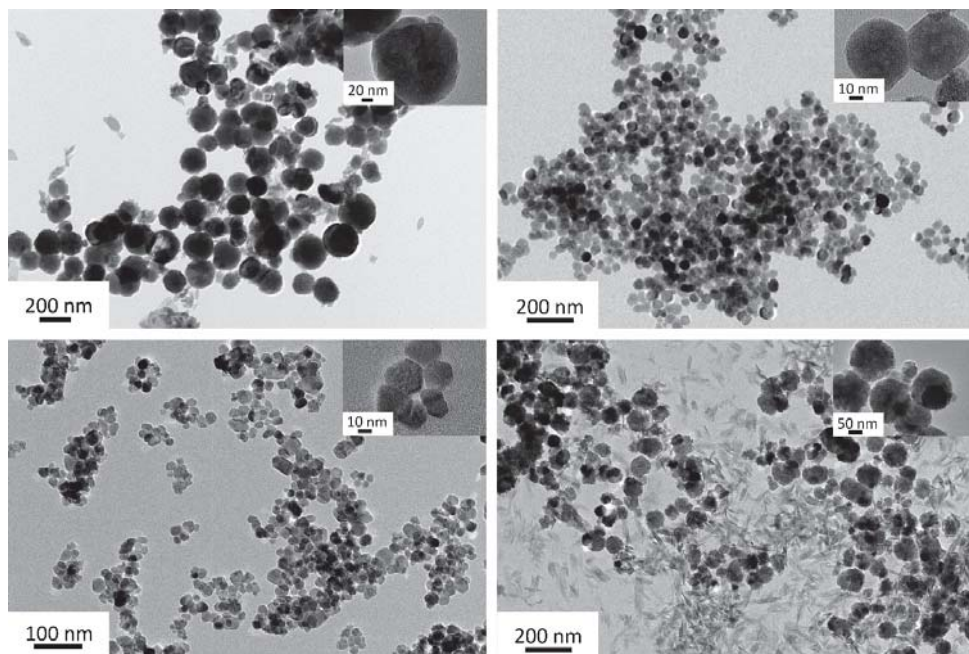


Figure 5.

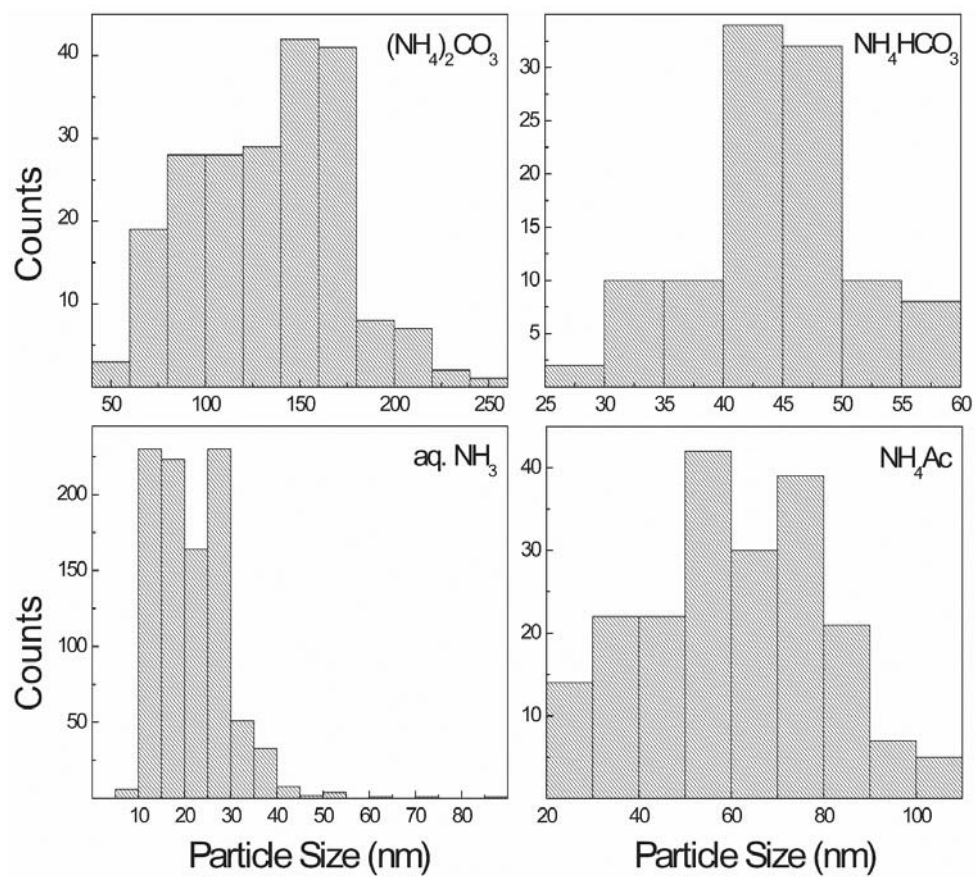


Figure 6.

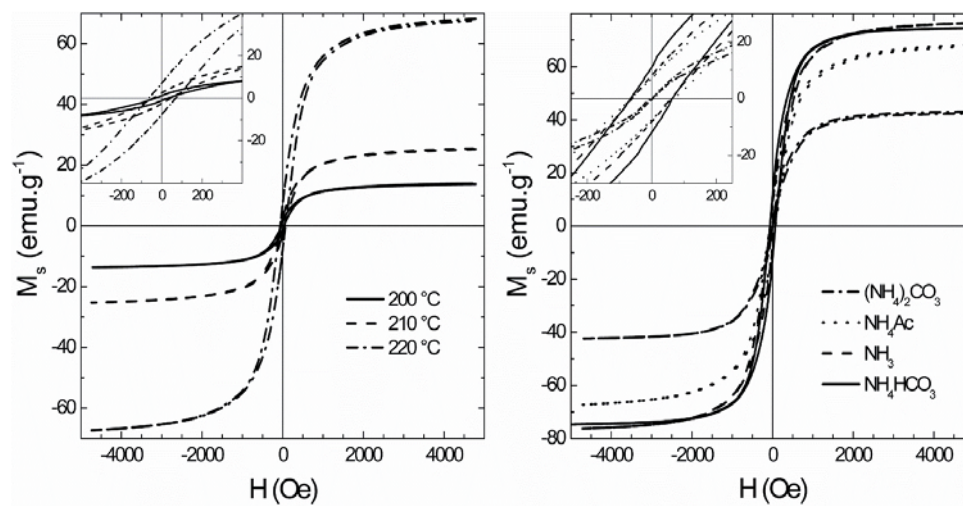


Figure 7.

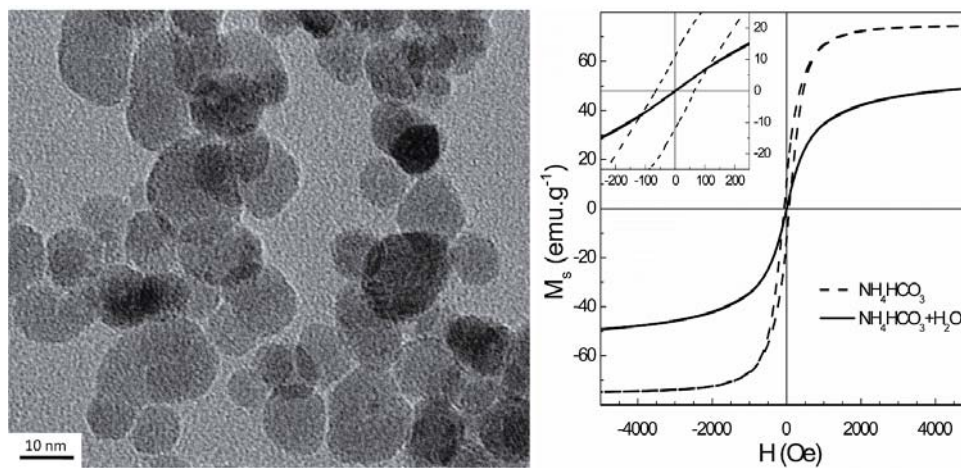


Table 1.

Paper III.

Kozakova, Z.; Kuritka, I.; Babayan, V.; Kazantseva, N.; Pastorek, M., Magnetic Iron Oxide Nanoparticles for High Frequency Applications. *Ieee Transactions on Magnetics* 2013, 49, (3), 995-999. (50%)

Magnetic Iron Oxide Nanoparticles for High Frequency Applications

Zuzana Kozakova^{1,2}, Ivo Kuritka^{1,2}, Vladimir Babayan^{1,2}, Natalia Kazantseva^{1,2}, and Miroslav Pastorek^{2,3}

¹Polymer Center, Faculty of Technology, Tomas Bata University, Zlín 762 72, Czech Republic

²Center of Polymer Systems, University Institute, Tomas Bata University, 760 01 Zlín, Czech Republic

³Department of Polymer Engineering, Faculty of Technology, Tomas Bata University, Zlín 762 72, Czech Republic

Magnetic properties of iron oxide nanoparticles synthesized by microwave solvothermal method are reported. The effect of the nucleating agent on the composition, size, morphology and microstructure of nanoparticles was studied with a view to their correlation with magnetic properties. It is shown that a soft magnetic material with high value of magnetization saturation and high-frequency dispersion of complex permeability can be obtained by an appropriate choice of the nucleating agent.

Index Terms—Inorganic materials, magnetic particles, microwave magnetics, nanoparticles, UHF measurements.

I. INTRODUCTION

IN the past decades, development and characterization of magnetic nanostructures occurred due to their numerous possible applications in many areas like medicine for controlled drug delivery, as a part of ferrofluids for, e.g., dumpers, data storage media, and reading or writing heads, materials for ultra high frequencies (UHF) such as antenna substrates, filters, and others [1]–[6].

The trend to miniaturization, performance increase and preparation of smart and portable communication and computer technologies results in the demand for miniaturization of electromagnetic components such as antennas, as well as for radio-absorbing materials with reduced dimensions and specific gravity [7]–[9]. For this purpose, soft magnetic nanoparticles that can be dispersed in polymer matrix seem to be the proper solution. Especially, ordered systems of superparamagnetic nanoparticles can be useful due to their high value of complex permeability and ferromagnetic resonance frequency in the microwave (MW) frequency range [10]. Nanoparticles with dimensions in the range between quantum and bulk materials are unique by their specific mesoscopic properties due to the finite dimensions. As a result, a noticeable increase in the surface to volume ratio leads to the domination of the surface effect, which can contribute to the orientation of spin and thus influence the magnetic properties [2], [3].

One of possible materials for the MW absorbing application is a magnetite with cubic inverse spinel structure and high magnetic and dielectric losses. Thanks to its simple crystalline structure, magnetite can be relatively simply prepared in laboratories by various already developed methods: chemical coprecipitation [11], hydrothermal [12], solvothermal [13], sonochemical [14], or sol-gel [15] syntheses. Present requirements for the increase of efficiency of synthetic methods and the importance of cost reduction and reduced impact on

environment lead to the development of new effective environmental-friendly methods. Successful experiences in the reaction acceleration with the use of MW irradiation in the field of organic chemistry [16] showed a possible way for preparation of magnetic nanoparticles [17]. Prospective benefit of MW heating techniques was already shown by several authors what motivated us to create a new method that would combine the simplicity and low cost of the ordinary solvothermal method using common non toxic chemicals and relatively low temperatures and, in addition, reduce the reaction times from 12 and more hours to 30 min [18]. A combination of the efficiency and simplicity of the MW-assisted method with the possibility to influence the morphology and the magnetic properties of the resulting product seems to be attractive for preparation of magnetic materials for high frequency applications.

II. EXPERIMENTAL PART

A. Materials and Methods

Soft magnetic materials based on the magnetite nanoparticles were prepared by a simple solvothermal method using ethylene glycol (EG) as a reaction and reduction medium. All the chemicals used in the method were obtained from Penta Ltd. (Czech Republic) in analytical purity and were used without further purification. In a typical procedure, ferric chloride as a source of Fe^{3+} cations (5 mmol) was dissolved in EG ($\text{C}_2\text{H}_6\text{O}_2$, 60 mL) and two different ammonium salts, ammonium bicarbonate (NH_4HCO_3 , 50 mmol) and ammonium carbonate ($(\text{NH}_4)_2\text{CO}_3$, 25 mmol) were added in order to serve as nucleation and precipitation agents. Moreover, one synthesis was modified by the water addition (2 mL) into the reaction system. Synthetic reactions were carried out in a MW pressurized reactor that enabled the control of reaction temperature due to the regulation of MW power. The selected reaction time of 30 minutes was considered to be sufficient due to the highly effective conversion of raw material into the product according to the previous experience [18]. The pressure of the synthesis can be influenced indirectly by setting the solvent and the operating temperature, as well as by adding of chemicals and the filling level of reaction vessels. In our case, the temperature was set to 220 °C, which is slightly above the boiling point of EG (197.3 °C), filling was 60 mL of EG to the 100 mL reaction vessel, and then the pressure during the synthesis varied from

Manuscript received September 14, 2012; revised October 29, 2012; accepted November 08, 2012. Date of current version February 20, 2013. Corresponding author: Z. Kozakova (e-mail: zkozakova@ft.utb.cz).

Color versions of one or more of the figures in this paper are available online at <http://ieeexplore.ieee.org>.

Digital Object Identifier 10.1109/TMAG.2012.2228471

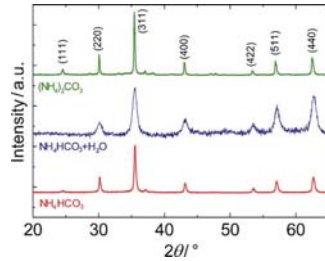


Fig. 1. XRD patterns of samples prepared by different nucleating agents.

900 to 3600 KPa depending on the added nucleating agent and the composition of the reaction medium (water content). The product obtained was separated by a permanent magnet and washed with water and ethanol several times by decantation.

B. Characterization

The structure and the phase composition of the materials prepared was determined by X-Ray diffraction (XRD, Bruker D8 diffractometer with SOL-X energy dispersive detector, and PANalytical X'Pert PRO) with $\text{CuK}\alpha$ radiation. The diffraction patterns were analyzed by the Rietveld method in FULLPROF software in order to determine crystallites size and composition of prepared materials. The particle size and the morphology, as well as the morphology of nanoparticle ensembles, were investigated with transmission electron microscopy (JEOL 1200, JEOL). Particle size was estimated by the TEM images analysis. The magnetization curves of the samples in the form of powders were measured on a VSM 7407 vibrating sample magnetometer (Lake Shore) at room temperature in air atmosphere. The complex magnetic permeability spectra of materials were studied in the frequency range from 1 MHz to 3 GHz by the impedance method using an Agilent E4991A Impedance/Material Analyzer. The permeability measurements were performed on toroidal samples with an inner diameter of 3.1 mm and an outer diameter of 8 mm. In order to measure the magnetic spectra, magnetic particles were mixed with 10 wt. % of polyvinyl alcohol, dried, and then compressed into toroids at 200 MPa.

III. RESULTS AND DISCUSSION

A. Structure and Morphology

XRD patterns of synthesized materials, shown in Fig. 1, can be attributed to the spinel structure of magnetite (Fe_3O_4) and/or maghemite ($\gamma\text{-Fe}_2\text{O}_3$) (these two magnetic phases are considered not to be distinguishable by XRD analysis). Further deeper analysis of the XRD results by the Rietveld method gave a detailed description of the crystalline phase composition of the materials obtained. Thus, the ammonium bicarbonate nucleated sample is composed of magnetite phase with minor fraction of $\text{Fe}_2\text{O}_3 \cdot \text{H}_2\text{O}$ (iron oxide hydrate) in accordance with the presence of a distinct peak in the position $24.3\ 2\theta$ and other peaks of low intensity. The mean crystal size of the particles calculated from the XRD peaks is about 32 nm. In the case of material prepared by adding of demineralized water into the system

nucleated by ammonium bicarbonate, these impurity peaks disappear. As a result, along with magnetite, this material contains a small amount of $\alpha\text{-Fe}_2\text{O}_3$ (hematite), as follows from the peak of low intensity in the position $49.2\ 2\theta$. The width and the low intensity of the peaks points to the small size of nanoparticles, which, according to calculations by the Rietveld method, is about 9 nm. The material obtained with the use of ammonium carbonate is also based on magnetite; nevertheless, the XRD patterns of this material exhibit low-intensity peaks observed at different angles ($24.3\ 2\theta$, $38.3\ 2\theta$, etc.) belonging to the iron oxide hydrate, hematite and goethite.

In the case of presented method, Fe^{3+} are dosed into the reaction system by $\text{FeCl}_3 \cdot 6\text{H}_2\text{O}$ and thus formation of maghemite, hematite and iron oxide hydroxide is probable via the hydrolysis of starting materials, subsequent formation of iron (III) hydroxide and its dehydration. However, presence of ethylene glycol causes reduction of Fe^{3+} into Fe^{2+} and so magnetite can occur in the system. From this reason, both, magnetite and maghemite phases are expected to be coexisting in presented material. Furthermore, goethite can occur in the system by partial dehydration of iron (III) hydroxide. Even if the reaction vessels are sealed, their content is not completely rid from oxygen and small amount can act in synthetic reactions. Therefore, under the heat treatment, magnetite can be oxidized into maghemite and about 200°C also to hematite [19]. Moreover, goethite can be formed by the oxidation of iron (II) hydroxide.

Fig. 2 shows the TEM images of magnetic particles prepared with the use of different nucleation agents. One can see that the use of ammonium bicarbonate leads to the formation of polyhedral single crystals with an average size of 40 nm, which is the value close to 32 nm obtained by XRD analysis. Moreover, the presence of crystalline impurities is also evident from the TEM image since they differ from the magnetite phase in their morphology. The addition of demineralized water to the reaction system lead to a decrease in the particle size from 40 to 10 nm; however, the shape of the magnetic nanoparticles remains similar to the shape of particles obtained without addition of water [Fig. 2(b)]. In advance, a relatively narrow size distribution is observed. Next, the size and shape uniformity of the nanoparticles points to the phase purity and homogeneity of the material prepared. An ammonium carbonate nucleated sample contains an appreciable amount of crystalline impurities [Fig. 2(c)] along with the nanoparticles of magnetite with an average size of 130 nm. Moreover, broad particle size distribution is evident since the presence of very small particles, except for those with a size greater than 100 nm, is observed. Microscopic observations are in agreement with the XRD phase analysis. The observed difference between TEM and XRD results can be caused by that: XRD analysis gave an average grain size of Fe_3O_4 , and TEM image indicates average particles size.

B. Magnetic Properties

Fig. 3 demonstrates the magnetization curves of iron oxides based on the materials prepared with the use of different nucleating agents. When ammonium bicarbonate is used, a soft magnetic material with a narrow hysteresis loop (coercivity H_c of 65 Oe) and high saturation magnetization M_s of $75\ \text{emu}\cdot\text{g}^{-1}$ was

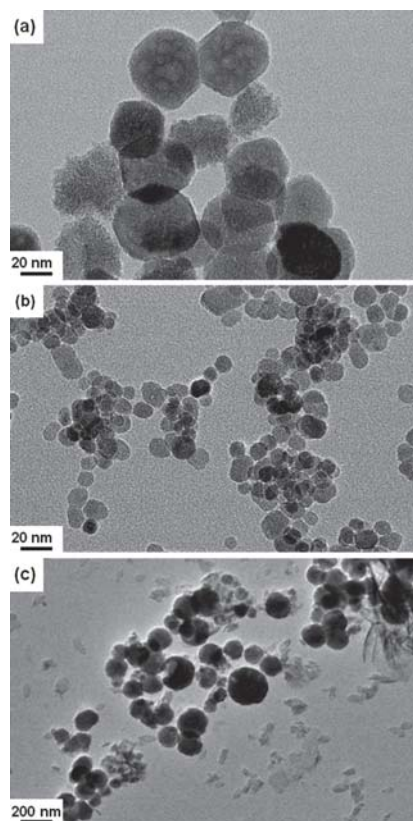


Fig. 2. TEM images of particles prepared with (a) NH_4HCO_3 , (b) $\text{NH}_4\text{HCO}_3 + \text{H}_2\text{O}$, and (c) $(\text{NH}_4)_2\text{CO}_3$.

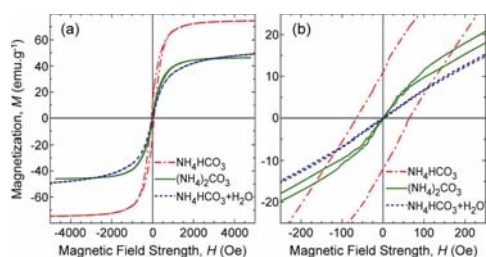


Fig. 3. (a) Hysteresis loops of materials obtained, and (b) the behavior of materials at low fields.

obtained. However, the addition of small amount of demineralized water to the reaction system (keeping other parameters unchanged) reduces the values of the M_s down to $52 \text{ emu}\cdot\text{g}^{-1}$ and H_c to 2 Oe, and drastically changes the form of the hysteresis loops. The material prepared with ammonium carbonate exhibits a lower value of M_s , reaching only $46 \text{ emu}\cdot\text{g}^{-1}$.

The decrease in the M_s of nanoparticles is usually correlated with the decrease in average grain and particle sizes. Moreover, the decrease in the M_s is usually accompanied by increased

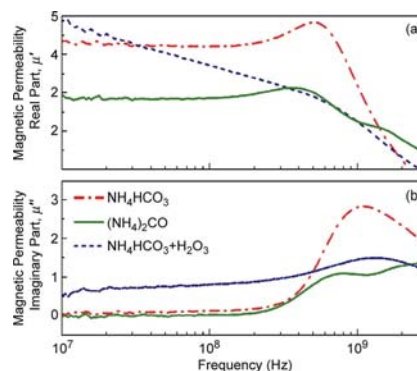


Fig. 4. Magnetic spectra of materials obtained. (a) Real part of complex magnetic permeability and (b) imaginary part.

H_c . It is explained by the core-shell structure of nanoparticles where the shell is characterized by significantly low magnetic properties [20], [21]. However, this trend is not observed in the case of iron oxide nanoparticles obtained in current work since they differ in composition. Here, a presence of coexisting phases (magnetite, maghemite, hematite, and goethite) has the main impact on the magnetic properties of iron oxide nanoparticles. It is known that formation of coexisting phases tends to change the hysteresis loop shape and decrease the M_s of nanomagnets [20]. Thus, the sample prepared by using ammonium carbonate shows the lower value of M_s and atypical shapes of the hysteresis loop due to a significant amount of hematite and goethite which was revealed by XRD measurements.

Dynamic magnetic properties allow better understanding of the magnetization mechanisms in magnetic nanostructures, as well as yield important frequency dependent characteristics for potential application in the high frequency range. Fig. 4 shows the frequency dependence of the complex permeability μ (magnetic spectra) for all materials. The complex permeability dispersion of ammonium bicarbonate and ammonium carbonate nucleated samples occupies a frequency interval from 300 MHz to 3 GHz, whereas a sample nucleated by ammonium bicarbonate with additional amount of demineralized water is characterized by a much broader frequency region of dispersion, from 10 MHz to 3 GHz. Moreover, the magnetic spectrum of ammonium carbonate nucleated sample has two regions of permeability dispersion with resonance frequencies at approximately 700 MHz and 3 GHz. This fact confirms the presence of different coexisting in this sample. Anyway, the permeability dispersion of all samples occurs in the frequency range of the natural ferromagnetic resonance (NFR), where the magnetization processes are determined by magnetization rotation in the effective magnetic anisotropy fields and demagnetizing fields [22]. Experimental evidence of NFR for single-domain specimens is suggested by Rado *et al.* [23], which has been further confirmed by numerous experimental and theoretical works. For example, the complex permeability spectra of composites filled with micro- and nanoparticles of barium ferrite were studied in [24]. In order to determine the contribution of domain wall resonance and NFR, the experimental magnetic spectra of these

TABLE I
STRUCTURAL AND MAGNETIC PROPERTIES OF IRON OXIDE NANOPARTICLES
OBTAINED BY DIFFERENT NUCLEATING AGENTS

Type of nucleating agent	Sample composition	Average grain size XRD (nm)	Average particle size TEM (nm)	M_s (emu.g ⁻¹)	H_c (Oe)	Gyromagnetic resonance f_R (GHz)	Magnetic losses at f_R
(NH ₄) ₂ CO ₃	Fe ₃ O ₄ (major) Fe ₂ O ₃ ·H ₂ O, α-Fe ₂ O ₃ (minor)	84	130	46	2	-0.7 and 3	-1.0
NH ₄ HCO ₃	Fe ₃ O ₄ (major) Fe ₂ O ₃ ·H ₂ O (minor)	32	40	75	65	-1	-2.5
NH ₄ HCO ₃ +H ₂ O	Fe ₃ O ₄ (major) α-Fe ₂ O ₃ (minor)	9	10	52	2	-1	-1.0

composites were approximated by the frequency dispersion formula [25]. The results of approximation have shown that for composites with nanoparticles, it is only the gyromagnetic susceptibility (permeability) that contributes to the total susceptibility. The similar results were obtained for composites filled with nanoparticles of magnetite which show the absorption peak in GHz region [26].

The magnetic anisotropy of nanoparticles includes various components: magnetocrystalline anisotropy, shape anisotropy, exchange magnetic anisotropy, surface magnetic anisotropy, anisotropy associated with magnetoelastic stresses, etc. [22]. Therefore, it is difficult to recognize the concrete factor responsible for the change in the magnetic properties of magnetic nanostructures. However, there is a correlation between μ and M_s of the samples obtained. The highest value of μ is demonstrated by a sample nucleated by ammonium bicarbonate, which, in turn, is characterized by the highest value of M_s . The low value of M_s of other two samples manifests itself in the low value of μ .

According to the results obtained from the XRD measurements, TEM analyses, and magnetic properties, the role of the precipitating and nucleating agents is crucial for tailoring the magnetic properties of iron oxide nanoparticles, since they change the composition, grain and particles sizes. Their action is based on the change of the reaction conditions such as pressure, total alkalinity thus ratio of FeCl₃·6H₂O hydrolysis [27] and the dosage of additional water into the reaction system. The influence of additional water was demonstrated to be important in the formation mechanism. Since other parameters were remained unchanged and the pressure during the synthesis did not change in serious rate (from 3100 to 3250 kPa) we consider two mechanisms of water impact to be prevailing. On the one hand, water can decrease viscosity of the system and increase the rate of nucleation stage and thus lead to the formation of many small crystals, on the other hand, solvation layer can be formed on the surface of particles preventing them from aggregation. The variation of the main properties of the prepared materials due to the variation of the nucleating and precipitating agents is illustrated in Table I.

IV. CONCLUSION

Simple and effective method for preparation of magnetic iron oxide nanoparticles has been demonstrated. A modified solvothermal synthesis using microwave heating reduces the reaction time from several hours to several minutes, increases the yield of the method, and provides a simple means for the variation of the material properties.

A strong influence of the nucleation agent and the composition of reaction medium has been established. These factors play a crucial role in the product composition, the presence of coexisting phases that differ in magnetic properties, and morphology of nanoparticles. As a result, the magnetic properties can be tailored for a particular application.

It is important for practice that soft magnetic material with a single-domain structure can be prepared in a single step. The relatively high saturation magnetization and complex permeability dispersion in the high-frequency range make them proper candidates for high frequency applications.

Moreover, the low cost and low toxicity of chemicals, along with the good economical and environmental character of microwave-assisted synthesis, make the method promising for the commercial and laboratory applications.

ACKNOWLEDGMENT

This work was supported in part by the Tomas Bata University, Zlín, Czech Republic, under internal Grant IGA/FT/2012/039, funded from the resource of specific university research; and by the Operational Program Research and Development for Innovations, cofunded by the European Regional Development Fund (ERDF) and the national budget of Czech Republic, within the framework of Project Center of Polymer Systems (Reg. No. CZ.1.05/2.1.00/03.0111). This contribution/article was written with support of the Operational Program Education for Competitiveness, cofunded by the European Social Fund (ESF) and the national budget of Czech Republic, within the framework of project Advanced Theoretical and Experimental Studies of Polymer Systems (Reg. No. CZ.1.07/2.3.00/20.0104).

REFERENCES

- [1] A. Thakur, P. Thakur, and J. H. Hsu, "Smart magnetodielectric nano-materials for the very high frequency applications," *J. Alloys Compounds*, vol. 509, no. 17, pp. 5315–5319, Apr. 2011.
- [2] Y. Koseoglu, H. Kavas, and B. Aktas, "Surface effects on magnetic properties of superparamagnetic magnetite nanoparticles," *Phys. Status Solidi A—Appl. Mater. Sci.*, vol. 203, no. 7, pp. 1595–1601, May 2006.
- [3] S. Kolev, T. Koutzarova, A. Yanev, C. Ghelev, and I. Nedkov, "Microwave properties of polymer composites containing combinations of micro- and nano-sized magnetic fillers," *J. Nanosci. Nanotechnol.*, vol. 8, no. 2, pp. 650–654, Feb. 2008.
- [4] A. Tomitaka, T. Koshi, S. Hatsugai, T. Yamada, and Y. Takemura, "Magnetic characterization of surface-coated magnetic nanoparticles for biomedical application," *J. Magn. Magn. Mater.*, vol. 323, no. 10, pp. 1398–1403, May 2011.
- [5] M. Sedlacik, V. Pavlinek, P. Saha, P. Svrčinová, P. Filip, and J. Stejskal, "Rheological properties of magnetorheological suspensions based on core-shell structured polyaniline-coated carbonyl iron particles," *Smart Mater. Struct.*, vol. 19, no. 11, Nov. 2010.
- [6] M. Pardavi-Horvath, "Microwave applications of soft ferrites," *J. Magn. Magn. Mater.*, vol. 215, pp. 171–183, Jun. 2000.

- [7] D. Souriou, J. L. Mattei, A. Chevalier, and P. Queffelec, "Influential parameters on electromagnetic properties of nickel-zinc ferrites for antenna miniaturization," *J. Appl. Phys.*, vol. 107, no. 9, May 2010.
- [8] H. Pang, M. Fan, and Z. F. He, "A method for analyzing the microwave absorption properties of magnetic materials," *J. Magn. Magn. Mater.*, vol. 324, no. 16, pp. 2492–2495, Aug. 2012.
- [9] Y. Shirakata, N. Hidaka, M. Ishitsuka, A. Teramoto, and T. Ohmi, "High permeability and low loss Ni-Fe composite material for high-frequency applications," *IEEE Trans. Magn.*, vol. 44, no. 9, pp. 2100–2106, Sep. 2008.
- [10] D. Hasegawa, H. T. Yang, T. Ogawa, and M. Takahashi, "Challenge of ultra high frequency limit of permeability for magnetic nanoparticle assembly with organic polymer-application of superparamagnetism," *J. Magn. Magn. Mater.*, vol. 321, no. 7, pp. 746–749, Apr. 2009.
- [11] U. S. Khan, N. S. Khattak, A. Rahman, and F. Khan, "Optimal method for preparation of magnetite nanoparticles," *J. Chem. Soc. Pakistan*, vol. 33, no. 5, pp. 628–633, Oct. 2011.
- [12] Q. Dong, N. Kumada, Y. Yonesaki, T. Takei, and N. Kinomura, "Hydrothermal synthesis of (Fe_3O_4) particles with various shapes," *J. Ceramic Soc. Japan*, vol. 117, no. 1368, pp. 881–886, Aug. 2009.
- [13] P. Hu, L. J. Yu, A. H. Zuo, C. Y. Guo, and F. L. Yuan, "Fabrication of monodisperse magnetite hollow spheres," *J. Phys. Chem. C*, vol. 113, no. 3, pp. 900–906, Jan. 2009.
- [14] M. N. Islam, L. V. Phong, J. R. Jeong, and C. Kim, "A facile route to sonochemical synthesis of magnetic iron oxide (Fe_3O_4) nanoparticles," *Thin Solid Films*, vol. 519, no. 23, pp. 8277–8279, Sep. 2011.
- [15] H. Z. Qi, B. Yan, C. K. Li, and W. Lu, "Synthesis and characterization of water-soluble magnetite nanocrystals via one-step sol-gel pathway," *Sci. China-Phys. Mech. Astronomy*, vol. 54, no. 7, pp. 1239–1243, Jul. 2011.
- [16] S. Mallakpour and Z. Rafiee, "Application of microwave-assisted reactions in step-growth polymerization: A review," *Iranian Polymer J.*, vol. 17, no. 12, pp. 907–935, Dec. 2008.
- [17] M. Tsuji, M. Hashimoto, Y. Nishizawa, M. Kubokawa, and T. Tsuji, "Microwave-assisted synthesis of metallic nanostructures in solution," *Chem.-A Eur. J.*, vol. 11, no. 2, pp. 440–452, Jan. 2005.
- [18] Z. Kozakova, P. Bazant, M. Machovsky, V. Babayan, and I. Kuritka, "Fast microwave-assisted synthesis of uniform magnetic nanoparticles," *Acta Phys. Polonica A*, vol. 118, no. 5, pp. 948–949, Nov. 2010.
- [19] P. Russo, D. Acierno, M. Palomba, G. Carotenuto, R. Rosa, A. Rizzuti, and C. Leonelli, "Ultrafine magnetite nanopowder: Synthesis, characterization, and preliminary use as filler of polymethylmethacrylate nanocomposites," *J. Nanotechnol.*, vol. 2012, p. 728326, 2012.
- [20] R. Skomski, "Nanomagnetics," *J. Phys.-Condens. Matter*, vol. 15, no. 20, pp. R841–R896, May 2003.
- [21] S. P. Gubin, Y. A. Koksharov, G. B. Khomutov, and G. Y. Yurkov, "Magnetic nanoparticles: Preparation, structure and properties," *Russian Chem. Rev.*, vol. 74, no. 6, pp. 489–520, Jun. 2007.
- [22] S. Chikazumi and C. D. Graham, *Physics of Ferromagnetism*, 2nd ed. Oxford; New York: Clarendon; Oxford Univ. Press, 1997.
- [23] G. T. Rado, R. W. Wright, and W. H. Emerson, "Ferromagnetism at very high frequencies. 3. 2 mechanisms of dispersion in a ferrite," *Phys. Rev.*, vol. 80, pp. 273–280, 1950.
- [24] Z. W. Li, G. Q. Lin, L. F. Chen, Y. P. Wu, and C. K. Ong, "Size effect on the static and dynamic magnetic properties of W-type barium ferrite composites—From microparticles to nanoparticles," *J. Appl. Phys.*, vol. 98, no. 9, p. 094310, Nov. 2005.
- [25] T. T. Nakamura, T. Tsutaoka, and K. Hatakeyama, "Frequency dispersion of permeability in ferrite composite-materials," *J. Magn. Magn. Mater.*, vol. 138, pp. 319–328, Dec. 1994.
- [26] S. Kolev, A. Yanev, and I. Nedkov, "Microwave absorption of ferrite powders in a polymer matrix," *Phys. Status Solidi C—Current Topics Solid State Phys.*, vol. 3, no. 5, pp. 1308–1315, 2006.
- [27] S. H. Xuan, F. Wang, Y. X. J. Wang, J. C. Yu, and K. C. F. Leung, "Facile synthesis of size-controllable monodispersed ferrite nanospheres," *J. Mater. Chem.*, vol. 20, pp. 5086–5094, 2010.

Paper IV.

Sedlacik, M.; Moucka, R.; Kozakova, Z.; Kazantseva, N. E.; Pavlinek, V.; Kuritka, I.; Kaman, O.; Peer, P., Correlation of structural and magnetic properties of Fe₃O₄ nanoparticles with their calorimetric and magnetorheological performance. *Journal of Magnetism and Magnetic Materials* 2013, 326, 7-13. (30%)



Correlation of structural and magnetic properties of Fe₃O₄ nanoparticles with their calorimetric and magnetorheological performance

M. Sedlacik^{a,b}, R. Moucka^{a,b}, Z. Kozakova^{a,b}, N.E. Kazantseva^{a,b,*},
V. Pavlinek^{a,b}, I. Kuritka^{a,b}, O. Kaman^c, P. Peer^d

^a Centre of Polymer Systems, University Institute, Tomas Bata University in Zlin, Nad Ovcirnou 3685, 760 01 Zlin, Czech Republic

^b Polymer Centre, Faculty of Technology, Tomas Bata University in Zlin, namesti T.G. Masaryka 275, 762 72 Zlin, Czech Republic

^c Institute of Physics, AS CR, v.v.i., Cukrovarnicka 10/112, 162 53, Prague 6, Czech Republic

^d Institute of Hydrodynamics, AS CR, v.v.i., Pod Patankou 5, 166 12, Prague 6, Czech Republic

ARTICLE INFO

Article history:

Received 4 May 2012

Received in revised form

21 August 2012

Available online 31 August 2012

Keywords:

Iron oxide

Nanoparticle

Ferrofluid

Hyperthermia

Embolization

Microwave synthesis

Magnetorheology

ABSTRACT

Magnetic particles based on Fe₃O₄ were prepared by means of the microwave solvothermal method under different reaction conditions with the intention of their utilization as a mediator in magnetic hyperthermia and material for reducing blood flow in the tumor area. The synthesized particles were characterized in terms of their structure, size, shape, and magnetic properties with an emphasis on the correlation between particle morphology and magnetic properties. Most importantly, their heat development when exposed to an alternating magnetic field was determined, as well as the rheological behavior of their suspensions under static magnetic field. Reasonable heat development and substantial flow resistance under the effect of magnetic field indicate their potential for applications such as hyperthermia mediators or substances for temporary embolization.

© 2012 Elsevier B.V. All rights reserved.

1. Introduction

Magnetic nanoparticles provide attractive possibilities in diagnostic and therapeutic biomedical applications. In diagnostics they can serve as contrast agents for magnetic resonance imaging used for detection of a disease in its early stage [1]. In therapeutic applications magnetic nanoparticles can be used for drug delivery and its subsequent triggered release [2]. By an external magnetic field the particles are delivered to the desired target area, in which they are fixed due to the surface functionalization by antibodies. This is followed by drug release, thus reducing the dosage of the medicine. Apart from these applications, magnetic nanoparticles can be employed for treatment of cancer.

Conventional cancer therapies comprise mainly surgery, radiotherapy and chemotherapy. While surgery is restricted to the cases of localized tumors and lack of distant metastases, radio- and chemotherapies strongly burden patient's organs. Recently, hyperthermia has evoked a tremendous increase in the interest of many researchers. Hyperthermic methods are based on cancer

cells undergoing irreversible changes and consequent necrosis and apoptosis when being exposed to temperatures above 42 °C. This occurs due to insufficient oxygen supply to the malignant tissue via blood vessels, whereas healthy cells are more temperature resistant [3]. The heat is most frequently delivered by means of electromagnetic radiation employing various wavelengths from radiofrequency [4] up to microwave region [5], even though ultrasound is used as well [6]. Selective heating of tumor cells proves to be an issue due to their large heterogeneity in terms of electrical conductivity which results in undesired heating of healthy cells.

The issue of localized heating can be solved by introducing magnetic particles to the treated site and their subsequent excitation by an alternating magnetic field. The specificity of this approach is based on the fact that the tissue is inherently non-magnetic hence and transparent to magnetic field. This method is called magnetic hyperthermia [7–9].

The ability to generate heat induced by external alternating magnetic field heating strongly depends on the characteristics of the field, i.e., amplitude and frequency, concentration of particles, and their intrinsic magnetic properties, which in turn vary with number of factors, their size and microstructure being only some of them. When disregarding eddy-current and dielectric losses, the main heating mechanisms comprise hysteresis

* Corresponding author at: Centre of Polymer Systems, University Institute, Tomas Bata University in Zlin, Nad Ovcirnou 3685, 760 01 Zlin, Czech Republic. Tel.: +420 576 038 114; fax: +420 576 031 444.
E-mail address: nekazan@yahoo.com (N.E. Kazantseva).

losses and relaxation processes, i.e. Neel relaxation and Brownian rotation [10].

Hysteresis losses are determined by magnetic anisotropy, which for nanosized materials consists of magnetocrystalline, shape and magnetic surface anisotropies, as well as strain induced anisotropy (magnetoelastic anisotropy) [11]. Magnetocrystalline anisotropy depends on the ratio of crystal-field energy to spin-orbital coupling and manifests itself by the rotation of magnetization along certain crystallographic directions (easy axis of magnetization). Shape and surface anisotropies play an important role in the reduction of magnetization of nanomagnets compared with bulk counterparts. The shape anisotropy causes demagnetizing field H_D , which for example for spherical particles is $H_D = -M_s/3$, where M_s is saturation magnetization [12]. The reason of M_s reduction due to the surface anisotropy is that with decrease of particle size the thickness of the shell with spin disorder (so-called dead layer) increases because of antiferromagnetic interactions. It leads to the hardening of particle surface and as a result the strain (magnetoelastic) anisotropy appears. Additionally, magnetoelastic anisotropy may occur due to the mechanical stresses induced in nanoparticles during synthesis.

The magnetic anisotropy energy of a particle is proportional, in first approximation, to the particle volume due to the magnetocrystalline and shape anisotropy [13]. With decreasing particle size to the size around single-domain-multidomain limit, magnetic anisotropy becomes comparable to thermal energy; thus the total magnetization of particles behaves as a super-spin which reverses coherently along the anisotropy direction. In an ensemble of single-domain particles the heat is mostly generated by relaxation of magnetic moments back to their equilibrium orientations cyclically (Neel relaxation) or by the rotational friction between the particles and the medium (Brownian relaxation) when exposed to AC magnetic field and, thus, the particles arrangement in carrier liquid is also an important factor [8,14].

The use of magnetic nanoparticles in magnetic hyperthermia imposes the following restrictions. The particles should have high monodispersity for effective heat generation and not exceed approximately 150–200 nm, because the larger the particles, the faster their elimination from the bloodstream [15]. It is also essential to take into account biomedical limitations, namely the restriction on using e.g. Ba, Mn or Co based magnetic materials. The biocompatibility has to be, consequently, guaranteed by surface functionalization [16]. On the other hand, recent studies with iron- and iron-oxide-based magnetizable particles showed no adverse effects on human body [17].

Other approaches to cancer therapy using magnetic nanoparticles include reducing blood circulation in the tumor area by clogging up blood vessels, which are feeding the tumor, with ferrofluid under an applied magnetic field [18,19]. The efficiency of this method is based on impairing *angiogenesis*, i.e., formation of new blood vessels that supply oxygen and nutrients to cancerous tissues. Ferrofluid becomes “solid-like”, its viscosity increases by several orders of magnitude when exposed to an external magnetic field, as magnetized particles are aligned into chain-like structures [20]. Such an inhibition of blood supply to the tumor in turn induces its necrosis. The properties of chain-like structures are proportional to the applied field strength, the magnetic susceptibility, and particles concentration. Unlike a normal embolus that stays solid once formed, the thermal energy causes the disintegration of aligned particles into randomly dispersed liquid immediately after the field has been removed [21,22].

The synthesis of uniform magnetic nanoparticles suitable for above mentioned applications is usually quite complicated or time consuming [23,24]. Recently, microwave (MW) dielectric heating techniques have been studied as a proper alternative to conventional heating. These methods are based on the

reorientation of dipolar molecules with respect to a dynamic electric field applied and, subsequently, transforming their energy into heat by molecular friction [25]. The use of MW synthesis can shorten the reaction time to several minutes, since the energy is directly transferred to the microwave absorbing materials. Moreover, in contrast to conventional heating, nucleation and growth conditions are uniform as they are not negatively affected by conduction or convection of the heat through the wall of reaction vessel or reaction mixture.

In the present study, magnetic properties, heating efficiency and magnetorheological behavior of Fe_3O_4 nanoparticles prepared via a simple and rapid one-pot solvothermal synthesis utilizing pressurized MW reactor, were investigated. Benefit of this method lies in obtaining particles with relatively narrow size distribution, whose mean size can be controlled through the choice of nucleating agent and reaction temperature.

2. Experimental

2.1. Materials

Iron(III) chloride hexahydrate $FeCl_3 \cdot 6H_2O$, ammonium acetate $NH_4C_2H_3O_2$, ammonium carbonate $(NH_4)_2CO_3$, aqueous ammonia solution (approximately 25 wt%), and ethylene glycol $C_2H_4(OH)_2$ used for the synthesis of Fe_3O_4 nanoparticles were of reagent grade and purchased from Penta Ltd. (Czech Republic). Other chemicals included distilled water and ethanol.

2.2. Synthesis of magnetic nanoparticles

Fe_3O_4 nanoparticles with rather narrow particle size distribution were obtained using the MW irradiation-assisted solvothermal method in ethylene glycol solution. In a typical preparation, 5 mmol of $FeCl_3 \cdot 6H_2O$ was dissolved in 60 ml of ethylene glycol. After that, a nucleating agent (50 mmol of $NH_4C_2H_3O_2$, 25 mmol of $(NH_4)_2CO_3$, or 50 mmol of NH_3 in the form of aqueous solution) was added to the mixture and the formed solution was placed in a 100 ml Teflon reaction vessel (XP-1500 Plus, CEM, USA). The solvothermal reaction was carried out in a MW reactor (Mars 5, CEM, USA) at 220 °C for 30 min and the yield was nearly 100%. Subsequently, the system was cooled naturally and the as-obtained product was collected with the help of a magnet and washed with distilled water and ethanol several times. The samples were dried under vacuum at 80 °C.

2.3. Characterization of prepared particles

The structural characteristics of prepared particles were examined via X-ray diffraction (XRD) patterns collected on a D8 diffractometer (Bruker AXS GmbH, Germany) with CuK_{α} radiation ($\lambda = 0.154$ nm) in the reflection mode and 2θ range from 20° to 100°. The Rietveld method was used for calculation of mean crystallite size (d_{XRD}). The particle size and shape were further observed with a transmission electron microscope (TEM, JEOL 1200, JEOL Ltd., Japan). Magnetic properties under static magnetic field were studied by using a vibration sample magnetometer (VSM, EG&G PARC 704, Lake Shore, USA) at a field of 5 kOe and 25 °C. The content of iron in the samples was estimated via an inductively coupled plasma optical emission spectrometer (ICP-OES, Jobin-Yvon, France).

The frequency dispersion of complex permeability μ (magnetic spectra) of the samples was studied in the frequency range from 1 MHz to 3 GHz by the impedance method using an Impedance/Material Analyser (Agilent E4991A, USA). The measurements were carried out on toroidal samples (mixture of nanoparticles with polyvinyl alcohol solution was dried and then compressed at

200 MPa) with inner diameter of 3.1 mm and an outer diameter of 8 mm.

2.4. Calorimetric determination of specific absorption rate

The magnetic heating experiment containing calorimetric determination of specific absorption rate (SAR) was performed with Fe_3O_4 nanoparticles suspended in an aqueous agarose gel (2.5 wt%). Samples (1.8 ml) in plastic test tubes were placed inside a coil and the temperature vs. time at an exposure to a dynamic magnetic field (field amplitude $H_{\text{max}}=7.5$ mT and frequency $\nu=960$ kHz) was recorded. All samples used in the measurement were freshly prepared. The temperature changes were automatically measured by an optical fiber probe (Luxtron STF-2, BFi OPTILAS SAS, France). Results were corrected for heat losses. For details of experimental setup see [26].

2.5. Characterization of suspensions under static magnetic field

The Fe_3O_4 nanoparticles were dispersed in viscous silicone oil (Dow Corning, Fluids 200, USA; viscosity $\eta_0 \approx 100$ mPa s) to prevent their sedimentation during measurement of the rheological response to direct magnetic field. Investigated concentration range of ferrofluids reflected their subsequent feasible clinical application at the physiological temperature of 37 °C. Thus the maximum tested concentration was chosen to be 20 wt%. The other four concentrations were 15, 10, 5 and 1 (wt%).

Steady-shear stress properties under static magnetic field were measured using a rotational rheometer Physica MCR501 (Anton Paar GmbH, Austria) with a Physica MRD 180/1T magnetocell at 37 °C. A parallel-plate measuring system with a diameter of 20 mm and a gap of 0.1 mm was used. True magnetic flux density was measured using a Hall probe and temperature was checked with the help of an inserted thermocouple. Both the Hall probe and the thermocouple were located on the bottom plate, for details see [27]. Temperature was set using an Anton Paar circulator Viscoterm VT2 with temperature stability ± 0.02 °C. Maximum magnetic flux density used in all measurements did not exceed 0.3 T to ensure sufficient homogeneity of a magnetic field perpendicular to the shear flow direction. All the steady-shear stress experiments were performed in the shear rate range 0.1–300 s^{-1} .

3. Results and discussion

3.1. Structural analysis

3.1.1. X-ray diffraction

The powder XRD patterns of prepared products via microwave-assisted solvothermal synthesis at 220 °C are shown in Fig. 1. It is worth noting that all diffraction peaks of aqueous ammonia nucleated material can be indexed to a pure cubic spinel Fe_3O_4 phase with lattice constant $a=8.396$ Å. However, close XRD analysis of materials nucleated by ammonium acetate and ammonium carbonate also showed, apart from magnetite or maghemite phase (indistinguishable from XRD), the presence of other phases. Especially in the case of ammonium acetate the substantial amount of goethite was recorded. Other phases were also detected for samples nucleated by ammonium carbonate, in this case dominated by ferrihydrite. From Rietveld refinement, employed for crystallite size determination, it clearly follows that grain size varied strongly depending on the nucleating agent used (see Table 1).

Note that the structural profile analysis of diffraction patterns showed a significant difference in the intensity of the diffraction

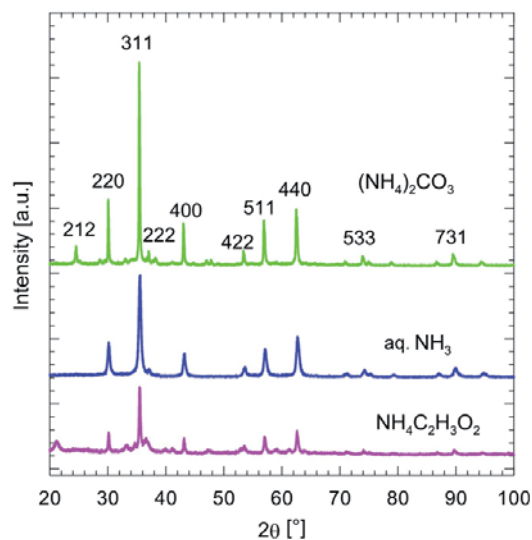


Fig. 1. X-ray diffraction patterns of the variously nucleated Fe_3O_4 particles.

peak {311}, which corresponds to the basic reflection of the face-centered cubic phase of Fe_3O_4 . The Fe_3O_4 nucleated by ammonium carbonate shows a twice higher intensity of the {311} peak. This occurrence may be attributed to the presence of the magnetic texture due to the orientational ordering among the nanocrystals which finally formed an individual nanoparticle.

3.1.2. Transmission electron microscopy

The changes in Fe_3O_4 particles size and shape resulting from the use of different nucleating agents were determined by means of TEM image analysis shown in Fig. 2. Comparison of mean crystallite size with particles size from TEM analysis gives close values indicating single crystallite particles of Fe_3O_4 nucleated by aqueous ammonia and ammonium acetate, whereas for Fe_3O_4 nucleated by ammonium carbonate the TEM analysis showed significantly higher values of particles size (see Table 1).

As can be seen in Fig. 2a, aqueous ammonia nucleated particles are mostly polyhedral with evident size distribution. However, smaller-sized nanocrystals are approximately spherical with mean particle size of about 10 nm. Fig. 2b shows that the use of ammonium acetate nucleation agent leads to the formation of particles of different morphologies, namely spherical particles and acicular particles. It is known that acicular morphology corresponds to the basic morphology of goethite [28]. It should be noted that ammonium acetate and ammonium carbonate nucleating agents yielded larger Fe_3O_4 -based spherical particles (Fig. 2b and c). In case of Fe_3O_4 nucleated by ammonium carbonate, some of the particles are formed by interlinking of smaller particles (crystallites) of irregular shape, which resembles the structure of polycrystalline materials (Fig. 2d). Thus, the difference between the values of particle size identified by TEM and XRD analysis can be explained by multiple hierarchical structure of the particles.

3.2. Magnetic properties

Saturation magnetization, M_s , remanent magnetization, M_R , coercivity, H_C , and magnetic permeability, μ , are the main technical parameters for the characterization of magnetic materials.

Table 1

Mean crystallite size (XRD), particle size (TEM), specific absorption rate, coercivity, saturation magnetization, remanent magnetization, real part of complex magnetic permeability and iron content of the Fe_3O_4 nucleated by different nucleating agents.

Nucleating agent used	d_{XRD} (nm)	d_{TEM} (nm)	SAR ($\text{W g}_{\text{Fe}}^{-1}$)	H_C (Oe)	M_S (emu g^{-1})	M_R (emu g^{-1})	μ' (at 10^7 Hz)	Fe content (%)
Aqueous NH_3	17	20	9.1	61	76	8	2.9	64
$\text{NH}_4\text{C}_2\text{H}_3\text{O}_2$	42	60	2.3	23	16	1	1.5	45
$(\text{NH}_4)_2\text{CO}_3$	84	130	2.7	20	42	3	2.9	58

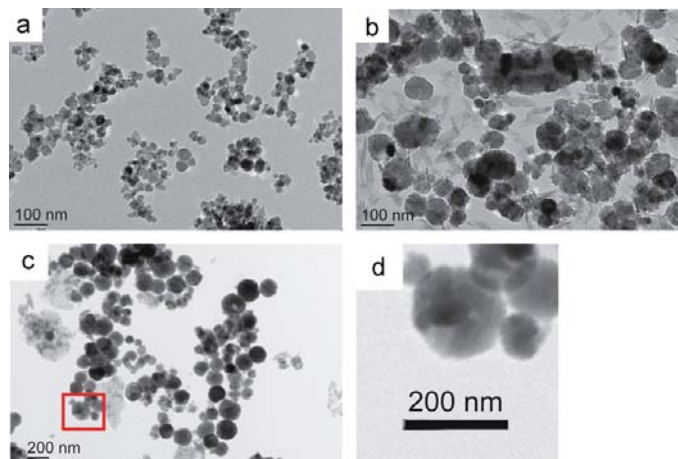


Fig. 2. TEM images of the Fe_3O_4 particles nucleated by (a) aqueous NH_3 ; (b) $\text{NH}_4\text{C}_2\text{H}_3\text{O}_2$; and (c) $(\text{NH}_4)_2\text{CO}_3$.

Fig. 3 shows the field dependence of magnetization for the synthesized Fe_3O_4 particles nucleated by different nucleation agents at 220°C . The corresponding magnetic parameters are listed in Table 1. According to the obtained results, all samples exhibit ferromagnetic behavior. However, they significantly differ in the value of M_S . The highest saturation was recorded for the Fe_3O_4 sample nucleated by aqueous ammonia. The Fe_3O_4 sample nucleated by ammonium carbonate has saturation approximately 1.8 times lower. Moreover, this sample exhibits a different shape of hysteresis loop. Lower value of M_S and atypical shape of the hysteresis loop can both be attributed to the presence of coexisting phases that differ in their magnetic properties. It is known that the presence of coexisting phases tends to change the hysteresis-loop shape and decrease magnetization of nanomagnets [11]. The lowest values of M_S , M_R and H_C have been recorded for Fe_3O_4 sample nucleated by ammonium acetate. In this case the presence of non-magnetic phase of goethite is responsible for sharp decrease of all parameters. Therefore, only Fe_3O_4 sample nucleated by aqueous ammonia demonstrates genuine soft magnetic properties. This characteristic feature of the sample can be explained by a pure cubic Fe_3O_4 spinel phase and absence of non-magnetic impurities.

The magnetostatic properties strongly correlate with dynamic magnetization processes which were studied in a broad frequency range. The permeability dispersion region of all samples appears in the frequency range which corresponds to the natural ferromagnetic resonance (Fig. 4), where the magnetization processes are determined by magnetization rotation in effective magnetic anisotropy fields and demagnetizing fields. The samples differ in the absolute value of μ and the curve shape of the magnetic losses. The sample prepared by ammonium carbonate exhibits two regions of permeability dispersion with two corresponding resonance frequencies, namely the first at about 800 MHz and the

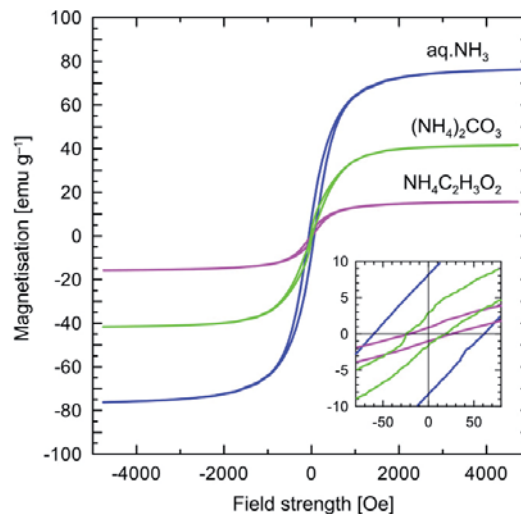


Fig. 3. Magnetization curves for synthesized Fe_3O_4 nanoparticles nucleated via various agents.

second close to 2 GHz. This can be explained by the presence of two coexisting phases that differ in magnetic properties. The Fe_3O_4 sample nucleated by ammonium acetate has the lowest value of μ among the samples due to the presence of goethite. Generally, the resonance frequency for all samples is around 1 GHz. This characteristic feature of the magnetic spectrum is typical for magnetic materials with single-domain particles.

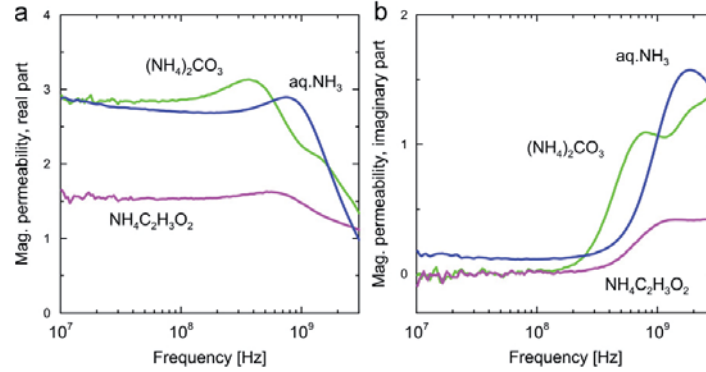


Fig. 4. Magnetic spectra of samples based on Fe_3O_4 nanoparticles nucleated via various agents.

Single-domain critical size for magnetite is about 20 nm [29]. Thus, according to the TEM and XRD results (see Table 1), only Fe_3O_4 nanoparticles nucleated by aqueous ammonia exhibit single-domain behavior and other samples should be multidomain. However, there is no contribution of domain wall motion to magnetic permeability in any sample.

Consequently, the main source of coercivity and high-frequency permeability presented in all Fe_3O_4 samples is magnetic anisotropy, more precisely, the sum of magnetocrystalline, shape, surface and strain induced anisotropy.

3.3. Evaluation of heat dissipation in terms of calorimetric measurement

The heat generation of aqueous suspension based on variously nucleated Fe_3O_4 particles prepared via the MW irradiation-assisted solvothermal method in terms of the time-dependent temperature curves in the applied AC magnetic field is shown in Fig. 5. As can be seen, inductive heating experiments reveal that given magnetic field is able to produce enough energy for temperature increase of the system to 43 °C in time interval 1–10 min for all samples. The temperature of aqueous ammonia nucleated Fe_3O_4 rose over 60 °C in 3 min, whereas the temperature of other two systems rose gradually against time and the heat generated was well below that of aqueous ammonia nucleated Fe_3O_4 sample.

A key feature of materials used for magnetic hyperthermia is the specific loss power of particles expressed in terms of SAR. The SAR values for particles dispersed in aqueous suspension can be calculated by using of the following equation [30]:

$$\text{SAR} = \frac{c_p}{m_{\text{Fe}}} \frac{dT}{dt} \quad (1)$$

where c_p is the sample-specific heat capacity under constant pressure ($c_p = 4.18 \text{ J g}^{-1}$ for water), m_{Fe} is the iron content per gram of the Fe_3O_4 , and dT/dt is the slope of the temperature (from 36 °C to 38 °C) vs. time dependence.

The SAR values at 37 °C (the body temperature, which is of primary interest for hyperthermia experiments) for studied systems with variously nucleated Fe_3O_4 nanoparticles are listed in Table 1. As can be seen, the highest SAR ($\sim 9 \text{ W g}_{\text{Fe}}^{-1}$) was measured for ammonium hydroxide nucleated Fe_3O_4 nanoparticles while for other nucleating agents these values were found to be systematically lower. The identification of specific mechanisms responsible for the resulting SAR for different samples is rather difficult as they have different particle morphologies and

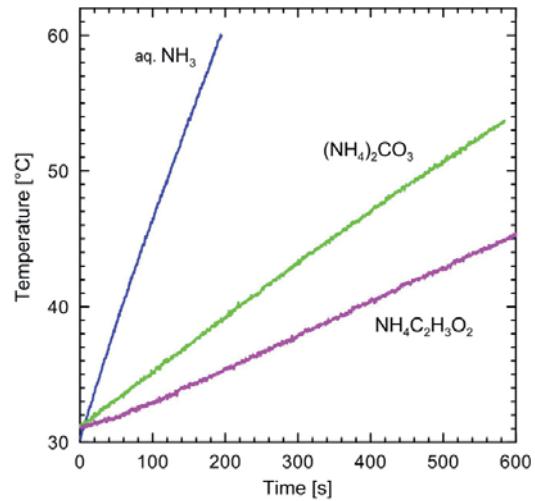


Fig. 5. Temperature increase triggered by Fe_3O_4 nanoparticles suspended in agarose gel measured at 960 kHz and magnetic field amplitude $H_{\text{max}} = 7.5 \text{ mT}$.

microstructures. There is still a lot of space for experimental and theoretical work for understanding all individual contributions (i.e. hysteresis losses and/or relaxation losses) to specific loss power which subsequently determines the efficiency of a certain material in magnetic hyperthermia. However, based on the structural and magnetic properties, we can assume that the higher value of SAR for aqueous ammonia nucleated Fe_3O_4 nanoparticles is caused by small particle size and narrow particle size distribution. In such a case the prevailing mechanism of heating in AC magnetic field is Neel relaxation.

Therefore, the obtained value of SAR can predestine the Fe_3O_4 nanoparticles prepared via the MW irradiation-assisted solvothermal method to applications such as heating agents in magnetic hyperthermia.

3.4. Rheological properties of ferrofluids under static magnetic field

According to the character of magnetization curve (Fig. 3) predestining the most effective magnetic dipole–dipole interactions between particles, aqueous ammonia nucleated Fe_3O_4

nanoparticles based ferrofluid was chosen for the evaluation of internal structure formation. Flow curves of shear stress as a function of shear rate for 15 wt% of ferrofluid based on aqueous ammonia nucleated Fe_3O_4 suspension in silicone oil under various magnetic flux densities (B) are shown in Fig. 6. The small pseudoplastic behavior in the absence of magnetic field at low shear rates can be attributed to strong interaction between Fe_3O_4 nanoparticles with large specific surface and silicone oil. When a magnetic field is applied to the ferrofluid, the shear stress increases abruptly with magnetic field, showing characteristic yield behavior of a Bingham fluid over the entire shear rate range [31]. This dramatic change in rheological properties (yield stress, τ_y , representing maximum seal pressure, increases by two orders in magnitude under application of magnetic field) is related to the formation of chain-like structures in ammonia nucleated Fe_3O_4 suspension. In external magnetic field the magnetized Fe_3O_4

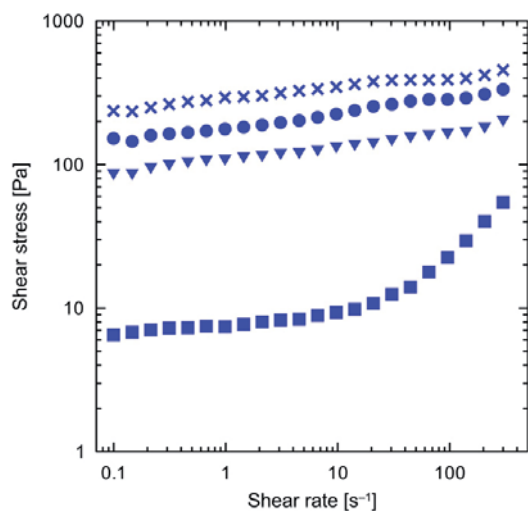


Fig. 6. Flow curves of 15 wt% suspension of aqueous ammonia nucleated Fe_3O_4 nanoparticles in silicone oil under various magnetic fields strengths; B (mT): ■ 0, ▽ 82, ● 168, and × 253.

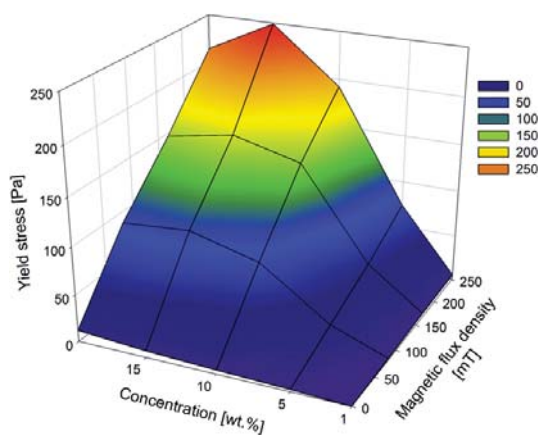


Fig. 7. Dependence of yield stress of ferrofluid on concentration of particles and applied magnetic field strength.

nanoparticles attract each other due to magnetic dipole–dipole interactions, forming chains of particles oriented along the field direction. Increase in B induces a higher dipole moment and the particular microstructures become stiffer [32].

Fig. 7 shows the dependence of the yield stress on the particle concentration in ferrofluid and magnetic flux density. Apparently the yield stress is proportional to both parameters, i.e., stronger internal structures are formed for highly concentrated ferrofluids and strong magnetic fields. The measured yield stress can be considered as a sealing pressure with respect to the intended embolization of tumors. Depending on the type of vessel to be occluded, required pressure can vary significantly from several units up to tens of mmHg. However, for occlusion of smaller blood vessels, sealing pressures of not more than 5 mmHg are sufficient [33].

Observed yield stress of 250 Pa (approximately 2 mmHg) for aqueous ammonia nucleated Fe_3O_4 nanoparticles ferrofluid under magnetic field used in this study (< 250 mT) may not prove to be sufficient to inhibit the blood flow in all types of blood vessels.

4. Conclusions

A one-step reproducible method of MW irradiation-assisted solvothermal synthesis was performed for the preparation of Fe_3O_4 nanoparticles which are different in their structure and magnetic properties. Based on the character of magnetic spectra, all prepared samples represent themselves as single-domain despite the fact that they differ significantly in particles size. In accordance with TEM and XRD results, only Fe_3O_4 nucleated by aqueous ammonia shows the particles size corresponding to the single-domain state. Other samples are characterized by particles size which is above the single-domain limit, but, in fact, big particles are formed by interlinking of smaller, single-domain particles.

The highest values of M_s , M_R , and H_C correspond to the Fe_3O_4 nucleated by aqueous ammonia due to the formation of a pure cubic Fe_3O_4 spinel phase, whereas in case of Fe_3O_4 nucleated by ammonium acetate and ammonium carbonate, the presence of additional weak antiferromagnetic phase of goethite and speromagnetic phase of ferrihydrite was detected. Thus the Fe_3O_4 nucleated by ammonium acetate and ammonium carbonate shows lower values of M_s , M_R , and H_C .

Preliminary heating experiments of Fe_3O_4 nanoparticles in AC magnetic field proved that the heat efficiency is determined by morphological and magnetic properties of nanoparticles. In particular, the experiments carried out with 20 nm aqueous ammonia nucleated Fe_3O_4 showed decent values of specific absorption rate at 37 °C, i.e. the body temperature. The highest value of SAR for aqueous ammonia nucleated Fe_3O_4 is due to the small particle size and narrow particle size distribution. In such a case the prevailing mechanism of heating in AC magnetic field is Neel relaxation.

Strong magnetic response of silicone oil suspensions filled with aqueous ammonia nucleated Fe_3O_4 nanoparticles was observed due to the chain formation caused by the interaction between magnetized particles resulting in flow resistance under DC magnetic field, which could be utilized for embolization of blood vessels.

Acknowledgment

Authors would like to thank the internal grant of TBU in Zlín no. IGA/25/FT/10/D funded from the resources of specific university research.

This article was written with support of Operational Programme Research and Development for Innovations co-funded by the European Regional Development Fund (ERDF) and national budget of the Czech Republic, within the framework of Centre of Polymer Systems project (Reg. number: CZ.1.05/2.1.00/03.0111).

References

- [1] J.W.M. Bulte, D.L. Kraitchman, Iron oxide MR contrast agents for molecular and cellular imaging, *NMR in Biomedicine* 17 (2004) 484–499.
- [2] T. Neuberger, B. Schopf, H. Hofmann, M. Hofmann, B. von Rechenberg, Superparamagnetic nanoparticles for biomedical applications: possibilities and limitations of a new drug delivery system, *Journal of Magnetism and Magnetic Materials* 293 (2005) 483–496.
- [3] R. Cavalier, E.C. Ciocatto, B.C. Giovanel, C. Heidelebe, R.O. Johnson, M. Margotti, B. Mondovi, G. Moricca, A. Rossifan, Selective heat sensitivity of cancer cells—biochemical and clinical studies, *Cancer* 20 (1967) 1351–1381.
- [4] G.S. Gazelle, S.N. Goldberg, L. Solbiati, T. Livraghi, Tumor ablation with radio-frequency energy, *Radiology* 217 (2000) 633–646.
- [5] T. Seki, M. Wakabayashi, T. Nakagawa, M. Imamura, T. Tamai, A. Nishimura, N. Yamashiki, A. Okamura, K. Inoue, Percutaneous microwave coagulation therapy for patients with small hepatocellular carcinoma—comparison with percutaneous ethanol injection therapy, *Cancer* 85 (1999) 1694–1702.
- [6] N. McDannold, C.M. Tempny, F.M. Fennessy, M.J. So, F.J. Rybicki, E.A. Stewart, F.A. Jolesz, K. Hynynen, Uterine leiomyomas: MR imaging-based thermometry and thermal dosimetry during focused ultrasound thermal ablation, *Radiology* 240 (2006) 263–272.
- [7] B. Samanta, H. Yan, N.O. Fischer, J. Shi, D.J. Jerry, V.M. Rotello, Protein-passivated Fe₃O₄ nanoparticles: low toxicity and rapid heating for thermal therapy, *Journal of Materials Chemistry* 18 (2008) 1204–1208.
- [8] A. Jordan, R. Scholz, P. Wust, H. Fahling, R. Felix, Magnetic fluid hyperthermia (MFH): cancer treatment with AC magnetic field induced excitation of biocompatible superparamagnetic nanoparticles, *Journal of Magnetism and Magnetic Materials* 201 (1999) 413–419.
- [9] T. Atsumi, B. Jeyadevan, Y. Sato, K. Tohji, Heating efficiency of magnetite particles exposed to AC magnetic field, *Journal of Magnetism and Magnetic Materials* 310 (2007) 2841–2843.
- [10] W. Andr , H. Nowak, *Magnetism in Medicine: A Handbook*, Wiley-VCH, Berlin, Chichester, 1998.
- [11] R. Skomski, Nanomagnetism, *Journal of Physics: Condensed Matter* 15 (2003) R841–R896.
- [12] R. Skomski, G.C. Hadjipanayis, D.J. Sellmyer, Effective demagnetizing factors of complicated particle mixtures, *IEEE Transactions on Magnetics* 43 (2007) 2956–2958.
- [13] R.H. Kodama, Magnetic nanoparticles, *Journal of Magnetism and Magnetic Materials* 200 (1999) 359–372.
- [14] A. Jordan, R. Scholz, P. Wust, H. Schirra, T. Schiestel, H. Schmidt, R. Felix, Endocytosis of dextran and silan-coated magnetite nanoparticles and the effect of intracellular hyperthermia on human mammary carcinoma cells in vitro, *Journal of Magnetism and Magnetic Materials* 194 (1999) 185–196.
- [15] C. Chouly, D. Pouliquen, I. Lucet, J.J. Jeune, P. Jallet, Development of superparamagnetic nanoparticles for MRI: effect of particle size, charge and surface nature on biodistribution, *Journal of Microencapsulation* 13 (1996) 245–255.
- [16] G. Baldi, D. Bonacchi, M.C. Franchini, D. Gentili, G. Lorenzi, A. Ricci, C. Ravagli, Synthesis and coating of cobalt ferrite nanoparticles: a first step toward the obtainment of new magnetic nanocarriers, *Langmuir* 23 (2007) 4026–4028.
- [17] A.S. Lubbe, C. Bergemann, W. Huhnt, T. Fricke, H. Riess, J.W. Brock, D. Huhn, Preclinical experiences with magnetic drug targeting: tolerance and efficacy, *Cancer Research* 56 (1996) 4694–4701.
- [18] G. Jacob, A.D. Ciochina, O. Bredeteian, M. Racuciu, Magnetite particle utilization for blood vessel embolization—a practical modeling, *Optoelectronics and Advanced Materials: Rapid Communications* 2 (2008) 446–449.
- [19] J. Liu, G.A. Flores, R.S. Sheng, In-vitro investigation of blood embolization in cancer treatment using magnetorheological fluids, *Journal of Magnetism and Magnetic Materials* 225 (2001) 209–217.
- [20] M. Sedlacik, V. Pavlinek, P. Saha, P. Svr cino, P. Filip, J. Stejskal, Rheological properties of magnetorheological suspensions based on core-shell structured polyaniline-coated carbonyl iron particles, *Smart Materials and Structures* 19 (2010) 115008.
- [21] R. Sheng, G.A. Flores, J. Liu, In vitro investigation of a novel cancer therapeutic method using embolizing properties of magnetorheological fluids, *Journal of Magnetism and Magnetic Materials* 194 (1999) 167–175.
- [22] G.A. Flores, J. Liu, Embolization of blood vessels as a cancer therapy using magnetorheological fluids, *Journal of Intelligent Material Systems and Structures* 13 (2002) 641–646.
- [23] R. Massart, Preparation of aqueous magnetic liquids in alkaline and acidic media, *IEEE Transactions on Magnetics* 17 (1981) 1247–1248.
- [24] W.W. Yu, E. Chang, C.M. Sayes, R. Drezek, V.L. Colvin, Aqueous dispersion of monodisperse magnetic iron oxide nanocrystals through phase transfer, *Nanotechnology* 17 (2006) 4483–4487.
- [25] M. Tsuji, M. Hashimoto, Y. Nishizawa, M. Kubokawa, T. Tsuji, Microwave-assisted synthesis of metallic nanostructures in solution, *Chemistry—A European Journal* 11 (2005) 440–452.
- [26] S. Vasseur, E. Duguet, J. Portier, G. Goglio, S. Mornet, E. Hadova, K. Knizek, M. Marysko, P. Veverka, E. Pollert, Lanthanum manganese perovskite nanoparticles as possible in vivo mediators for magnetic hyperthermia, *Journal of Magnetism and Magnetic Materials* 302 (2006) 315–320.
- [27] H.M. Laun, C. Gabriel, Measurement modes of the response time of a magnetorheological fluid (MRF) for changing magnetic flux density, *Rheologica Acta* 46 (2007) 665–676.
- [28] R.M. Cornell, U. Schwertmann, *The Iron Oxides: Structure, Properties, Reactions, Occurrences and Uses*, VCH, Weinheim, Cambridge, 1996.
- [29] K.M. Krishnan, Biomedical nanomagnetism: a spin through possibilities in imaging, diagnostics, and therapy, *IEEE Transactions on Magnetics* 46 (2010) 2523–2558.
- [30] R. Hergt, W. Andra, C.G. d'Ambly, I. Hilger, W.A. Kaiser, U. Richter, H.G. Schmidt, Physical limits of hyperthermia using magnetite fine particles, *IEEE Transactions on Magnetics* 34 (1998) 3745–3754.
- [31] F.F. Fang, H.J. Choi, W.S. Choi, Two-layer coating with polymer and carbon nanotube on magnetic carbonyl iron particle and its magnetorheology, *Colloid and Polymer Science* 288 (2010) 359–363.
- [32] D.J. Woo, M.H. Suh, E.S. Shin, C.W. Lee, S.H. Lee, Electrorheological behavior of suspensions of a substituted polyaniline with long alkyl pendants, *Journal of Colloid and Interface Science* 288 (2005) 71–74.
- [33] M.E. Klingensmith, *The Washington Manual of Surgery*, Wolters Kluwer Health, Lippincott Williams & Wilkins, Philadelphia, 2008.

Paper V.

Kozakova, Z.; Kuritka, I.; Bazant, P.; Pastorek, M. and Babayan, V., Synthesis of needle-like iron oxide particles by microwave-assisted thermal decomposition technique. *Manuscript submitted to Materials Letters*. (50%)

Elsevier Editorial System(tm) for Materials Letters
Manuscript Draft

Manuscript Number:

Title: Magnetic Needle-Like Iron Oxide Particles Prepared by Microwave-Assisted Thermal Decomposition Technique

Article Type: Letter

Keywords: Magnetic materials, Crystal growth, Phase transformation, Nanocrystalline materials

Corresponding Author: Ms. Zuzana Kozakova,

Corresponding Author's Institution: Tomas Bata University in Zlin

First Author: Zuzana Kozakova

Order of Authors: Zuzana Kozakova; Ivo Kuritka; Pavel Bazant; Miroslav Pastorek; Vladimir Babayan

Abstract: Iron oxide particles were prepared by a simple organic precursor assisted thermal decomposition technique. Microwaves were used as a source of energy for both, precursor synthesis and generation of heat required for thermal decomposition. Ferrous oxalate dehydrate prepared within the microwave-assisted solvothermal process possess needle-like particle morphology with the length of about 20 μm and submicrometric diameter. Magnetic iron oxide was formed by a topotactic decomposition of prepared precursor in a microwave reactor thus the final product also preserves needle-like shape and possesses soft ferromagnetic behavior.

Suggested Reviewers: Martin Hermanek Doctor
Research assistant, Department of Experimental Physics, Palacky University, Czech Republic
martin.hermanek@upol.cz
Expert in the field of thermal decompositions.

Kaibin Tang Professor
Professor, Department of Chemistry, University of Science and Technology of China
kbtang@ustc.edu.cn
Expert in the field of thermal decompositions.

Inna P. Borovinskaya Professor
Head of laboratories of Self-Propagating High-Temperature Synthesis, Institute of Structural Macrokinetics and Materials Science, Russian Academy of Sciences
inna@ism.ac.ru
Expert in the field of thermal decompositions.

Highlights (for review)

- Magnetic needles of 20 μm were prepared by a two step microwave-assisted synthesis
- This method is simple, effective and uses available cheap and low-toxic chemicals
- Prepared particles possess soft ferromagnetic behavior typical for nanoparticles
- Elongated shape, size and magnetic properties predict high application potential

1
2 **Magnetic Needle-Like Iron Oxide Particles Prepared by Microwave-Assisted Thermal**
3 **Decomposition Technique**
4

5
6
7
8 Zuzana Kozakova*, Ivo Kuritka, Pavel Bazant, Miroslav Pastorek, Vladimir Babayan
9

10
11 Centre of Polymer Systems, University Institute, Tomas Bata University in Zlin, Nad Ovcirnou 3685, 760
12
13 01 Zlin, Czech Republic
14

15
16
17 List of email addresses and phone numbers:

18 Zuzana Kozakova, zkozakova@ft.utb.cz, +420773184823 * Corresponding author

19 Ivo Kuritka, ivo@kuritka.net, +420603254579

20 Pavel Bazant, bazantik@centrum.cz, +420 57 603 8049

21 Miroslav Pastorek, pastorek@ft.utb.cz, +420 57 603 8128

22 Vladimir Babayan, babayan@ft.utb.cz, +420 57 603 1451
23
24
25
26
27
28

29 **Abstract**
30

31 Iron oxide particles were prepared by a simple organic precursor assisted thermal decomposition technique.
32
33 Microwaves were used as a source of energy for both, precursor synthesis and generation of heat required
34 for thermal decomposition. Ferrous oxalate dehydrate prepared within the microwave-assisted solvothermal
35 process possess needle-like particle morphology with the length of about 20 μm and submicrometric
36 diameter. Magnetic iron oxide was formed by a topotactic decomposition of prepared precursor in a
37 microwave reactor thus the final product also preserves needle-like shape and possesses soft ferromagnetic
38 behavior.
39
40
41
42

43 *Keywords* — Magnetic materials, Crystal growth, Phase transformation, Nanocrystalline materials
44
45

46 **1. Introduction**
47

48
49 In recent years, preparation of iron oxide one-dimensional nano- and submicro-structures gets great
50 attention due to their unique properties resulting from the shape anisotropy [1,2]. Especially, spinel ferrites
51 are interesting due to possible utilization for magnetic refrigeration, as a promising component of
52 ferrofluids and materials for the high density data storage [3]. Moreover, their incorporation into the
53 polymeric matrix under the influence of an external magnetic field provides the anisotropic reinforced
54 materials [4], materials with tunable elastic modulus [5] or microwave absorbing materials [6].
55
56 Among the most common synthesis techniques, hydrothermal and solvothermal methods are most used and
57
58 there is number of publications dealing with preparation of magnetic nanostructures; however, these
59
60
61
62
63
64
65

1
2
3 methods predominantly lead to the formation of spherical or polyhedral particles [7-12]. On the other hand,
4 publications devoted to the preparation of magnetic iron oxides with elongated shape are significantly less
5 extended. As an example, Lian et al. described preparation of single crystalline Fe₃O₄ nanorods from
6 FeSO₄·7H₂O, NaOH and PEG-1000 at 150°C in sealed Teflon autoclaves, however, information on the
7 magnetic properties is missing in this publication [13].
8
9

10
11 Another way how to obtain elongated magnetic structures is the use of template-assisted synthesis.
12

13 Methods that utilize organometallic precursors that decompose at relatively low temperature appear to be
14 the most suitable [1]. “Precursor syntheses” are interesting from technological point of view since these
15 methods are simple, cost effective and enable large-scale production [14].
16
17

18 Several types of precursors are commonly used for thermal decomposition techniques. As an example,
19 solution-combustion methods utilize metal nitrates as the source of metal cations and organic compounds
20 such as citric acid, glycine or urea as reducers (fuels). Firstly, the precursor is dissolved in proper solvent
21 and obtained gel is combusted. Combustion procedure is accompanied by generation of gaseous products
22 which suppress the aggregation of forming metal oxide particles thus remaining in nanoscale [15,16].
23
24

25 However, these combustion methods do not lead to the formation of elongated rod- or wire-like structures.
26
27 For this purpose, ferric and ferrous oxalates appear to be proper candidates due to their preferred growth in
28 one dimension at proper conditions thus forming rod-like structures [1,17-19]. Conversion of precursor into
29 the final product is a topotactic reaction thus the forming particles preserve the shape given by the
30 precursor [1].
31
32

33 The difficulty to control the crystalline phase composition is considered to be the biggest disadvantage of
34 oxidative decomposition techniques and is caused by numerous experimental parameters involved into the
35 oxidative reactions (temperature, time, reaction atmosphere, precursor particle morphology and also
36 thickness of precursor layer). Iron (α -Fe), iron carbide (Fe₃C), siderite (FeCO₃), wüstite (FeO) magnetite
37 (Fe₃O₄) and various Fe₂O₃ can be formed within the oxidative decomposition of Fe(II) oxalate precursor
38 [14]. Another disadvantage is considered to be the necessity to use the surfactants which are not only
39 expensive but also can be harmful [20]. According to Zhou et al., controlling the reaction atmosphere of
40 ferrous oxalate thermal decomposition can provide various products: hematite (α -Fe₂O₃) on air, maghemite
41 (γ -Fe₂O₃) under inert atmosphere or magnetite under limited air conditions [1].
42
43
44
45
46
47
48
49
50
51
52

53 In order to achieve uniform elongated precursor particles with high aspect ratio in short synthetic times we
54 developed a microwave-assisted procedure providing material with such properties. Moreover, we showed
55 that the desired product can be prepared in a good quality without the use of surfactants. To minimize the
56 synthetic time and maximize efficiency of synthetic procedure, the process of thermal decomposition of the
57 precursor was performed in microwave oven in a ceramic kiln accompanied with microwave absorbing
58
59
60
61
62
63
64
65

1
2 layer on the inner wall. This two-step setting enables to reach high temperature in short times and thus
3 perform rapid conversion of precursor into the desired product. Limited amount of air involved in the
4 reaction system was provided through the sealing of precursor into glass tube.
5
6
7

8 9 **2. Materials and methods**

10
11 Magnetic needles based on iron oxides were prepared by a thermal decomposition of organometallic
12 precursor. Microwaves were used in both steps of procedure: they served as a source of energy for the
13 formation of precursor and for generation of heat required for the thermal decomposition.
14
15
16

17 **2.1. Precursor Synthesis**

18
19 Organometallic precursor was prepared by a microwave-assisted solvothermal method. All of the chemicals
20 used within the synthesis were purchased from Penta Company (Czech Republic) in an analytical purity
21 and were used as-received without further purification. Iron (II) sulfate heptahydrate (20 mmol) and oxalic
22 acid dihydrate (20 mmol) were dissolved separately in a mixed solvent containing water and ethylene
23 glycol in a ratio of 1:3. Prepared solutions were filtered off and then the solution of oxalic acid was added
24 into the solution of iron (II) sulfate slowly while constant stirring. As-prepared solution was then
25 transferred into the Teflon liner, sealed and placed into the cavity of a pressurized microwave reactor CEM
26 Mars 5 (USA). The solution was then treated for 30 minutes at 100°C and the obtained yellow precipitate
27 was filtered-off and rinsed with distilled water.
28
29
30
31
32
33
34
35
36

37 **2.2. Thermal Decomposition of Organometallic Precursor**

38
39 Magnetic needles were prepared by the thermal decomposition of organometallic precursor obtained by the
40 described solvothermal procedure. Small amount (10 mg) of precursor was sealed into the glass tube with
41 the total volume of about 2 ml. Tubes were then placed into the ceramic kiln equipped with the microwave
42 absorbing layer and the kiln was heated in the cavity of common domestic microwave oven (Hyundai,
43 MWM 1417 W) at 750 W for 15 minutes. This setup enables reaching of high temperature in short times
44 and therefore, the decomposition of precursor was complete after 15 minutes. Temperature measured
45 immediately after the decomposition using the contactless pyrometer was found to be of about 450 °C.
46
47
48
49
50
51
52

53 **2.3. Characterization of Prepared Materials**

54
55 First of all, macroscopic appearance of prepared powder was observed by naked eye and by digital
56 microscope DVM 2500 (Leica Microsystems, Germany). Crystalline composition of prepared materials
57 was studied with the help of X-ray Diffraction (XRD, PANalytical X'Pert PRO) with Cu K α 1 radiation (λ
58 = 1.540598 Å). Particle size and morphology were investigated with the help of Scanning Electron
59
60
61
62
63
64
65

Microscopy (SEM, VEGA\LMU, Tescan). Magnetic properties were measured by a Vibrating Sample Magnetometer (VSM, VSM 7400, Lake Shore) at the room temperature and air conditions.

3. Results and Discussion

Crystalline composition of prepared magnetic particles was determined by XRD. Figure 1 shows XRD patterns of precursor and the final product obtained by its thermal decomposition.

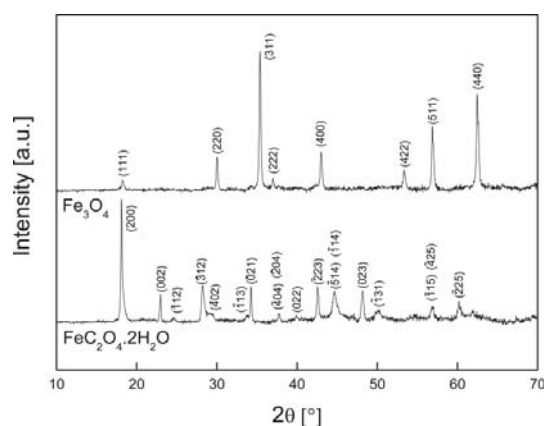


Figure 1. XRD patterns of precursor and product of the thermal decomposition

Prepared precursor is composed solely of the ferrous oxalate dehydrate with monoclinic crystal system (ICDD-JCPDS PDF-2 entry 01-072-1305). In next, all peaks that were observed in XRD pattern of the decomposition product can be attributed to the spinel cubic structure of magnetite (or maghemite). Even if the distinction of magnetite and maghemite by XRD method is not explicit, one can expect that the prepared black powder is consisted of magnetite phase majority due to the limited air conditions within the decomposition of precursor. To investigate the structure of prepared oxalate precursor and final product, the crystallites size was calculated from the broadening of the diffraction peaks from XRD diffractograms according to the Scherrer's equation and was estimated to be about 40 nm in both cases.

Morphological investigation was performed with the help of SEM. A representative captured image of the product can be seen in Figure 2.

1
2
3
4
5
6
7
8
9
10
11
12
13
14
15
16
17
18
19
20
21
22
23
24
25
26
27
28
29
30
31
32
33
34
35
36
37
38
39
40
41
42
43
44
45
46
47
48
49
50
51
52
53
54
55
56
57
58
59
60
61
62
63
64
65

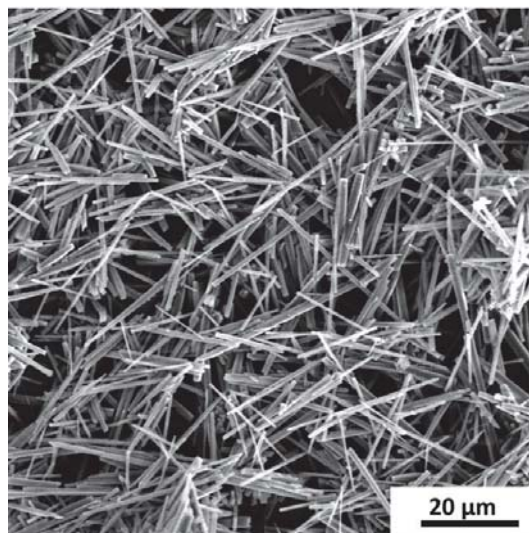


Figure 2. SEM image of prepared magnetic iron oxide needle-like particles

Prepared precursor particles have the shape of long needles and their diameter is less than 1 μm . Due to the topotactic character of the decomposition process, the shape of the converted product remains preserved.

The length of about 20 μm and diameter less than 1 μm gives to our product uniquely high aspect ratio.

Figure 3 shows static magnetic properties measured by the VSM at a room temperature. Obtained magnetization-demagnetization curves show that the prepared iron oxide particles possess ferromagnetic behavior with the saturation magnetization (M_S) of about 43 $\text{emu}\cdot\text{g}^{-1}$ and coercivity 124 Oe.

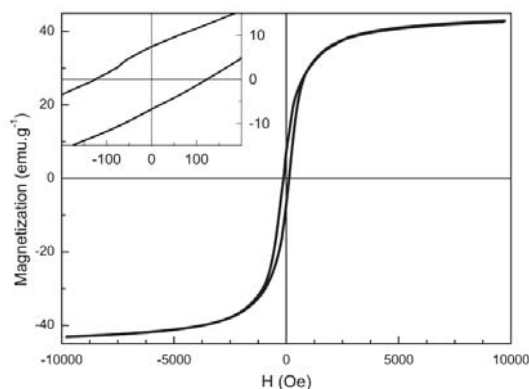


Figure 3. Magnetostatic properties of prepared iron oxide measured by VSM

It is well known, that nanoscaled magnetite has lower value of magnetization saturation (M_S) than the bulk

1
2 form (92–100 emu.g⁻¹) and can be attributed to the canted spins on the surface [21-23]. No
3
4 superparamagnetic behavior was observed which is in agreement with the fact that the critical size of
5
6 superparamagnetism in magnetite is 29 nm [24]. On the other hand, the observed coercivity is much larger
7
8 than values observed for magnetite nanoparticles with 40 nm diameter synthesized by common [25] or
9
10 microwave-assisted [26,27] technique. Anisotropic effects oppose the magnetization rotation and determine
11
12 the coercivity of single-domain particles. For this kind of particles, magnetization switching occurs due to
13
14 the coherent magnetization rotation and curling. Energy of uniformly magnetized elongated particles then
15
16 depends on the direction of magnetization: non-spherical sample is easily magnetized along the long axis
17
18 (easy magnetization axis) while to magnetize the sample along the short axes (non-easy magnetization
19
20 axis), an extra energy called magnetocrystalline anisotropy energy is needed [22,28]. Thus resulting large
21
22 coercivity can be expected for this kind of materials which inherits elongated morphology and anisotropy
23
24 from its precursor by topotactic transformation similarly as it was discussed in [29] by Angermann. In
25
26 comparison to Angermann, our particles are very well shaped, at least ten times longer and have much
27
28 larger aspect ratio. However, the particles evidently keep the characteristic magnetic properties of their 40
29
30 nm sized nanoparticulate building blocks.

31 **4. Conclusions**

32
33 Unique magnetic needle-like particles of submicrometric diameter and length of about 20 μm were
34
35 prepared by a rapid two step synthesis. Microwaves were used within the preparation procedure to provide
36
37 oxalate precursor and subsequent formation of iron oxide particles by its thermal decomposition. Prepared
38
39 iron oxide particles possess ferromagnetic behavior with moderate value of magnetic saturation and large
40
41 value of coercivity with respect to common related nano-materials. Presented novel method of synthesis is
42
43 simple, effective and uses common available, non-costly and low-toxic chemicals. Synthetic time is
44
45 significantly shortened due to the acceleration of the reaction rates within the solvothermal process and
46
47 faster formation of heat required for the thermal decomposition. Prepared particles have demonstrated
48
49 nearly ideal size, shape and properties for their future utilization is several branches using their magnetic
50
51 performance either during fabrication or in the function of the product itself.

52 **Acknowledgment**

53
54 This work was supported by the internal grant of TBU in Zlín No. IGA/FT/2013/014 funded from the
55
56 resource of specific university research.

57
58 This article was written with support of Operational Program Education for Competitiveness co-funded by
59
60 the European Social Fund (ESF) and national budget of Czech Republic, within the framework of project
61
62 Advanced Theoretical and Experimental Studies of Polymer Systems (reg. number:
63
64
65

1
2 CZ.1.07/2.3.00/20.0104).

3
4 This article was written with support of Operational Program Research and Development for Innovations
5 co-funded by the European Regional Development Fund (ERDF) and national budget of Czech Republic,
6 within the framework of project Centre of Polymer Systems (reg. number: CZ.1.05/2.1.00/03.0111).
7
8
9

10 **References**

- 11
12
13 [1] Zhou WW, Tang KB, Zeng SA, Qi YX. Room temperature synthesis of rod-like Fe_2O_3 center dot $2\text{H}_2\text{O}$
14 and its transition to maghemite, magnetite and hematite nanorods through controlled thermal decomposition.
15 *Nanotechnology*. 2008;19.
16
17 [2] Park SJ, Kim S, Lee S, Kim ZG, Char K, Hyeon T. Synthesis and magnetic studies of uniform iron nanorods
18 and nanospheres. *J Am Chem Soc*. 2000;122:8581-2.
19
20 [3] Sivakumar P, Ramesh R, Ramanand A, Ponnusamy S, Muthamizhchelvan C. Synthesis and characterization of
21 NiFe_2O_4 nanoparticles and nanorods. *J Alloys Compd*.563:6-11.
22
23 [4] Jestin J, Cousin F, Dubois I, Menager C, Schweins R, Oberdisse J, et al. Anisotropic reinforcement of
24 nanocomposites tuned by magnetic orientation of the filler network. *Advanced Materials*. 2008;20:2533-+.
25
26 [5] Varga Z, Filipcsei G, Zrinyi M. Magnetic field sensitive functional elastomers with tuneable elastic modulus.
27 *Polymer*. 2006;47:227-33.
28
29 [6] Ramajo LA, Cristobal AA, Botta PM, Lopez JMP, Reboredo MM, Castro MS. Dielectric and magnetic
30 response of Fe_3O_4 /epoxy composites. *Composites Part a-Applied Science and Manufacturing*. 2009;40:388-
31 93.
32
33 [7] Cao SW, Zhu YJ, Chang J. Fe_3O_4 polyhedral nanoparticles with a high magnetization synthesized in mixed
34 solvent ethylene glycol-water system. *New J Chem*. 2008;32:1526-30.
35
36 [8] Chen XY, Zhang ZJ, Li XX, Shi CW. Hollow magnetite spheres: Synthesis, characterization, and magnetic
37 properties. *Chem Phys Lett*. 2006;422:294-8.
38
39 [9] Deng H, Li XL, Peng Q, Wang X, Chen JP, Li YD. Monodisperse magnetic single-crystal ferrite
40 microspheres. *Angewandte Chemie-International Edition*. 2005;44:2782-5.
41
42 [10] Hu P, Yu LJ, Zuo AH, Guo CY, Yuan FL. Fabrication of Monodisperse Magnetite Hollow Spheres. *J Phys*
43 *Chem C*. 2009;113:900-6.
44
45 [11] Xuan SH, Wang YXJ, Yu JC, Leung KCF. Tuning the Grain Size and Particle Size of Superparamagnetic
46 Fe_3O_4 Microparticles. *Chem Mater*. 2009;21:5079-87.
47
48 [12] Zhu LP, Xiao HM, Zhang WD, Yang G, Fu SY. One-pot template-free synthesis of monodisperse and single-
49 crystal magnetite hollow spheres by a simple solvothermal route. *Cryst Growth Des*. 2008;8:957-63.
50
51 [13] Lian SY, Kang ZH, Wang EB, Jiang M, Hu CW, Xu L. Convenient synthesis of single crystalline magnetic
52 Fe_3O_4 nanorods. *Solid State Commun*. 2003;127:605-8.
53
54 [14] Jia ZG, Ren DP, Xu LX, Zhu RS. Preparation, characterization and photocatalytic activity of porous zinc oxide
55 superstructure. *Mater Sci Semicond Process*.15:270-6.
56
57
58
59
60
61
62
63
64
65

- 1
2
3 [15] Barinova, TV, Borovinskaya, IP, Ignate'va, TI, Belikova, AF, Khomenko, NY, Shchukin, AS, Bakhtamov SG.
4 Combustion Synthesis of Nanosized Iron Oxides: The Effect of Precursor Composition. *International Journal*
5 *of Self-Propagating High-Temperature Synthesis*. 2010; 19:276-80.
6
7 [16] Barinova, TV, Borovinskaya, IP. Solution-Combustion Synthesis of Nanosized Iron Oxide from Ferric
8 Oxalate. *International Journal of Self-Propagating High-Temperature Synthesis*. 2012; 21: 1-6.
9
10 [17] Jia ZG, Ren DP, Xu LX. Generalized preparation of metal oxalate nano/submicro-rods by facile solvothermal
11 method and their calcined products. *Mater Lett*.76:194-7.
12
13 [18] Guo LM, Arafune H, Teramae N. Synthesis of Mesoporous Metal Oxide by the Thermal Decomposition of
14 Oxalate Precursor. *Langmuir*.29:4404-12.
15
16 [19] Hermankova P, Hermanek M, Zboril R. Thermal Decomposition of Ferric Oxalate Tetrahydrate in Oxidative
17 and Inert Atmospheres: The Role of Ferrous Oxalate as an Intermediate. *Eur J Inorg Chem*.1110-8.
18
19 [20] Liu XH, Guo Y, Wang YG, Ren JW, Wang YQ, Guo YL, et al. Direct synthesis of mesoporous Fe₃O₄ through
20 citric acid-assisted solid thermal decomposition. *J Mater Sci*.45:906-10.
21
22 [21] Cornell RM; Schwertmann, U. The iron oxides: structure, properties, reactions, occurrences, and uses. 2nd ed.
23 Weinheim: Wiley-VCH; 2003.
24
25 [22] Vereda F, de Vicente J, Hidalgo-Alvarez R. Physical Properties of Elongated Magnetic Particles:
26 Magnetization and Friction Coefficient Anisotropies. *ChemPhysChem*. 2009;10:1165-79.
27
28 [23] Morales MP, Veintemillas-Verdaguer S, Montero MI, Serna CJ, Roig A, Casas L, et al. Surface and internal
29 spin canting in gamma-Fe₂O₃ nanoparticles. *Chem Mater*. 1999;11:3058-64.
30
31 [24] Dunlop DJ. SUPERPARAMAGNETIC AND SINGLE-DOMAIN THRESHOLD SIZES IN MAGNETITE.
32 *Journal of Geophysical Research*. 1973;78:1780-93.
33
34 [25] Muerbe J, Rechtenbach A, Toepfer J. Synthesis and physical characterization of magnetite nanoparticles for
35 biomedical applications. *Mater Chem Phys*. 2008;110:426-33.
36
37 [26] Kozakova Z, Bazant P, Machovsky M, Babayan V, Kuritka I. Fast Microwave-Assisted Synthesis of Uniform
38 Magnetic Nanoparticles. *Acta Physica Polonica A*.118:948-9.
39
40 [27] Kozakova Z, Kuritka I, Babayan V, Kazantseva N, Pastorek M. Magnetic Iron Oxide Nanoparticles for High
41 Frequency Applications. *IEEE Trans Magn*.49:995-9.
42
43 [28] Lee WY, Cheng WY, Yeh YC, Lai CH, Hwang SM, Hsiao CW, et al. Magnetically Directed Self-Assembly of
44 Electrospun Superparamagnetic Fibrous Bundles to Form Three-Dimensional Tissues with a Highly Ordered
45 Architecture. *Tissue Engineering Part C-Methods*.17:651-61.
46
47 [29] Angermann A, Toepfer J. Synthesis of magnetite nanoparticles by thermal decomposition of ferrous oxalate
48 dihydrate. *J Mater Sci*. 2008;43:5123-30.
49
50
51
52
53
54
55
56
57
58
59
60
61
62
63
64
65

